Dynamics of Co-Behaviour of Climate Processes over Southern Africa

Kwesi Akumenyi QUAGRAINE

Thesis Presented for the Degree of

DOCTOR OF PHILOSOPHY

in the Department of Environmental and Geographical Science

Faculty of Science

UNIVERSITY OF CAPE TOWN

JANUARY 2020

Declaration for inclusion of Publications

I confirm that I have been granted permission by the University of Cape Town's Doctoral Degrees Board (DDB) to include the following publication(s) in my PhD thesis, and where co-authorships are involved, my co-authors have agreed that I may include the publication(s):

Quagraine, K. A., B. Hewitson, C. Jack, I. Pinto, and C. Lennard, 2019: A Methodological Approach to Assess the Co-Behaviour of Climate Processes over Southern Africa. *Journal of Climate*, **32**, 2483–2495, https://doi.org/10.1175/JCLI-D-18-0689.1.

Quagraine, K. A., B. Hewitson, C. Jack, P. Wolski, I. Pinto, and C. Lennard, 2019: Using Co-Behaviour Analysis to Interrogate the Performance of CMIP5 GCMs over Southern Africa. *Journal of Climate,* **33,** 2891–2905, https://doi.org/10.1175/JCLI-D-19-0472.1.

Quagraine, K. A., C. Jack, B. Hewitson, P. Wolski, I. Pinto, and C. Lennard, 2019: Process-Based Evaluation of the Co-Behaviour of Regional Climate Drivers over Southern Africa. This article is to be submitted to a journal.

For when the time is right, I will make it happen!

Abstract

Large-scale climate processes such as El Niño-Southern Oscillation (ENSO), Antarctic Oscillation (AAO), and many others, play varying roles in regional climate variability across the world. While the role of singular processes have been explored in many studies, the combined influence of multiple large-scale processes has received far less attention. Key to this is the challenge of developing methodologies to support the analysis of multiple processes interacting in potentially non-linear ways (co-behaviour) in a particular region. This study details the development of such a methodology and demonstrates its utility in the analysis of the co-behaviour of large-scale process interactions on regional precipitation and temperature variability over southern Africa.

The study defines co-behaviour as the interaction of large-scale processes that may influence regional circulation leading to climate variability. A novel methodology which involves a combination of analysis techniques such as Self-Organizing Maps (SOM) and Principal Component Analysis (PCA) is developed to identify and quantify such co-behaviour which accommodates potentially non-linear interactions. This methodology is evaluated in the context of southern African regional climate using three key processes, namely ENSO, AAO and Inter-tropical Convergence Zone (ITCZ), and characterizations of regional circulation, and temperature and rainfall variability.

Analysis of co-behaviour under observed conditions identifies results that concur with prior studies, in particular the dominant regional response to ENSO, but also establishes key examples of co-behaviour such as the role of the AAO in moderating and altering the regional response to ENSO which is important for understanding regional climate variability. Application of the approach to Global Climate Model (GCM) simulations of past climate reveals that while many GCMs are able to capture individual processes, in particular ENSO, they fail to adequately represent regional circulation variability and key observed co-behaviour. The study therefore clearly demonstrates the importance of co-behaviour in understanding regional climate variability as well as showing the usefulness of the new methodology in investigating co-behaviour. Finally, the new insights into evaluating model performance through the

lens of core climate processes and their interaction provides a significant step forward in both model development and application for decision making.

Supervision, Funding and Declaration

Supervisors

Prof Bruce Hewitson
Climate System Analysis Group, ENGEO, University of Cape Town, South Africa

Dr Christopher Jack
Climate System Analysis Group, ENGEO, University of Cape Town, South Africa

Dr Christopher Lennard
Climate System Analysis Group, ENGEO, University of Cape Town, South Africa

Funding

I am thankful for funding assistance from the University of Cape Town, the Climate System Analysis Group (CSAG) under the Future Resilience for African CiTies and Lands (FRACTAL) project and the National Research Fund of South Africa for the various support given me throughout this research.

Declaration

I declare that this thesis is my own work and that apart from the normal guidance from my supervisor, I have received no assistance except as acknowledged. I declare that neither the substance nor any part of the above thesis has been submitted in the past, or is being, or is to be submitted for a degree at this University or at any other university.

Chapter two of this manuscript has been published in Journal of Climate. Chapter three has been accepted by Journal of Climate while Chapter 4 is in review in Climate Dynamics. I confirm that this above declaration holds true for all publications, and authorship of my two supervisors represents their assistance with improving style and grammar, and advice in managing the paper through the peer-review process.

Signed by candidate

Kwesi Akumenyi Quagraine

Dedication

To my lovely, adorable daughter, Nana Aba, you bring great joy to the world!!

and

To my Granny who passed away midway into my studies, Your Grandson made it!

Miss you so much!!

Acknowledgements

The past three and a half years have been special for me as I was given the freedom and opportunity to think and to explore the world of science and research. I therefore would like to thank my supervisors, Prof. Bruce Hewitson, Dr. Christopher “CJ” Jack, Dr. Christopher Lennard and Dr. Izidine Pinto for their trust, support, guidance, encouragement and numerous helpful discussions from the beginning to the successful completion of my research. I am particularly grateful to CJ for all the time and energy spent on helping me improve my writing. To all my supervisors, your contributions have really paid off and they are immeasurably immense. Thank you!

I am also grateful to Prof Mark New and Prof. Corinne Le Quere for the opportunity to partake in the University of Cape Town (UCT) - University of East Anglia (UEA) Newton PhD Partnership Program awarded through the African Climate and Development Initiative (ACDI), Tyndall Centre for Climate Change Research, Climatic Research Unit (CRU) and funded by the National Research Foundation (NRF) of South Africa and the Research Councils United Kingdom (RCUK). Also, my sincere gratitude to Dr. Clare Goodess for her support and guidance during my stay at UEA. The interactions and experience gained during my stay helped improve my first paper for the thesis.

I thank all CSAGers for welcoming me when I arrived to undertake my PhD and for keeping me part of the family. Will cherish the friendships I have developed for a long time. I also want to warmly thank Prof. Piotr Wolski for all the great discussions that triggered new ideas and helped shape my thoughts on how to proceed with this research. A warm thanks to Sharon Barnard for being a mother to me and Melanie Rustin-Nefdt for all the assistance and support. Phillip Mukwenha is thanked for providing technical assistance during my research. In the distance, I want to thank Prof. Babatunde Abiodun for the words of encouragement given in the hallways of the EGS building and for motivating me to keep going.

To my office mates and colleagues, Portia, Temi, Rusere, Siya, Nokwe, Tlakale, Jess, Stefaan, Mira, Michel, Sabina, Koketso, Peter and Luleka thanks for the excellent

working environment we shared. I am most grateful for all those interesting conversations along this wonderful journey. Wish you all the best!

I will like to thank my family, especially Maa Baaba and Dada Kofi, Mama Dora and Mama Faustie for all their prayers, support and their unwavering belief in me to complete this work. My siblings TQ and Ato Kwamena for always keeping a smile on my face and constantly asking for updates with my work. To cousin Emmanuel I say thank you for all the support, encouragement and motivation.

To my loving, caring, beautiful wife, Esi, thank you for the encouragement, patience and support, and for sharing in the ups and downs of my PhD journey, long after the many expected completion dates. My deepest gratitude to you for being there in the good and the bad and for always reminding me of the important things in life. Love you to bits Bebey!

Contents

List of Figures

List of Tables

Acronyms

Notation	Description
AAO	Antarctic Oscillation
ARR	All-year Rainfall Region
CHIRPS	Climate Hazards Infrared Precipitation with Stations
CM	Co-behavior Mode
CMIP5	Coupled Model Intercomparison Project Phase 5
CRU	Climatic Research Unit
ENSO	El Niño-Southern Oscillation
GCM	Global Climate Model
ITCZ	Intertropical Convergence Zone
PCA	Principal Component Analysis
SOM	Self-Organizing Map
SRR	Summer Rainfall Region
TRBI	Tropical Rain Belt Index
TTT	Tropical Temperate Trough
WRR	Winter Rainfall Region

Chapter 1

1 Introduction

Regional climate variability over southern Africa is partly driven by a number of large-scale climate processes, such as El Niño-Southern Oscillation (ENSO) and Inter-tropical Convergence Zone (ITCZ). These large-scale processes do not operate in isolation but interact with each other, and the regional response to these interactions largely conditions the resulting regional climate variability and extreme climate events (Mason and Jury 1997; Muñoz et al. 2015; Stocker et al. 2013). The majority of regional climate variability studies focus on individual large-scale drivers (e.g. Reason and Jagadheesha 2005; Pohl et al. 2010; Suzuki 2011) or, if multiple drivers are considered, they are considered as independent rather than interacting drivers (e.g. James et al. 2015; Pinto et al. 2018). Relatively few studies have examined the interaction of these large-scale processes in a regional context (e.g. Fauchereau et al. 2009; Pascale et al. 2019; Hoell et al. 2017a; Hart et al. 2018; Pohl et al. 2018; Meehl et al. 2001; Pohl et al. 2010), and their potential changes in a warming climate. For instance, Pohl et al. (2010) examined the possible relationship between Antarctic Oscillation (AAO), the Madden-Julian Oscillation (MJO) and ENSO and its consequence for rainfall. The study found that MJO does not influence AAO fluctuations on the inter-annual timescale but rather a strong teleconnection with ENSO is found during peak austral summer season. Similarly, to develop an understanding of large-scale interactions, Hart et al. (2018) investigated the impact of ENSO on the likelihood of the formation of tropical-extratropical cloud bands in the South Indian Convergence Zone (SICZ) and found that during La Niña events, there is an increased likelihood of more cloud bands developing than during El Niño events. The Indian Ocean Dipole has also been found to either disrupt or enhance southern African precipitation response to ENSO events (Hoell et al. 2017).

The ability to unpack these interactions has the potential to provide new insights to improve our understanding of regional climate variability and change, climate model representation of regional climate variability, and potential future regional climate

shifts. It may provide a better understanding into the nature of these interactions while identifying their influence on surface expressions (e.g. precipitation and temperature) especially for regions with no individual large-scale driver of the regional climate, such as southern Africa (see Garreaud et al. 2008; Tyson and Preston-Whyte 2000). The region has been widely recognized as one of the most vulnerable regions to climate variability and change (Niang et al. 2014) as shown by the past occurrence and projected increase in droughts (Abiodun et al. 2018) and extreme precipitation events (Pinto et al. 2016). This dissertation assesses how interactions among large-scale processes are influencing the regional climate over southern Africa. Hereafter, these interactions between two or more large-scale climate processes that individually influence the climate variability in a region is defined as co-behaviour. Thus, the core of the dissertation is:

Investigating the co-behaviour of synoptic to global scale climate processes as a driver of regional climate variability and change over southern Africa.

The concept of co-behaviour is not trivial as it involves addressing the complexity of the non-linearity of the climate system; this implies that the interactions between climate processes may not be merely linear (e.g. Qian et al. 2010; Moron et al. 2015). Co-behavior explicitly recognises that interactions between climate processes are unlikely to be simply linear combinations both with respect to regional circulation responses as well as precipitation and temperature. For example, we cannot assume that the regional rainfall response to the combined and potentially co-behaving ENSO and ITCZ variability in southern Africa is simply a linear combination of the response to each driver individually.

To handle this complexity appropriate methods that can accommodate non-linearity are required. For instance, neural network techniques such as the Self-Organizing Maps (SOM; Kohonen 1982, 2001) are useful in relating synoptic circulation types to surface expressions through non-linear mapping of synoptic states to variability in surface variables. The SOM approach has been effectively and efficiently used in classifying synoptic circulation patterns over many regions in climate science (see Hewitson and Crane 2002; Rousi et al. 2015; Wolski et al. 2017). Likewise, when identifying underlying structures in datasets, principal component analysis (PCA) has

been extensively used and proved valuable (see Lever et al. 2017). Finally, composite mapping of surface responses to different modes of co-behaviour accommodates non-linear surface responses. The power of these methods does not only lie in their individual ability but also how their combination can be useful in tackling the complexity, possible non-linearity and cross timescale challenge of co-behaviour. Hence in this dissertation, a combination of these methods is employed to tackle the core objective of the dissertation.

1.1 Aims and Objectives

The aim of this study is to develop a methodology to examine the co-behaviour of large-scale processes as a driver of regional climate variability over southern Africa and to apply this to the evaluation of Global Climate Models (GCM). Underlying this aim are the following research questions:

1. *What is the co-behaviour of key climate processes and how do we assess the impact over southern Africa? and*
2. *How well do climate models capture co-behaviour as identified in reanalysis datasets?*
3. *What are the possible mechanisms responsible for how the models are representing co-behaviour?*

The immediate section that follows from here provides an exposition on the southern African climate as this is not covered extensively in the embedded publications. The subsections that follow describe in detail key processes that govern the southern African climate. This is by no means an exhaustive list of processes as we only examine those relevant to this research. The subsequent section addresses the thesis overview.

1.2 An overview of the climate of southern Africa

The region of southern Africa considered here is bounded to the north by latitude 10°S, and the south by 35°S, to the west by 5°E and the east by 45°E (as shown in Figure 1.1). Climatic conditions vary over the region; typically the south-western part of the region experiences Mediterranean conditions, the north and east parts experience humid subtropical conditions while the west experiences predominantly arid conditions (Daron 2014).

The southern African climate and its variability is moderated by the complex interactions between atmospheric and oceanic processes over several spatial and temporal scales (Tyson 1986; Buckle 1996a; Tyson and Preston-Whyte 2000; Chase and Meadows 2007). The climate is primarily governed by the adjacent relatively warm Indian and cool Atlantic Oceans, the location of the atmospheric high and low pressure systems, Angola low, Tropical Temperate Troughs (TTTs) and the migration of the ITCZ. For instance, the ITCZ conditions precipitation over the region (Nicholson 2000), while heavy rainfall events are commonly associated with TTTs (e.g. Hart et al. 2010; Nicholson 2000; Ratna et al. 2014; Suzuki 2011). Also, global teleconnections resulting from the effects of ENSO and Antarctic Oscillation (AAO) are known to modulate the regional climate of southern Africa. For example, the ENSO teleconnection affects regional rainfall variability as the region experiences dryer (wetter) than normal rainfall conditions under El Niño (La Niña) events (e.g. Meque and Abiodun 2015). Dieppois et al. (2019) found that ENSO is linked to southern African rainfall variability at three (interannual, quasi-decadal and interdecadal) timescales. The Antarctic Oscillation (AAO) teleconnection is generally responsible for precipitation over the south-western coast of South Africa during winter (e.g. Reason and Rouault 2005).

As described in Chapter 2, three climate processes and feature that govern the southern African climate are used in this research, namely the ENSO, AAO and ITCZ which have been shown to be important to the southern African climate (e.g. Klutse et al. 2016; Meque and Abiodun 2015; Reason and Rouault 2005; Weldon and Reason 2014; Suzuki 2011). The ITCZ is a feature of the regional climate of southern Africa. Together these processes and feature are understood and described in literature (e.g.

Nicholson, 2000; Philippon et al. 2012; Reason and Rouault, 2005) and have established indices for describing their variability. Their roles are described into detail in the next subsection.

Generally, most parts of the region (Figure 1.1) predominantly receives rainfall in summer (December-January-February) with the exception of the relatively small areas along the south-eastern and south-western coast of South Africa that receives rainfall throughout the year and during winter (June-July-August) (D'Abreton and Lindesay 1993; Taljaard 1996; Tyson et al. 2002). These regions are therefore known as the summer rainfall region (SRR), all-year rainfall region (ARR) and winter rainfall region (WRR) as shown in Figure 1.1.

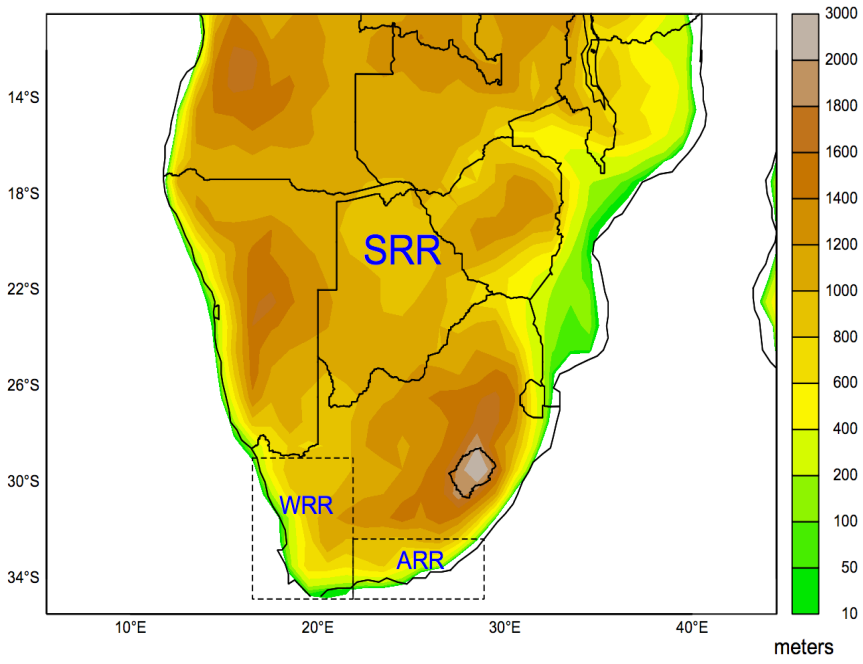

Figure 1.1: A map of southern African domain showing topography and the rainfall regions; SRR=summer rainfall region, WRR=winter rainfall region, ARR=all-year rainfall region

1.2.1 Roles of key large-scale processes modulating southern African climate

1.2.1.1 Inter-Tropical Convergence Zone (ITCZ)

The ITCZ also referred to as the tropical rain belt is a cloud band region of intense convective precipitation formed as a result of the convergence of south-easterly and north-easterly trade winds (dotted lines in figure 1.2). Rains associated with the ITCZ are as a result of local thermal instability and the rains are enhanced by the low-level wind convergence within the zone (Nicholson 2018). Its position controls the intensity and timing of moisture flow while it migrates over the African continent from south to north (shown in figure 1.2) following the apparent path of the sun (Nicholson 2000; Klutse et al. 2016; Suzuki 2011). The ITCZ stays largely parallel to the equator and is located in the Southern Hemisphere during austral summer whereas in austral winter, it is located in the Northern Hemisphere (Reason et al. 2006). Southern Africa generally experiences wet conditions when the ITCZ migrates southward of the equator (Figure 1.2a).

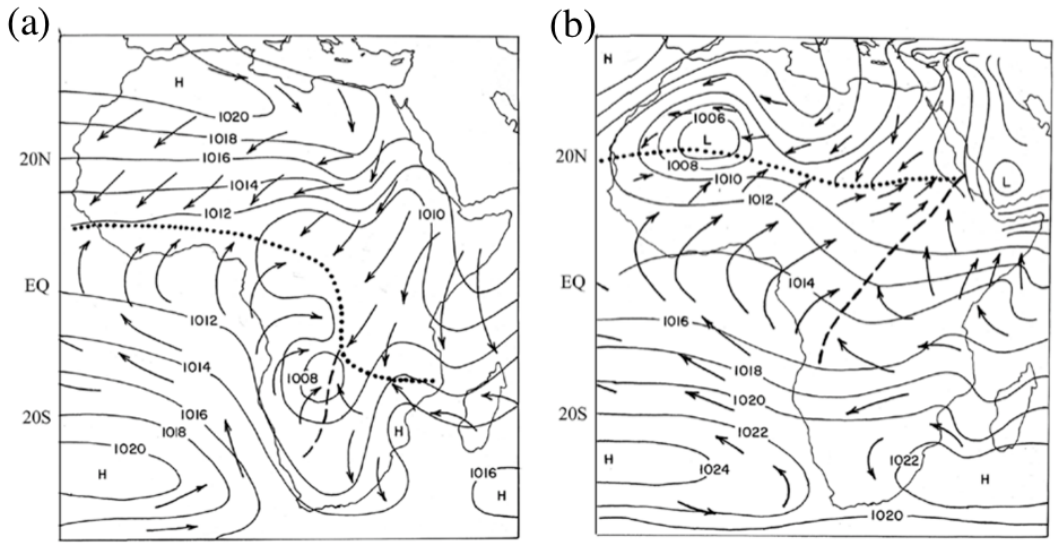

Figure 1.2: General circulation features over Africa using mean pressure and wind fields for (a) austral summer and (b) austral winter with ITCZ as a dotted line. Source: Nicholson (2011).

The migration of the ITCZ southwards (figure 1.2(a)) is due to the increase in tropical east Atlantic sea surface temperatures (SSTs) between August and November. This

condition induces a strong convection over the Congo basin and northern Angola thereby bringing moisture on to the sub-continent (Reason et al. 2006; Nicholson 2011). However, during the austral winter, convective systems are inhibited and rather a strong high pressure system persists over the region. At the higher latitudes, sometimes, mid-latitude low-pressure systems interferes with the existing high pressure thereby bringing some cooling over the region during winter (Nicholson 2011).

1.2.1.2 El Niño-Southern Oscillation (ENSO)

ENSO is a global phenomenon that modulates rainfall in many regions of the world (Ropelewski and Halpert 1987; Nicholson 2011). Although the phenomenon was initially understood to be a localised meteorological event which brought intense rains to coastal areas of Peru, it is now understood to be a global phenomenon (Figure 1.3) with impacts in most parts of the world (see Fogt et al. 2006; Nicholson 2011; Philippon et al. 2012). The phenomenon which is associated with SST changes in the Pacific Ocean has been well documented to impact the regional climate of southern Africa. Particularly, rainfall variability and increasing temperatures have been attributed in part to ENSO (Camberlin et al. 2001; Meque and Abiodun 2015). Southern Africa experiences dryer than normal conditions when ENSO is in the warm phase (El Niño) whereas conditions in the region is wetter than normal when in the cold phase (La-Niña). However, there exist a non-linear relationship between the magnitude of rainfall impacts during ENSO over southern Africa and the strength of the ENSO event. A typical example is the 1997/98 El Niño event that did not lead to the expected severe drought over the southern African sub-region, although the event was recorded as one of the strongest of the last century (see Reason 2017). Typically, coastal (west to east) areas of southern Africa are known to experience positive rainfall anomalies with negative rainfall anomalies across the majority of the region during El Niño events while the reverse is true for La-Niña (Cook 2000; Daron et al. 2019). Earlier studies by Todd and Washington (1999) and Washington and Todd (1999) identified a northwest-southeast (NW-SE) dipole structure associated with TTTs. Consequently a later study by Fauchereau et al. (2009) also identified the existence of a NW-SE dipole pattern in rainfall anomalies during ENSO events and went on to show that positive outgoing longwave radiation (OLR) anomalies suggests less cloud cover leading to

reduced precipitation. However, due to the different climate regimes present in the region (mainly attributed to orographic differences) the effects of the phenomenon varies across the region. According to Boulard et al. (2013) some of the mechanisms behind southern Africa's response to rainfall under ENSO conditions are not fully understood. Cook (2000) in an attempt to understand these mechanisms has attributed the modulation of the amplitude of rainfall response to large-scale atmospheric response of Rossby waves while the study of Misra (2003) suggests spatial distribution of rainfall anomalies is SST dependent. Nicholson (2003) further clarified the latter relationship by suggesting rainfall is reduced across the region during El Niño events which causes an unusually high SST in the surrounding oceans of southern Africa.

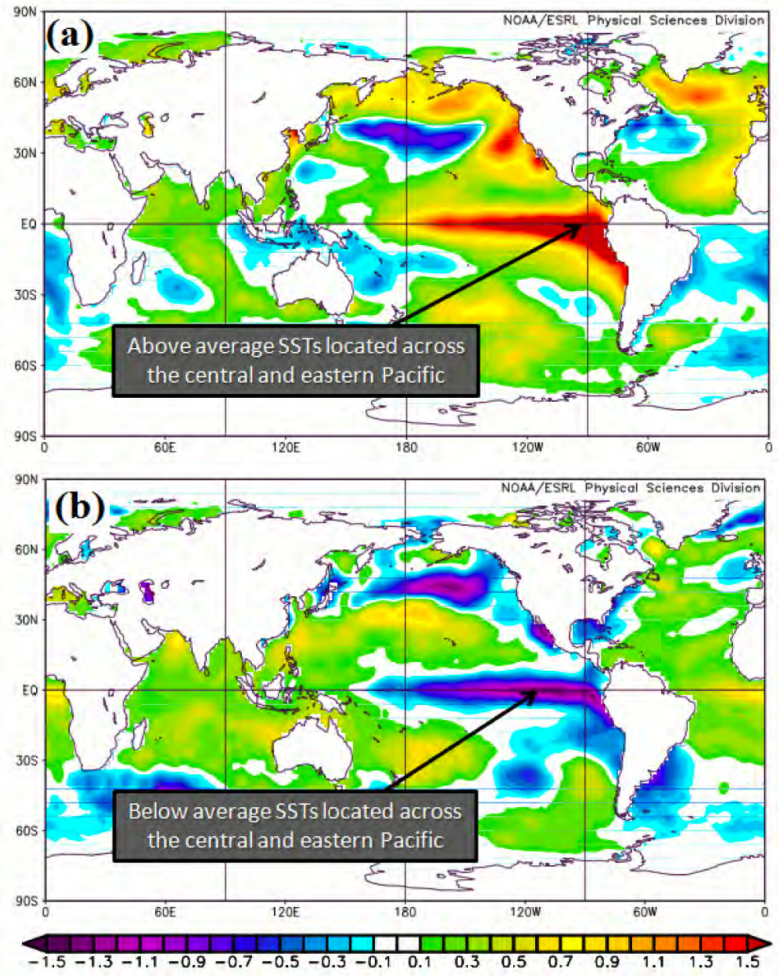

Figure 1.3: Global SST anomaly maps for (a) El Niño (positive phase ENSO) and (b) La-Nina (negative phase ENSO). Source: https://climate.ncsu.edu/climate/patterns/enso

1.2.1.3 Antarctic Oscillation (AAO)

The Antarctic Oscillation (AAO) is the leading mode of variability south of 20°S (poleward) and is characterised by variations in atmospheric pressure between the Antarctic region and the southern mid-latitudes (Thompson and Wallace 2000a; Pohl et al. 2010). The AAO is a hemispheric phenomenon typically associated with the Southern Hemisphere. The modes of variability are generally represented with an index which is computed usually by finding the leading empirical orthogonal function (EOF) mode of the 700/850 hPa geopotential height south of 20°S (Mo 2000). Another approach for computing the index uses the normalised difference of the zonal sea level pressure between the Antarctic and the mid-latitude (Reason and Rouault 2005).

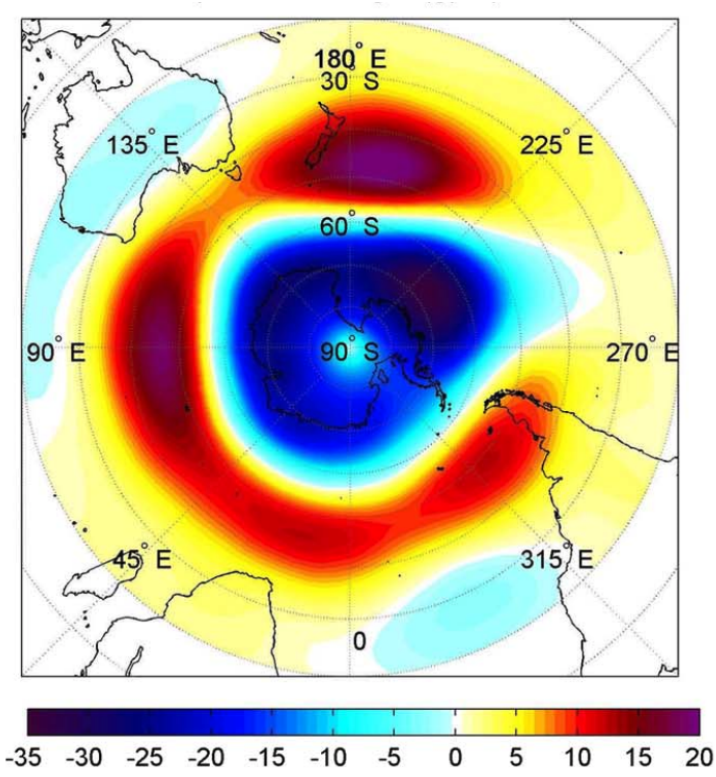

Figure 1.4: Spatial pattern of the leading EOF mode accounting for 26.8% of the total variance for 700 hPa geopotential height anomalies using Climate Forecast System Reanalysis (CSFR) dataset. Source: Stopa, Justin and Cheung (2014).

The phenomenon is an essential feature of the region as it has been found to influence winter rainfall in southwestern part of South Africa as a result of shifts in the subtropical jet and changes in the low-level moisture flux over the South Atlantic (Reason and Rouault 2005).

1.3 Thesis Overview

This dissertation is structured in three core parts where each part is a journal article. Chapters 2 and 3 are already published, Chapter 4 is submitted for publication. Each includes an introduction section where relevant literature is discussed. For readability and coherence, when results in previous parts are mentioned, they will be cited according to the journal article reference.

Although each part is individually written, they are linked to address the broader scope of the dissertation research of understanding the dynamics of the co-behaviour of climate processes that govern the regional climate variability of southern Africa.

The first article (Chapter 2) addresses objective one, where the term co-behaviour is defined and a methodology is developed to evaluate response to co-behaviour. The article also identifies the various modes of co-behaviour and their respective influence on southern African climate. This directly feeds into tackling objective two where the second article (Chapter 3) assesses how Global Climate Models (GCMs) are representing co-behaviour modes identified in article one using eight GCMs from the Coupled Model Intercomparison Project Phase 5 (CMIP5; Taylor et al. 2012). The third and final objective is addressed in article three (Chapter 4) which describes a process-based model evaluation of co-behaviour. In this article, the underlying mechanisms that are responsible for how the different GCMs capture co-behaviour is explored. Findings are synthesized in Chapter 5.

As a means of guiding the reader through the dissertation, each part commences by reiterating these overarching questions with specific questions answered in the article.

1.4 Synopsis

The motivation for this study is to formulate and test a methodology to investigate the combined roles of large-scale processes (co-behaviour) over southern Africa. Co-behaviour is particularly important as the regional climate is governed by an interaction between multiple processes and thus understanding the nature of these interactions may provide useful insights on what drives regional climate variability and change. The thesis is built on three academic journal articles that seek to elucidate understanding on co-behaviour through the answering of scientific questions pertaining to interactions amongst large-scale processes.

In Chapter 2 (first article), three key large-scale processes, namely the ITCZ, ENSO and AAO, that are essential to the regional climate of southern Africa through their individually established influences on regional precipitation and temperature are considered for the formulation and testing of the methodology. These processes are understood in literature and their variability is easily described by means of a climate index hence making it convenient for the study. By means of a combination of methods (e.g. SOMs and PCA), the approach examines precipitation and temperature response to co-behaviour over the southern African region. The SOM is used to characterise circulation patterns over the region, while the PCA is applied to explore relationships between regional climate variability and the key climate processes selected for the study. More details of these methods are found in Chapter 2. The study identifies eight co-behaviour modes with varying consequences on the climate of southern Africa. The influence of these modes on regional precipitation and temperature is then explored using observation and reanalysis datasets. This chapter directly addresses the first objective of this thesis.

With co-behaviour defined and the methodology developed, the responses over southern Africa are explored in Chapter 2, while the subsequent chapter (second article) uses the methodology to evaluate how eight GCMs from CMIP5 are representing identified co-behaviour modes from the reanalysis and observation datasets. Although the methodology is modified to cater for the complexity that the new analysis provides, the modification allows for comparison of SOM node frequencies across the GCMs while providing comparable inputs to the PCA analysis.

The responses for regional precipitation and temperature across the GCMs under different co-behaviour modes is then established.

Chapter 4 (final article) assess how the key large-scale processes: ITCZ, ENSO and AAO are being captured within the eight GCMs from CMIP5 whose precipitation and temperature responses were determined in the preceding chapter. This chapter addresses the third objective of the thesis through the comparison of model representations of the large-scale processes to that of the observed. This is done to ascertain the sources of variability in their depiction of co-behaviour influence on regional precipitation and temperature. It is expected that some models will capture some processes better than others, and this will feed directly into how they represent co-behaviour.

Finally, Chapter 5 synthesizes the findings of the thesis by drawing on the three articles of the thesis. This chapter establishes the importance of this thesis to the broader understanding of the regional climate variability and change over southern Africa.

Chapter 2

A Methodological Approach to Assess the Co-Behavior of Climate Processes over Southern Africa

What is co-behaviour of climate processes and how do we assess its impact over southern Africa?

Specific Questions?

- How do we define the concept of co-behaviour?
- Can a generalised methodology be developed?
- How has it influenced observed regional precipitation and temperature?

Abstract

The study develops an approach to assess co-behaviour of climate processes. The regional response of precipitation and temperature patterns over southern Africa to the combined roles (co-behaviour) of El Niño-Southern Oscillation (ENSO), Antarctic Oscillation (AAO) and Inter-Tropical Convergence Zone (ITCZ) is evaluated. Self-Organizing Maps (SOMs) classify circulation patterns over the subcontinent and Principal Component Analysis (PCA) is used to identify related patterns across the data. The Tropical Rain Belt Index (TRBI), a measure of the ITCZ, is generally in phase with the AAO but mostly out of phase with ENSO. The phases of AAO may enhance or suppress ENSO impact on the location and distribution of regional precipitation and temperature over the region. This understanding of the co-behaviour of large-scale processes is important to assess the impact these processes collectively have on precipitation and temperature, especially under future climate forcings.

A paper based on this part has been published in the Journal of Climate:

"A Methodological Approach to Assess the Co-Behavior of Climate Processes over Southern Africa"

https://doi.org/10.1175/JCLI-D-18-0689.1

***K. A. Quagraine**, B. Hewitson, C. Jack, I. Pinto and C. Lennard*

2 Introduction

A regional climate is typically conditioned by a number of climate processes operating on multiple spatial and temporal scales. Evaluating the regional response to the collective co-behaviour of these processes is thus central to understanding a region's climate variability. Most especially for southern Africa, where there is no dominant large-scale driver of the regional climate, this is important. The regional climate variability of southern Africa is influenced by multiple processes such as the migration of the tropical rainfall belt (also referred to as Inter-Tropical Convergence Zone, ITCZ), which influences the intensity and timing of rainfall through the seasons (Nicholson 2000; Suzuki 2011), and the El Niño-Southern Oscillation, ENSO, which influences the timing and spatial distribution of rainfall (Dieppois et al. 2015; Meque and Abiodun 2015). Additionally, there are also relevant small-scale processes that modulate the impact of such large-scale processes. An example is the effect of mountain winds and convection on rainfall (Houze 2012). Variability of these large-scale processes, and their interactions across spatial and temporal scales ranging from global and decadal through to regional and sub-daily leads to regional climate variability and extreme events (Frei et al. 2006; IPCC 2012; Mason and Jury 1997; Meehl and Tebaldi 2004; Nicholson 2000; Stocker et al. 2013).

Earlier studies have dealt with how individual processes influence regional climate variability and change (see Hope et al. 2006; Hoell et al. 2017; Manatsa et al. 2017; Pohl et al. 2010; Suzuki 2011; Sheridan and Lee 2012). However, there arises a challenge when we want to examine the combined influence of these processes on regional climate. Investigating the combined influence of large-scale processes on the regional climate becomes increasingly complex due to the non-linearity of the climate system which then implies the combined impact of individual climate processes are not merely their linear combinations. For example, recent studies have focused on the relevance of the impact of cross-time scale interactions of multiple climate drivers on improving the predictive skills of extreme rainfall (Muñoz et al. 2015), establishing a framework for considering the influence of cross-time scale interactions in establishing weather types using coupled circulation models (Muñoz et al. 2017) and exploring the predictability of weather type variability over Maritime Continent using k-means clustering algorithm (Moron et al. 2015).

The concept of co-behaviour in this study is defined as an interaction between two or more large-scale climate processes that have an influence on regional weather and climate. Hence our ability to develop methodologies to address collective co-behaviour of important climate processes will aid in understanding the nature of these interactions and will improve robustness of seasonal and inter-annual predictions to accurately present the regional information and consequently address regional climate change.

The aim of the present study is to develop a methodology to examine co-behaviour through identifying and examining its influence on precipitation and temperature. However, examining the dynamics of the process driving the rainfall and temperature responses are not the main focus of this study. The next subsection provides a brief review of the southern African climate while identifying the influence of important large-scale processes on the regional climate. Section 2 explains the data and methods adopted for the study. The results are presented and discussed in Section 3 with summary and conclusion in Section 4.

2.1 Processes affecting southern African climate

The processes affecting the climate of southern Africa has been well documented (see Buckle 1996b; Chase and Meadows 2007; Tyson and Preston-Whyte 2000) and we describe some of the main processes below to provide a context for the paper. Southern Africa, defined here as region bounded to the north by latitude 10°S, to the south by 35°S, to the west by 5°E and the east by 45°E consists primarily of arid or semi-arid climatic regions (Figure 2.1). The domain was selected in order to include relevant atmospheric climate processes occurring immediately around the sub-continent such as the subtropical high pressure systems and mid-latitude wave systems. Most parts of the region is known to experience summer rainfall while the south-western coast and eastern coast of South Africa experiences winter and all-year rainfall and are together shown in Figure 2.1 as regions; summer rainfall region (hereafter SRR), winter rainfall region (hereafter WRR) and all-year rainfall region (hereafter ARR) respectively. These regions exist as a result of four vital synoptic features; namely a the presence of a semi-permanent high pressure system inland,

baroclinic disturbances in the mid-latitudes leading to Rossby waves over the south-western and southern parts of the region, a barotropic, quasi-stationary sub-tropical easterly wave low-pressure over the interior linking up with mid-latitude westerlies and ridging highs eastwards from south Atlantic to the south Indian Oceans (see Hart et al. 2010; Lennard and Hegerl 2014; Shulze and Maharaj 2007; Taljaard 1996).

Atmospheric controls of regional climate variability in the region includes regional processes such as the Tropical Temperate Troughs (TTT) and the tropical rainfall belt migration which have been identified as important drivers of precipitation over the subcontinent. The former has been known to contribute substantially to heavy precipitation in summer over the region (Hart et al. 2010; Lennard et al. 2013; Macron et al. 2014; Ratna et al. 2014) while the position of the latter controls the intensity, and timing of moisture flow across the African continent (Nicholson 2000; Suzuki 2011).

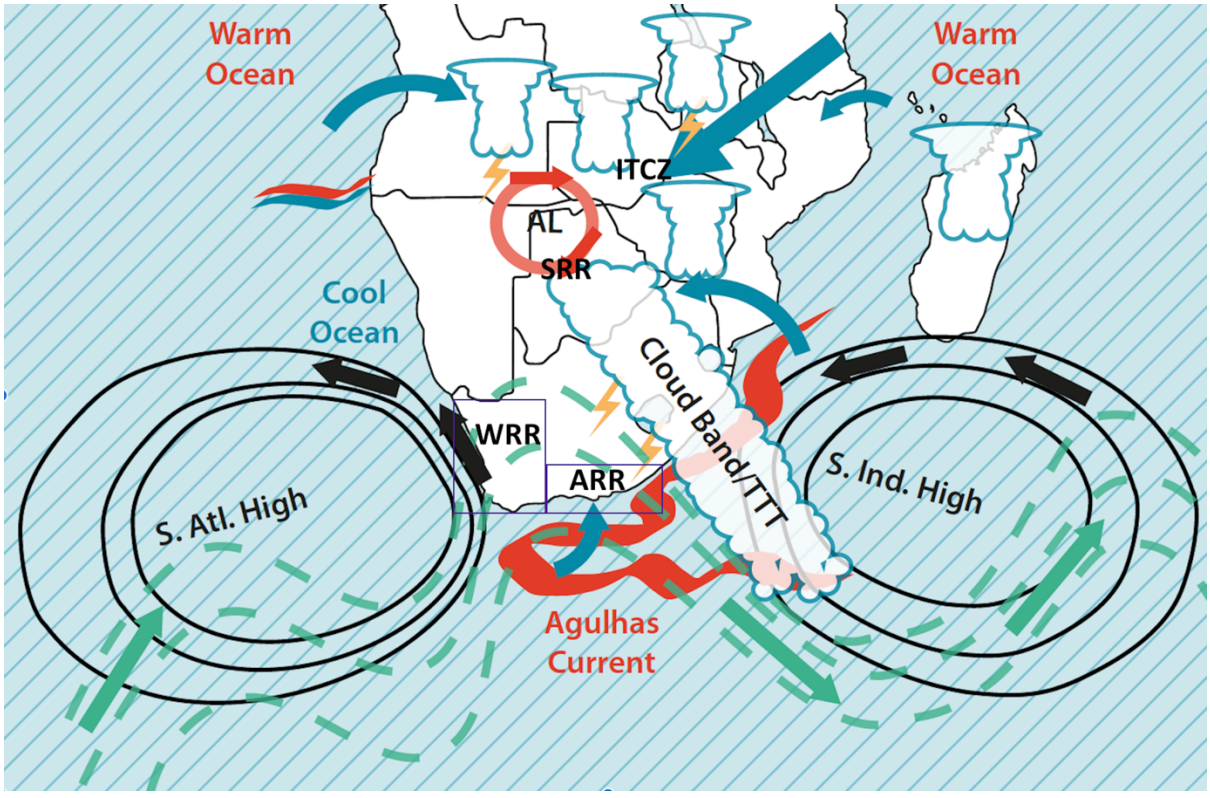

Figure 2.1: A schematic detailing key processes over southern Africa. AL = Angola low, ITCZ = intertropical convergence zone, and TTT = tropical temperate trough. Also shown here are three climatic regions: summer rainfall region (SRR), winter rainfall region (WRR), and all-year rainfall region (ARR) (modified from Hart et al. 2016).

Westerly waves bring cold fronts from the South Atlantic Ocean to the western and southern parts of the country during winter (Makarau and Jury 1997; Tyson and Preston-Whyte 2000). Additionally, the South Atlantic and South Indian high pressure systems advect dry air and warm moist air respectively to the western and eastern parts of the country and potentially controls the latitudinal movement of mid-latitude westerly waves poleward or equatorward (DeBlander and Shaman 2017).

Teleconnection processes also influence southern African rainfall variability, e.g. ENSO teleconnection (Camberlin et al. 2001; Engelbrecht et al. 2013; Fauchereau et al. 2003; Hulme et al. 2001; Jury and Freiman 2002; Lennard et al. 2013; Meque and Abiodun 2015). The region generally experiences dryer (wetter) than normal austral summer rainfall conditions when the phenomenon is in the El Niño (La Niña) phase, however the regional response to ENSO is varied both spatially, and under different ENSO events. There have been a number of notable exceptions where strong El Niño has occurred with little or no regional rainfall response (see Lyon and Mason 2007). Another teleconnective feature is the Antarctic Oscillation (AAO), which is known to affect variability in mid-latitude circulations that have direct influence on precipitation and temperature over the region (Hart et al. 2010; Lennard and Hegerl 2014; Mason and Jury 1997) such as in the south-western coast of South Africa during the winter season (Fogt et al. 2006; Pohl et al. 2010; Reason and Rouault 2005; Weldon and Reason 2014a).

In our study of co-behaviour, we analyse three of the important processes that govern the southern African regional climate, ENSO, AAO and intensity of ITCZ. It is worth mentioning that other processes could have equally been used, but for the purposes of exploring the methodology we focus on processes that are well known and described in literature and have relatively convenient established indices describing their variability.

2.2 Data and Methods

2.2.1 Data

For the classification of circulation patterns over southern Africa domain we used geopotential height data at 700-hPa from the European Centre for Medium-Range Weather Forecasts (ECMWF) ERA-interim reanalysis data (Dee et al. 2011) with a grid resolution of 0.75^0 for the period 1980-2013. The 700-hPa level is chosen over other levels because it effectively captures both tropical and mid-latitude synoptic weather systems, such as easterly waves, westerly waves, subtropical high pressures, and continental low pressures over the region (e.g. Bartman et al. 2003).

We use three indices that describe and analyse the state and changes in ENSO, AAO and ITCZ intensity. For ENSO, we use the Multivariate ENSO Index (Wolter and Timlin 1993, 1998) which accounts for changes in both atmospheric and oceanic fields and best describes the coupled nature of the phenomenon. We also use AAO index constructed by projecting the daily 700-hPa height anomalies poleward of 20°S onto the leading pattern of the AAO (see Thompson and Wallace 2000b). This index was obtained from KNMI Climate Explorer (ftp.cpc.ncep. noaa.gov/cwlinks). The intensity of the ITCZ is characterised using the Tropical Rain Belt Index, TRBI, which is an index based on methodology used by Nikulin et al. (2012) and Nikulin and Hewitson, (2019). The reader is referred to Nikulin and Hewitson (2019) for further reading. A positive TRBI is associated with higher rainfall intensities within the tropical rain belt.

We further analyse the co-behaviour of these indices on surface temperature and rainfall variability in the region. We use temperature data from Climate Research Unit, CRU-TS v4.01 (Harris et al. 2014) and precipitation data from Climate Hazards Group Infra-Red Precipitation with Station, CHIRPS (Funk et al. 2015) which is known to give a good representation of the rainfall regimes across the region (Dunning et al. 2016).

2.2.2 Methods

The study uses self-organising maps (Kohonen 2001) to characterise regional circulation variability, and Principal Component Analysis (PCA) (see Abdi and Williams 2010; Jolliffe 2002; Wilson et al. 1992) to explore co-behaviour of climate processes and regional circulation variability. Figure 2.2 shows a schematic diagram of the phases of methods employed in this study.

We use the SOM to produce 12 characteristic 700-hPa anomaly fields circulation patterns over the study period 1981-2013 (see below for more detail on the SOM technique). Daily 700-hPa anomaly fields are used to train a 12 node SOM, after which each day in the study period is mapped to one of the 12 circulation patterns. From this, a 3-month frequency of occurrence of each synoptic type are determined. The 3-month frequencies (using a centered moving average 3-month window) is used to construct a monthly time series matrix of each synoptic type's frequencies. The moving average window serves as a low pass filter to eliminate short-term trends and highlight longer-term trends.

This matrix is augmented with additional columns for climate indices for ENSO, AAO and TRBI. PCA is then used to identify the dominant modes of independent variability within the augmented matrix. Using the N-Rule test (Peres-Neto et al. 2005), which is based on randomization and assessment of significance at 90% confidence level, 3 Principal Components (PCs) were retained for the analysis. This allows for an exploration of the frequency of occurrence of synoptic types in relation to the co-behaviour of the conditioning large-scale drivers represented by the indices. The PCA loadings indicate the relation between the frequency of occurrence of synoptic types and the conditioning by the three large-scale processes.

In order to investigate the regional precipitation and temperature response under different combined teleconnection and circulation states, 3-month periods are identified where the score of each of the 3 retained PCs identified by the PCA exceeds plus or minus one standard deviation in different combinations (details below). Plus or minus one standard deviation is selected as a threshold for considering each PC to be a "strong" driver of the regional climate. As each PC relates to the indices of large-

scale processes, this assists in evaluating the co-behaviour role in conditioning the regional climate response on seasonal time scales. Precipitation and temperature anomalies are then calculated for each of the sub-periods for each grid cell using the CHIRPS and CRU-TS v4.01 datasets. Standard bootstrapping with replacement (details below) is used to determine the standard error of this anomaly and anomalies that exceeded the 90th percentile of the error estimate are deemed statistically significant.

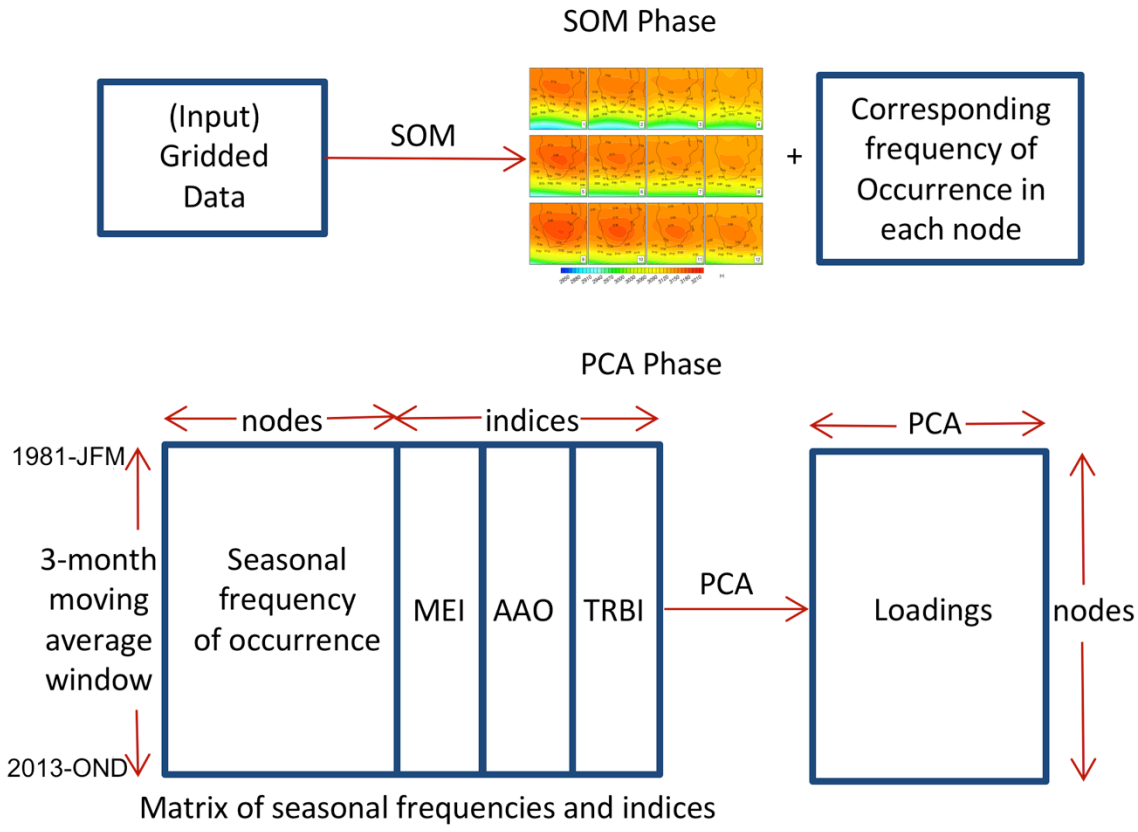

Figure 2.2: A schematic diagram of the implementation of the SOM and PCA.

i. Self-Organizing Map (SOM)

The SOM is a form of artificial neural network (Kohonen 1982, 2001) and may be thought of as a topologically sensitive clustering technique that has been used in studying synoptic climatology (Hewitson and Crane 2002; Lee 2017; Richardson et al. 2003; Sheridan and Lee 2012). The method aids in objectively classifying archetypal circulation patterns (nodes) over a region and quantifying the frequency of occurrence

of each node. The strongest attribute of SOM is that it preserves relationships between weather states by maintaining the data as a continuum while presenting both the basic and transitional patterns as an array making classified patterns readily understood and visualised, which is a challenge in other methods (Rousi et al. 2015). For a more detailed explanation of the workings of SOM, the reader should see (Lennard and Hegerl 2014). The SOM is randomly initialised with different SOM node sizes while being trained with the daily 700-hPa geopotential height anomalies of ERA Interim data and after testing the different sizes for the SOM, a 12-node SOM size was selected as it was found to adequately represent the generalized synoptic circulation patterns over the region. Other studies (Mackellar et al. 2010; Tadross et al. 2005) have also successfully used a 12-node SOM to also determine circulation patterns for the region. The SOM produced 12 archetypal 700-hPa patterns and each day in the training dataset is then mapped to one of these nodes thereby generating corresponding frequency mappings for each node. These nodal mappings are then grouped seasonally to aid in understanding the seasonal variability of the 700-hPa field.

ii. Rotated Principal Component Analysis (PCA)

Principal Component Analysis (PCA) is a multivariate statistical technique used in identifying the dominant phases of variance within data that consists of several generally related variables. PCA is used as it reduces the dimensionality of large datasets while maintaining its interpretability and preserving information (Abdi and Williams 2010; Jolliffe 2002; Jolliffe and Cadima 2016; Wilson et al. 1992). PCA aids in revealing the hidden structure of a dataset (Shlens, 2005) by computing new variables called Principal Components (usually containing coefficients of correlation or loadings) obtained as linear combinations of the original variables. The principal component axis may be rotated to facilitate the interpretation of the components by maximizing the variance of the rotated squared loadings.

In this study, PCA is used to examine the interrelations that may exist amongst climate processes and the circulation patterns identified through the SOM by reducing the dimensions of the data into its simplest form to establish the relationship with minimal

change in fundamental structure of data (see Abdi and Williams 2010). The N-Rule test is used to determine the number of components to retain in the PCA (Peres-Neto et al. 2005). The Psych package from R programming software is used here. This package uses eigenvalue decomposition and returns the loadings for components of a correlation matrix. Component loadings are produced by rescaling the eigenvectors by finding the square root of the eigenvalues. The principal components are varimax rotated[1].

iii. Evaluating regional precipitation and temperature response, and assessing significance

In assessing the significant differences in average regional precipitation and temperature from the long term average (anomalies), we use a bootstrapping approach. The approach, which is a resampling method, assumes the unknown cumulative distribution function of a sample (in this instance; precipitation and temperature series) can be estimated reasonably by the empirical cumulative distribution function (see Efron and Tibshirani 1994). This normally highlights the fact that the empirical density function approximates the population density function (Xu 2006).

On the above premise, we bootstrapped with replacement the precipitation and temperature anomalies during the months/seasons whose PC scores exceed the preselected threshold. We then constructed 10,000 randomised composites from the anomalies and a statistical significance for each grid cell determined from the resampled distribution. Anomalies greater than 90th percentile or lower than 10th percentile of the resample distribution was calculated and deemed significant (Brown 2017). These are then used to characterise precipitation and temperature uncertainty in obtained results.

[1] Varimax rotation is applied to the retained principal components. Rotation can considerably simplify interpretation (see Jolliffe and Cadema, 2016).

2.3 Results and Discussion

2.3.1 SOM Mapping of Geopotential Height at 700 hPa

The circulation patterns of geopotential height at 700-hPa are shown in Figure 2.3. To the leftmost part of the SOM, (that is, nodes 1-2-5-9), we identify passing mid-latitude frontal systems that cause rains over the south-western parts of South Africa during winter (wet winter states). However, under these same conditions, the strong high pressure (also known as the Kalahari High) of the interior suppresses convection and typically results in dry conditions (dry summer) (Tyson and Preston-Whyte 2000). The circulation in the rightmost part of the SOM (nodes 4-8-12), represent disturbances in the easterly flow caused by interactions between the Inter-tropical convergence zone (ITCZ) and the warm, humid easterly wave, forces the semi-permanent subtropical high to migrate south due to continental heating. These conditions allow warm air masses to converge humid air over the interior leading to rainfall in the region during summer (wet summer).

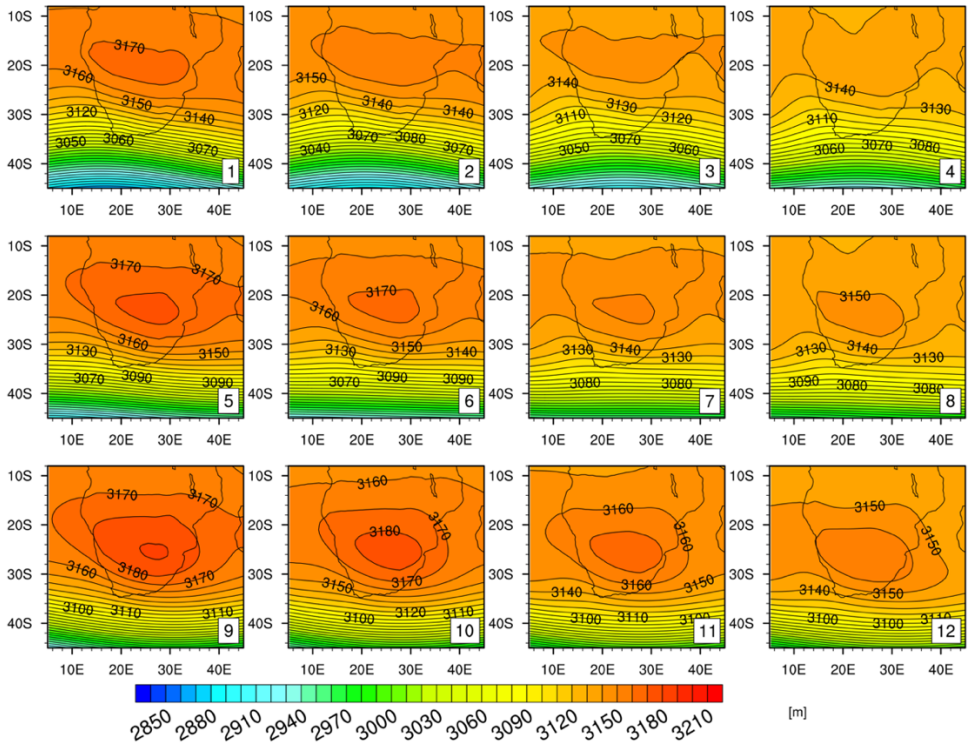

Figure 2.3: The 4 x 3 SOM using daily ERA-Interim geopotential height Z at 700 hPa for southern Africa for the period 1981-2013. Node numbers are shown on bottom right.

The frequency of circulation patterns across the SOM shows a characteristically even distribution across the nodes (Figure 2.4). Seasonally, nodes 1-2-5-9 occur primarily in winter (JJA) days and accounted for 17%, 14.8%, 14.9% and 15.5% respectively of the total days of occurrence in each of those nodes. Nodes 4-8-12 are also mostly associated with summer (DJF) days accounting for 16%, 18% and 13% of the total days of occurrence. Nodes 3 and 6 accounted for 12% and 9.5% of the total days of occurrence which were predominantly spring (SON) days whereas in nodes 10 and 11 they accounted for 12% and 14% of the total days of occurrence and were predominantly autumn (MAM) dominated days. Node 7 occurs in both summer (DJF) and spring (SON) with both accounting for 9.5% of the days of occurrence.

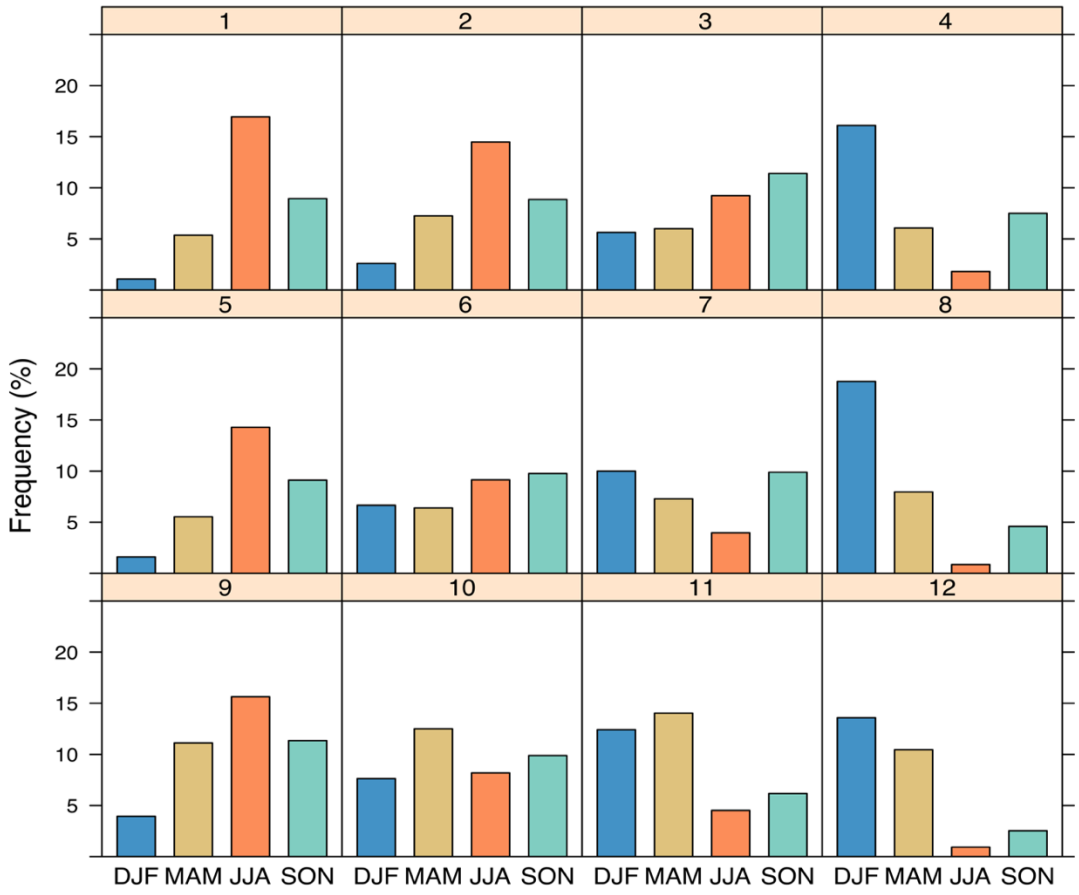

Figure 2.4: Seasonal variation of the frequency of occurrence (%) mapped to each SOM node for the training period 1980–2013. The node numbers (top center) correspond to that of Figure 2.3 with DJF = summer, MAM = autumn, JJA = winter, and SON = spring, respectively.

2.3.2 Rotated Principal Component Analysis (PCA)

To analyse the co-behaviour between the seasonal SOM frequencies and the climate indices, we applied PCA. The PCA loadings and explained variance for the three retained PC are presented in Table 2.1 below.

Table 2.1: Loading matrix for the first three varimax rotated PCs of the SOM node frequencies with MEI, AAO, and TRBI with PC1, PC2, and PC3. Bold numbers in each row (same as node arrangement in Figure 2.3) represent loadings statistically significant at the 95% level associated with circulation processes identified by the SOM in Figure 2.3. Truncation of PCs is based on N-Rule and with explained variance expressed as percentage in bold.

PC1 [MEI = −0.10, AAO = 0.06, TRBI = 0.07(30.0%)]			
0.87	**0.74**	0.16	**−0.46**
0.83	0.23	**−0.53**	**−0.66**
0.62	−0.17	**−0.76**	**−0.71**
PC2 [MEI = 0.72, AAO = −0.09, TRBI = −0.32(19.8%)]			
0.09	0.09	−0.23	**−0.70**
0.27	**0.48**	−0.06	**−0.58**
0.56	**0.81**	0.25	**−0.34**
PC3 [MEI = 0.09, AAO = 0.40, TRBI = 0.22(12.6%)]			
−0.03	0.29	**−0.81**	−0.01
−0.20	**0.50**	**−0.58**	**−0.30**
−0.30	0.07	−0.21	**−0.36**

The first rotated principal component (hereafter called PC1) accounted for 30% of the explained variance of the data across the period examined. MEI, AAO and TRBI show weak correlations with PC1, while strong correlations are seen across the SOM node loadings. PC1 is strongly negatively correlated with the summer synoptic states on the right hand side of the SOM and strongly positively correlated with winter synoptic states suggesting that PC1 is capturing the seasonal cycle. The MEI is negatively correlated with AAO and TRBI on the second rotated principal component (hereafter called PC2). However, MEI dominates PC2 by exhibiting a strong positive correlation

(0.72), AAO exhibiting a weak negative correlation of -0.09, and TRBI a moderate negative correlation of -0.32 respectively in Table 2.1 suggesting that this component is largely an ENSO response. This component also accounted for 19.8% of the explained variance. The strong positively correlated MEI points to an increase in dry summer states (winter circulation; nodes 1-2-5-9) and a decrease in wet summer states (summer circulation; nodes 4-8-12). The moderate negative correlation of PC2 with TRBI (-0.32) is likely explained by the tendency for positive MEI (El Niño) to suppress regional convection (see Dieppois et al. 2015; Cook 2000). The third rotated principal component (PC3) is dominated by a positively correlated AAO, a weak MEI and a positively weak TRBI which suggests this component is largely an AAO mode. An increase in both dry and wet summer states are associated with these conditions. This component also accounted for 12.6% of the explained variance across the data also shown in Table 2.1. In the first two components, AAO and TRBI are found to be out of phase with MEI whereas this is not the same for the third component. The PCA result indicates that the three process indices contribute significantly to the total variance and their exclusion would significantly alter the PCA results.

2.3.3 Links between climate processes, regional precipitation and temperature

In this section, we investigate how circulation patterns identified by the SOM influences the distribution of precipitation and temperature over the SRR, WRR and ARR of southern Africa by considering their composite anomalies. Figures 2.5 and 2.6 show precipitation and temperature composite anomalies when PC1, PC2 and PC3 are in positive (when scores are greater than 1 standard deviation) and negative (when scores are less than -1 standard deviation) phases. In order to ascertain the potential influence of each phase on regional precipitation and temperature we examine the variations in their spatial distribution. To reduce redundancy, we only mention areas of statistical significance for the sake of summary, discussion and interpretation.

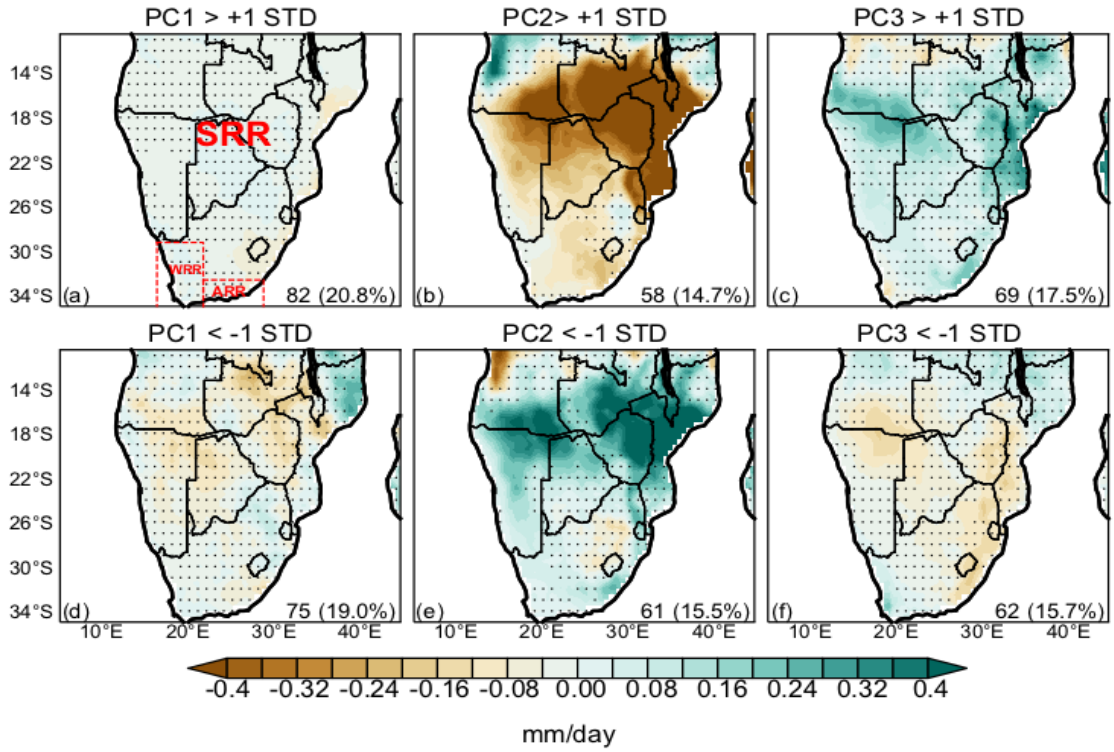

Figure 2.5: Composite precipitation anomaly patterns associated with (a)–(c) positive and (d)–(f) negative phases for SRR, WRR, and ARR for retained PCs. Stippling denotes grid cells not statistically significant at 90% level. At the lower right corner is the number of data points and its corresponding percentage that contributed to each phase.

From Figure 2.5a we note that both positive and negative phases of PC1 produce very weak and largely statistically insignificant precipitation anomalies. This is to be expected as the composites are calculated taking into account months in which the positive or negative phase events occurred and PC1 is strongly dominated by the seasonal cycle. As the method of calculating anomalies removes the seasonal cycle from the observations we expect and observe very weak anomalies for PC1. This is likely due to inter-seasonal variance differing. However, we only record significant precipitation anomalies (although negative) for the east of SRR, particularly northern Mozambique when PC1 is in positive phase (Figure 2.5a).

For PC2 in positive phase (Figure 2.5b), we see dryness in SRR and to the north of WRR. Since PC2 is largely an ENSO response as shown in our PCA, we suggest here that the positive phase of ENSO (El Niño) is largely responsible in suppressing convective systems, such as the South Indian Ocean Convergence Zone (SIOCZ), due to the weakening of convergence zones during El Niño events as a result of changes in Walker Circulation (Dieppois et al. 2015; Mason and Jury 1997; Reason et al. 2000) and its effect is particularly strong in the SRR. Again, the wetness in central parts of SRR could be attributed to the negative phase ENSO (La Niña) enhancing convective systems (Figure 2.5e) convective systems are enhanced leading to wetter and cooler than normal conditions in SRR (Trujillo and Thurman 2011). For PC3, which is also seen largely as the AAO response, when in positive phase, the central parts of SRR and the east of ARR are marginally wet (Figure 2.5c). On the other hand, WRR is wet while central parts of SRR is dry when PC3 is in negative phase (Figure 2.5f). This in previous studies has been attributed to the reduction in the typical subsidence over the interior of the region as a result of weaker South Atlantic and South Indian subtropical anticyclones shifting frontal systems northwards (Reason and Rouault 2005).

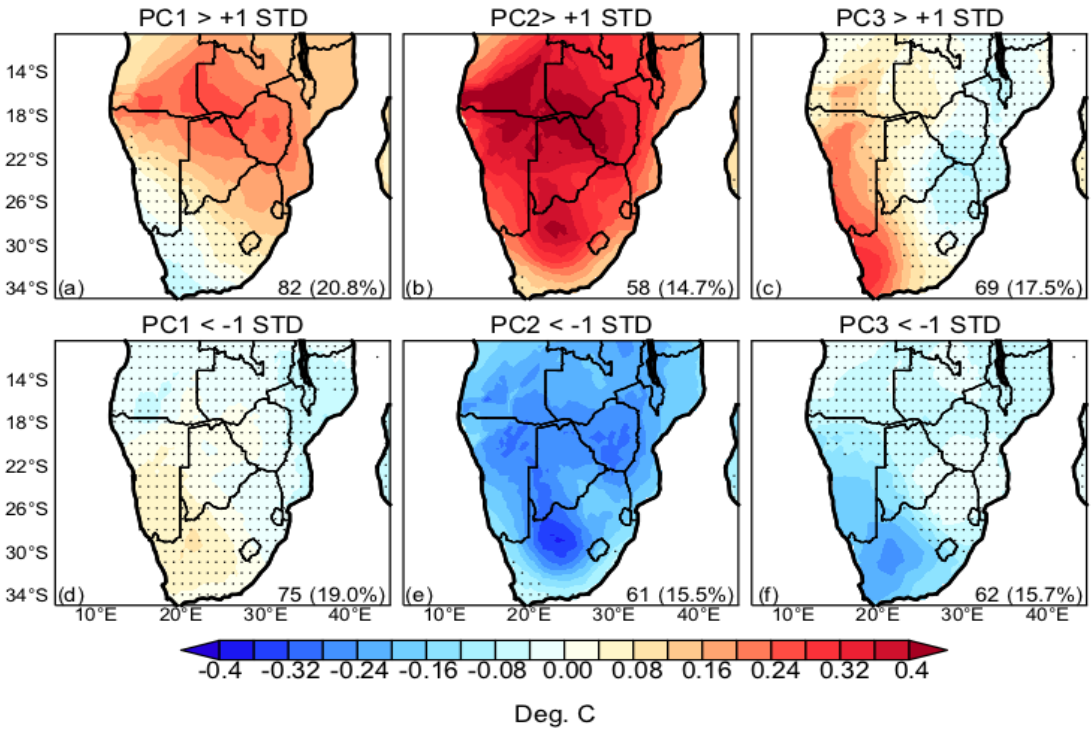

Figure 2.6: As in Figure 5, but for composite temperature anomaly.

For spatial distribution of temperature associated with PC1 (Figure 2.6a and d), we identify warming in SRR when in positive phase. Again, although SRR, WRR and ARR are warm during PC2 (Figure 2.6b) positive phase, we find SRR much warmer when compared to WRR and ARR. We also identify the SRR and ARR are cold when PC2 is in negative phase (Figure 2.6e). With PC3 in positive phase, WRR and ARR appears to be warm showing an east to west gradient (Figure 2.6c). WRR and ARR are however cold when PC3 is in negative phase (Figure 2.6f). The conditions in PC2 and PC3 are quite typical of ENSO and AAO individual influence over the subcontinent as mentioned earlier.

2.3.4 Analysing Co-behavior

In the next step we evaluate co-behaviour by assessing the eight possible combinations that may likely influence regional precipitation and temperature based on the PCs identified from the rotated PCA. These combinations are realized by the mixing of the alternating phases of PC1, PC2 and PC3 and the results presented.

If we focus on significant dry conditions in the SRR in Figure 2.7 (d and g), we see that these dry conditions are regionally extensive (d) under dry summer conditions (PC1 > 1 std), El Niño (PC2 > 1 std) and positive AAO (PC3 > 1 std). If AAO is strongly negative (Figure 2.7 g) the dry pattern becomes more northerly suggesting that AAO is moderating the regional precipitation response to El Niño.

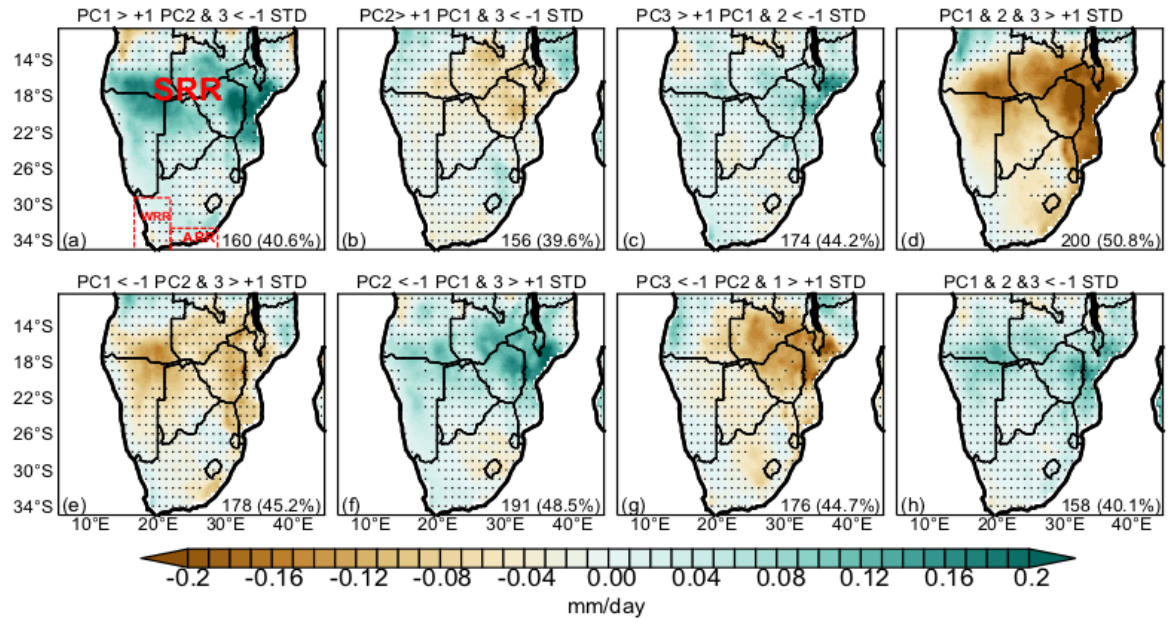

Figure 2.7: Composite precipitation anomaly patterns associated with eight possible combinations of positive and negative phases for retained PCs. Stippling denotes grid cells not statistically significant at 90% level. At the lower right corner is the number of data points and the corresponding percentage that contributed to each combination.

Similarly, if we focus on significant wet conditions in the SRR (Figure 2.7 a and f), we see that summer conditions (PC1 > 1 std), La Niña (PC2 < -1 std), and negative AAO (PC3 < -1 std) are associated with broad wet conditions across central and northern parts of the region. If AAO shifts to positive (PC3 > 1 std) then this wet region is concentrated more in the east and northern Namibia and southern Angola is only marginally wetter. Again, this suggests that the AAO is moderating the regional precipitation response to ENSO, in this case under La Niña conditions.

For significant wet conditions in the WRR (Figure 2.7c), we find areas around the south-western Cape of South Africa marginally wet under winter conditions (PC1 < -1 std), positive AAO (PC3 > 1 std), and La Niña (PC2 < -1 std).

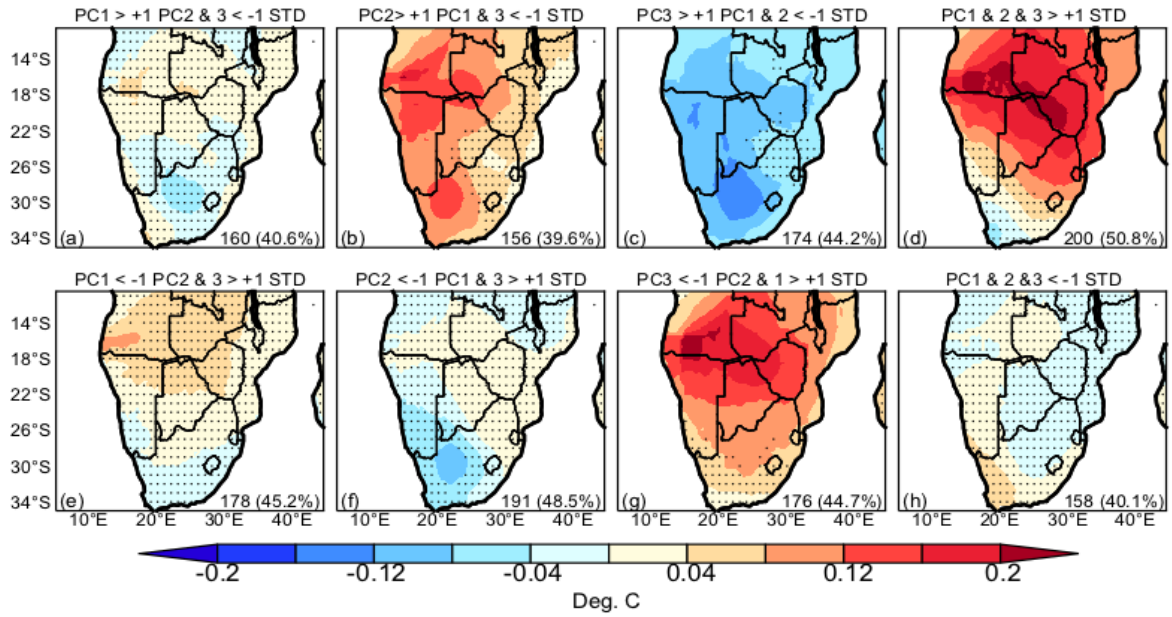

Figure 2.8: As in Figure 7, but for composite temperature anomaly.

Additionally, focusing on significant warm conditions in the SRR (Figure 2.8b, d and g), we see the centre/north of the region is anomalously warm and the south western areas are cool (though not statistically significantly) under summer conditions (PC1 > 1 std), El Niño (PC2 > 1 std) and positive AAO (PC3 > 1 std) in Figure 2.8d. The AAO shifting to negative (Figure 2.8g) shifts the center of the warm anomaly westwards and is concentrated around southern Angola with Zimbabwe and northern Botswana. With El Niño and a negative AAO phase co-behaving (Figure 2.8b), most parts to the west of the subcontinent is warm spreading from the south to the north. In totality, this is similar to the precipitation response, which suggests that the AAO does moderate the El Niño temperature responses as well when they co-behave.

A positive AAO co-behaving with La Niña in winter is the only identified condition where all the rainfall regions are cold.

2.4 Summary and Conclusion

The study develops a methodology to objectively identify co-behaviour between climate processes and drivers of the southern African regional climate. We developed a PCA based on indices of seasonal circulation types, ENSO, AAO and the ITCZ and the resulting loadings were associated with characteristic circulation patterns. Composites of precipitation and temperature for the first three components of the PCA were then produced and statistical significance at each grid cell determined.

We analyse the large-scale circulation types over the subcontinent as a proxy to understanding the influence of co-behaviour, results show the SOM was effective in capturing the dominant circulation patterns leading to the identification of the seasonal evolution patterns. Circulation types represented in nodes 1-2-5-9 are primarily associated with winter (wet conditions for the WRR and ARR) and dry conditions over the interior of the SRR. Conversely, circulation types in nodes 4-8-12 represent weak high pressure systems and are associated with summer and precipitation over the SSR.

From the PCA analysis, we associate PC1 with the seasonal cycle as the loading matrix correlates strongly with winter (positive correlation) and summer (negative correlation) circulation types. The loading matrix of PC2 is identified as largely an ENSO response with strong MEI index loading on the matrix and moderate negative TRBI pointing to the expected suppression of convection under warm ENSO conditions. PC3 appears to be largely representing the variability of AAO and to a smaller extent the TRBI.

The PCA enables us to further examine the influence of individual teleconnective drivers on precipitation and temperature over the SRR, WRR and ARR. We identified already established associations in literature, for instance the influence of a strongly negative AAO on precipitation in the WRR (PC3) and the ENSO influence on temperature and precipitation (PC2) in the SRR validating the strengths of the developed methodology.

Addressing our primary objective, combining the different combinations and variability of our retained PCA components, we are able to analyse the co-behaviour of teleconnective drivers on regional precipitation and temperature. Results show conditions in SRR to be extensively dry and warm when El Niño episodes co-behave with a strongly positive AAO during summer. However, when AAO shifts to strongly negative in summer conditions, the dry pattern is more northerly and warming peak shifts westwards. Broadly wet conditions persist in the SRR and parts of the ARR when La Niña episodes co-behave with a strongly negative AAO during summer. Conversely, a shift in AAO to strongly positive drives wet conditions in central and northern parts of the SRR although peak conditions are centered to the east.

We demonstrate that the WRR is both marginally wet and cold, with ARR only cold and the SRR much colder to the west when La Niña episodes co-behave with a strongly positive AAO during winter. However, during summer, this co-behaviour enhances wet conditions in central to northern parts of the WRR. While further investigation would be required, Pohl et al. (2010) identifies a slowdown in the subtropical jet speed as a result of the combined effect of positive phase of the AAO and La Niña which may lead to rain-causing synoptic systems. During winter, a co-behaviour of El Niño and a strongly negative AAO augments very warm conditions in the SRR while both the WRR and ARR are moderately warm.

Despite our analysis of co-behaviour between drivers of climate over the study region, it must be noted that there are additional regional circulation features such as the Angola Low, Botswana high, the subtropical South Indian high pressure system together with local soil moisture feedbacks and local topographic effects, particularly of the escarpment, that may modulate the local response to these co-behaving systems (Mackellar et al. 2010; Blamey et al. 2018). Although the large-scale processes and their co-behaviour studied here establish the environment for the surface responses in rainfall and temperature, these additional drivers of local variability in the region may modulate the effect of the large-scale forcing (e.g. Wolski et al. 2018). However, it is beyond the scope of this study to investigate these relationships.

In conclusion, the methods developed in this study have demonstrated that the impact of co-behaving climate processes may be analysed. The method identified already established relationships over the subcontinent and further identified significant relationships between different phases of ENSO, AAO and ITCZ with precipitation and temperature distribution across the southern African region. The methodology developed aims to underpin future work to advance the study of co-behaviour of climate processes relevant to any given region. The present method can also be used to analyse climate drivers at multiple timescales. This type of analysis is essential for climate model evaluation and in subsequent studies we will assess how well co-behaviour is captured in climate models and how co-behaviour may change in future climate scenarios.

Acknowledgements

This work was conducted under the Future Resilience for African CiTies and Lands (FRACTAL) project, which is part of Future Climate for Africa (FCFA) program funded by UK's Department of International Development and National Environmental Research Council. The authors are grateful to Grigory Nikulin at Rossby Centre, Swedish Meteorological and Hydrological Institute, Sweden for the provision and use of the Tropical Rain belt Index. The first author is grateful to the University of Cape Town for funding assistance. Additionally, the first author is thankful to African Climate and Development Initiative (ACDI) of University of Cape Town, Tyndall Centre for Climate Change and Climatic Research Unit (CRU) under the Newton PhD Partnering Scheme funded by Research Councils UK (RCUK) and the National Research Foundation (NRF) of South Africa.

Chapter 3

Using Co-Behavior Analysis to Interrogate the Performance of CMIP5 GCMs over Southern Africa

How well do climate models capture co-behaviour as identified in reanalysis datasets?

Specific Questions?

- How are climate models representing observed co-behaviour?
- What are the possible variations in precipitation and temperature response across models under the different co-behaviour modes?

Abstract

As established in earlier research (Quagraine et al. 2019a), analysis of the combined roles (co-behaviour) of multiple climate processes provides useful insights into the drivers of regional climate variability, especially for regions with no dominant large-scale circulation controls. Here, we extend the previous study in order to examine the performance of 8 models from the Coupled Model Intercomparison Project Phase 5 (CMIP5) in representing co-behaviour influence on surface expressions over southern Africa. We find that although models broadly simulate observed precipitation responses over southern Africa, they fail to produce statistically strong response signals for an important drought pattern (El Niño co-behaving with positive AAO during summer) for the region. We also demonstrate that the models show statistically strong temperature response signals to co-behaviour that agree well with observed responses over the region. The multi-model ensemble mean although consistent with observations shows a larger spread. By elucidating the performance of models in representing observed co-behaviour of climate processes, we are able to evaluate models while establishing important information for understanding of climate variability.

A paper based on this part has been published by Journal of Climate:

"Using Co-Behavior Analysis to Interrogate the Performance of CMIP5 GCMs over Southern Africa"

https://doi.org/10.1175/JCLI-D-19-0472.1

***K. A. Quagraine**, B. Hewitson, C. Jack, P. Wolski, I. Pinto and C. Lennard*

3 Introduction

Understanding the drivers of regional scale climate variability and change is key to understanding and interrogating climate projections for regions which in turn provides the foundation for informing increasingly urgent adaptation decision making. Studies have often focused on individual processes in attempts to understand regional climate variability and change by establishing statistical relationships with climate variables. While this approach has improved our understanding of regional climate to an extent, not much has been done to understand the response to multiscale interactions among climate processes driving regional climate variability and change. As such alternative approaches are required to help interpret the nature of these interactions and their impact on the present and future climate (Daron et al. 2019).

Interactions amongst climate processes; co-behaviour, can influence regional weather and climate. Co-behavior recognises that regional climate variability is an outcome of multiple, potentially interacting climate processes operating across varying temporal and spatial scales, and a better understanding of co-behaviour may advance our understanding of regional climate variability. Quagraine et al. (2019) described an approach to identifying and analysing co-behaviour in observation based and climate reanalysis data. For the purposes of improving understanding of regional climate variability there may be a need to extend this approach to Global Climate Models (GCMs).

GCMs are our primary tool to understand past and future changes in our climate (see Frame and Stone 2013; Knutti and Sedláček 2013). The ability of GCMs to reasonably simulate already identified co-behaviour modes in observed datasets may permit climate model weighting and the evaluation of climate model simulations by making available consistent set of GCMs pertaining to any region of interest.

Over time, we have significantly improved how GCMs are able to simulate the observed climate and to some extent make robust future predictions in the presence of uncertainties through improving our understanding of the physics and refinement to model configuration and numerical algorithms (Miao et al. 2014; Ramirez-Villegas

et al. 2013; Su et al. 2013). Experiments like the Coupled Model Intercomparison Project phase 5 (CMIP5; Taylor et al. 2012) have certainly helped in this direction. Few studies have used CMIP5 models in tackling a wide range of climate issues over southern Africa. The studies include but are not limited to the modelling of the present and future African climate (Dike et al. 2015), exploration of climate processes associated with rainfall bias (Munday and Washington 2018), analysing how models reproduce teleconnections between El Niño-Southern Oscillation (ENSO) and southern African rainfall (Dieppois et al. 2015) and how models have identified drivers of rainfall decline over southern Africa in recent past and near future projections (James and Washington 2013).

However, co-behaviour of climate processes in climate models remain weakly explored, yet may offer a valuable source of information to understand regional climate variability as well as aid in assessing the robustness of climate model results. Few recent studies have directly focused on the role of interactions between climate processes on surface manifestations of climate. Muñoz et al. (2015) investigated the relevance of multiple climate drivers across multiple timescales to improve extreme rainfall predictability. These studies used observation and reanalysis datasets. A study by Muñoz et al. (2017) used five members each of two versions of a GCM to develop a framework for understanding the influence of cross-time scale interactions on weather types. Daron et al. (2019) also uses related theoretical concepts in highlighting the relationship that exists among climate processes.

In this paper we examine how a set of GCMs from the CMIP5 experiment represent observed co-behaviour over southern Africa (10°S-35°S; 5°E-45°E). The rest of the paper is organized as follows: section 3.1 summarizes the datasets and methodology adopted for the study. The results are discussed in section 3.2 with summary and conclusions presented in section 3.3.

3.1 Data and methods

3.1.1 Data

ERA-Interim data (Dee et al. 2011) at 700-hPa geopotential height with a grid resolution of 0.75° is used for the self-organising map (SOM; Kohonen 1982, 2001) classification of circulation patterns over southern Africa (see Quagraine et al. (2019) for details of the approach).

In the present study, we select only eight models (Table 3.1) from the set of CMIP5 GCMs based on the availability of climate variables needed for the study and the ability of the models to reasonably represent the southern African climate (see McSweeney et al. 2015).

For observed temperature, we use the Climatic Research Unit (CRU-TS v4.01; Harris et al. 2014) data, and Climate Hazards Infrared Precipitation with Stations (CHIRPS; Funk et al. 2015) for precipitation.

3.1.2 Methods

i. Climate Indices

We calculate three indices that describe and analyse the state of changes occurring in ENSO, Antarctic Oscillation (AAO) and the Intertropical Convergence Zone (ITCZ) intensity for each of the CMIP5 models used (see Table 3.1). Here, the Niño 3.4 index (Trenberth 1997; Trenberth and Stepaniak 2001), is computed using sea surface temperature anomalies, and used to characterise ENSO, while the AAO index is constructed by projecting daily 700-hPa height anomalies poleward of 20°S onto the leading pattern of the AAO as described by Thompson and Wallace (2000b) as is similarly done in Chapter 2, section 2.2. The tropical rain belt index (TRBI) which captures the intensity of the ITCZ and is based on methodology from (Nikulin et al. 2012; Nikulin and Hewitson 2019) is generated. For higher rainfall intensities within the tropical rain belt, TRBI is positive. These above mentioned processes are chosen because of their importance to the southern African regional climate (see Klutse et al. 2016; Lennard and Hegerl 2014; Meque and Abiodun 2015; Reason and Rouault

2005; Weldon and Reason 2014). We stress here that other processes could have equally been used but we use these processes as they are well understood in literature and conveniently easy to compute their indices for the study.

Table 3.1: Details of CMIP5 model simulations used in the study.

Model Version	Modelling Center	Reference	Period
CanESM2	Canadian Centre for Climate Modelling and Analysis (CCCMA), Canada	Arora et al. (2011)	1980-2013
CNRM-CM5	Météo-France (CNRM-CERFACS), France	Voldoire et al. (2013)	1980-2013
GFDL-ESM2M	NOAA Geophysical Fluid Dynamics Laboratory (NOAA GFDL), USA	Dunne et al. (2012)	1980-2013
HadGEM2-ES	Met Office Hadley Centre, United Kingdom	Collins et al. (2011)	1980-2013
IPSL-CM5A-LR	Institut Pierre-Simon Laplace (IPSL), France	Dufresne et al. (2013)	1980-2013
MIROC-ESM	Japan Agency for Marine-Earth Science and Technology (JAMSTEC), Atmosphere and Ocean Research Institute (University of Tokyo) and National Institute for Environmental Studies (MIROC), Japan	Watanabe et al. (2011)	1980-2013
MPI-ESM-LR	Max Planck Institute for Meteorology (MPI-M), Germany	Raddatz et al. (2007)	1980-2013
MRI-CGCM3	Meteorological Research Institute (MRI), Japan Meteorological Agency (JMA), Japan	Yukimoto et al. (2012)	1980-2013

Ii. Self-Organizing Map (SOM)

In this study, we identify archetype synoptic circulation patterns over the region by training a 12-node self-organizing map (SOM; Kohonen 1982, 2001) with daily 700 hPa ERA-Interim geopotential anomaly fields to produce 12 characteristic circulation patterns over the study period 1980-2013 (Figure. 3 in Quagraine et al. 2019 from hereafter Figure. S3.1). At 700-hPa geopotential height level the important climate systems such as subtropical high and low pressures, easterly and westerly waves around southern Africa are effectively captured (e.g. Bartman et al. 2003).

A SOM is a topologically sensitive clustering technique which uses unsupervised training to cluster training data (Kim and Seo 2016; Lennard and Hegerl 2014). The SOM analysis typically consists of two main processes: the training phase and the mapping phase. The technique as applied in synoptic climatology is particularly effective as it maintains clusters as a continuum which in turn preserves relationships between weather states and presents the output as a readily understood and visualized array of classified patterns (Hewitson and Crane 2002; Kim and Seo 2016; Lee 2017; Rousi et al. 2015; Sheridan and Lee 2012). The classified patterns can aid in developing an understanding of linkages between large-scale regional circulation and local weather expressions (see Cassano et al. 2015; Gibson et al. 2017; Hewitson and Crane 1996). The implementation of the SOM in this study is shown in Figure 1a.

The choice of the SOM size is compromise between, on the one side, the need to generalize circulation field structure for analytical purposes, and on the other side, the need to capture the dominant spatial features of that field that have implications to local climate. Mackellar et al. (2010) and Tadross et al. (2005) found the 12-node SOM size captures the generalized synoptic circulation patterns over southern Africa, and we have used this SOM size in earlier analysis (Quagraine et al. 2019). For this analysis, the benefit of reducing variance to representative time series outweighs the temporal and spatial information loss in using this SOM size, thus we use the 12-node SOM (see Wolski et al. 2018). Here, we first use the daily 700-hpa anomaly field of the reanalysis to train a 12-node SOM, where each day in the study period is mapped on to one of the 12 circulation patterns identified by the SOM (Figure 3.1a(i)). Each model is then mapped through the reanalysis SOM space as shown in Figure 3.1a(ii).

The purpose of mapping the models to the reanalysis SOM space is to allow for comparison of SOM node frequencies between the GCMs and ERA-Interim representation of the observed frequencies and to further provide comparable inputs to the PCA analysis (Figure 3.1b(i)). The implicit assumption here is that the GCM patterns fall within the data space represented by the reanalysis, that is, that the archetype synoptic patterns of the ERA-Interim data encompasses the range of synoptic states in the GCMs. To test this assumption, we calculate the mean error of each day's pattern when compared to the reference pattern of the SOM node to which it maps. By comparing the error mapping of the GCMs to that of the ERA-Interim data, one can assess whether the GCM patterns have a greater error than the reanalysis which would indicate that the GCM is representing synoptic patterns that go out of the data space of the ERA-Interim data. In all cases, except some very few nodes in one model, the GCM patterns have errors smaller than the ERA-Interim data mapped to the ERA-Interim trained SOM as shown in Table 3.2. This is in some ways not unexpected as the GCMs are a reduced complexity system and hence would be expected to have less variance than the ERA-Interim data which is constrained by observations. Further, it indicates no significant departure by the GCMs from the archetype patterns determined from the ERA-Interim data and thus allowing us to proceed to examine the differences in the frequency of occurrence which is our initial intention.

As a next step, we generate frequency of occurrence histograms for the reanalysis and all eight models. A monthly time series matrix of each synoptic type is then generated from the daily frequency of occurrence and then from this a 3-month centered moving average window which serves as a low-pass filter is used to eliminate short-term variability while highlighting long-term variability (see Quagraine et al. 2019). This seasonal grouping aids in analyzing seasonal variability of the SOM.

Table 3.2: Quantization error (q_{err}, the Euclidean distance between an input vector and the best-matching unit (BMU) SOM reference vector) as calculated for each pattern with respect to each SOM. Values larger than the values for the ERA-Interim data indicates the GCM is producing some synoptic systems that go out of the bounds of the patter space represented by ERA-Interim.

SOM Node Number	SOM Node Quantization Error (q_{err})								
	ERA-Interim	**CanESM2**	**CNRM-CM5**	**GFDL-ESM2M**	**HadGEM2-ES**	**IPSL-CM5A-LR**	**MIROC-ESM**	**MPI-ESM-LR**	**MRI-CGCM3**
1	41.3	40.6	41.9	38.2	38.5	34.9	25.1	40.4	42.9
2	41.9	38.8	38.1	37.3	35.7	32.4	24.9	37.5	39.8
3	44.4	38.9	38.5	38.0	37.5	34.7	29.8	38.0	40.9
4	46.6	42.8	44.1	37.3	41.9	40.7	56.9	41.1	45.7
5	39.6	36.5	35.7	31.3	34.6	34.1	24.7	36.2	37.5
6	36.3	33.0	33.8	31.7	31.8	28.6	25.0	33.0	34.6
7	35.4	33.4	34.8	31.7	32.4	29.6	33.5	33.7	35.5
8	39.5	38.5	39.9	32.0	37.4	36.5	52.3	38.2	43.5
9	40.8	34.2	32.8	30.9	30.2	30.5	24.6	32.8	34.1
10	35.2	32.7	32.9	31.3	30.5	30.6	29.8	32.7	33.6
11	35.1	32.7	35.1	30.8	31.1	31.5	39.6	33.3	34.6
12	34.9	37.9	41.3	31.5	37.0	38.9	48.1	39.1	39.6
Mean	**39.3**	**36.7**	**37.4**	**33.5**	**34.9**	**33.6**	**34.5**	**36.3**	**38.5**

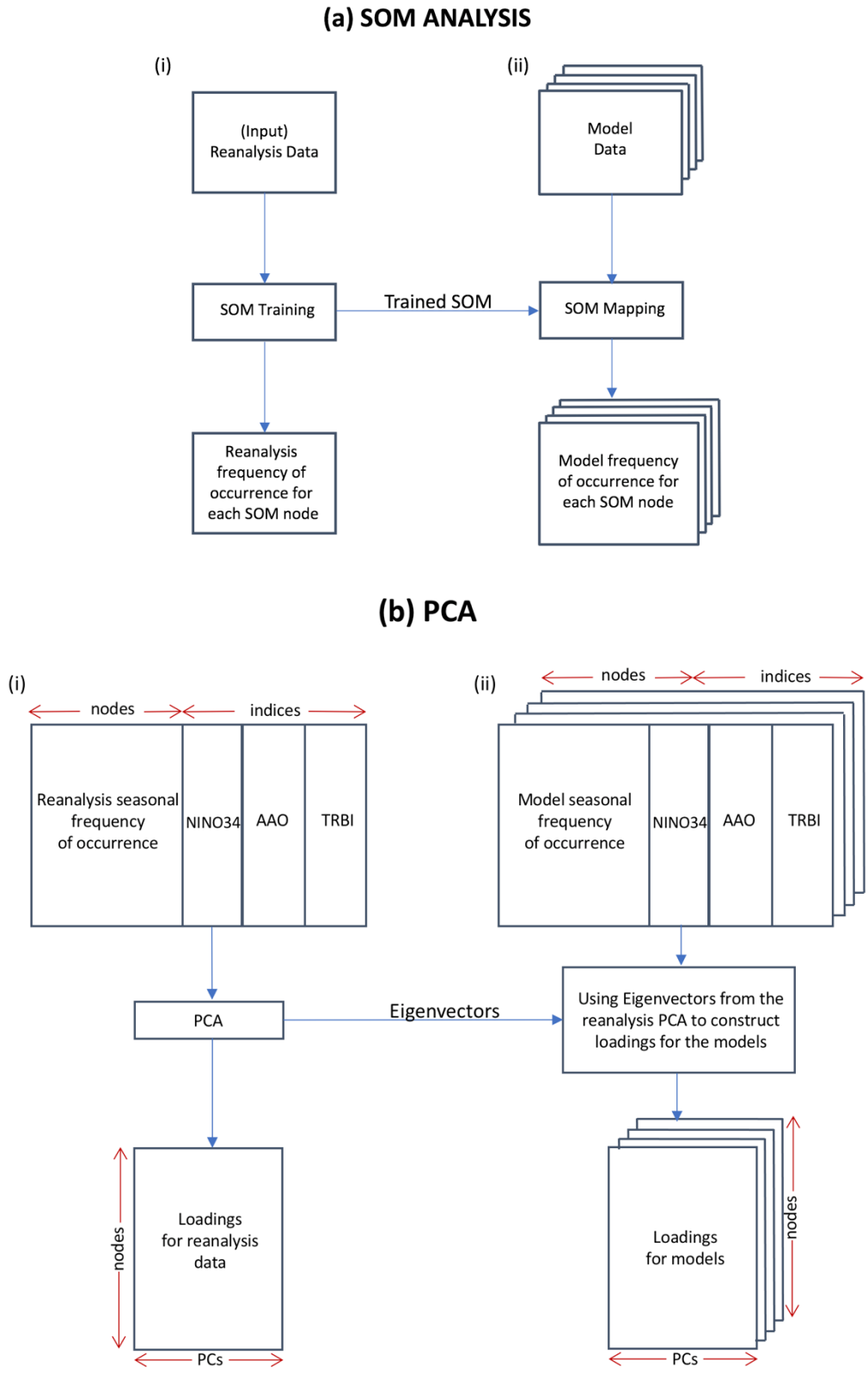

Figure 3.1: A schematic representation of the implementation of the (a) Self-Organising Map (SOM) and (b) Principal Component Analysis (PCA; modified after Quagraine et al. 2019).

iii. Rotated PCA

To explore the frequencies of occurrence of the synoptic circulation types in relation to the co-behaviour of the conditioning large-scale drivers (represented by climate indices), we use principal component analysis (Jolliffe and Stephenson 2012; Jolliffe and Cadima 2016; Lever et al. 2017), shown in Figure 3.1b. In Figure 3.1b(i), the input to the PCA is an extended matrix of seasonal frequencies with additional columns for the climate indices for ENSO, AAO and TRBI derived from the ERA-Interim reanalysis data (hereafter, training dataset). A similar matrix is generated for each model to serve as input for the PCA (Figure 3.1b(i)).

PCA is a multivariate technique which produces a set of abstract variables known as principal components (PCs) which are weighted linear combinations (coefficients) of the original variables (Jolliffe and Cadima 2016) and these coefficients are then stored in a loading matrix with the goal of finding the best summary of the data using limited number of PCs (Lever et al. 2017). The data is rotated by the loading matrix (also known as rotating matrix) in a way that the projection with the greatest variance maps along the first axis (first PC). By eliminating PCs that represent only small amounts of the total original variance, the complexity of a high-dimensional data can be simplified while retaining trends and patterns by transforming the data into fewer dimensions which are summaries of features and has previously been used as a dimension reduction approach in distribution modelling (Lever et al. 2017; Robertson et al. 2001). Hence the output of our PCA as applied to our extended matrix, identifies dominant modes of independent variability within our data and three PCs were retained based on randomization and assessment of their significance at 90% confidence level using the N-Rule test as a stopping rule (see Peres-Neto et al. 2005). Through the PCA loadings, we are able to establish the relationship between the frequency of occurrence of the synoptic circulation types and the conditioning large-scale processes. A modified version of scikit-learn python module which incorporates a function for varimax rotation is used for the PCA (https://scikit-learn.org/; Pedregosa et al. 2011).

iv. GCM Analysis

In order to analyze how the 8 GCMs represent the observed relationships between synoptic variability and large-scale climate indices we first re-grid the GCMs to the same resolution as the ERA-Interim dataset using nearest neighbour interpolation. For the period of study, each GCM is a combination of the historical period (1980-2005) and the future scenario (2006-2013) for Representative Concentration Pathway (RCP) 8.5, as this was the likely pathway at that period in time. Similarly to what has been done for the reanalysis, we then combine the timeseries of the ENSO, AAO and TRBI indices with the SOM node frequencies for each GCM: these data vectors are then used with the original reanalysis derived PCA loadings to produce PCA score timeseries for each GCM. This sort of approach has been frequently and effectively applied in climate science and the reader is referred to Maraun and Widmann (2018) for detailed understanding.

v. Assessing regional precipitation and temperature response, and significance

In order to assess how each GCM represents local responses to co-behaviour of large-scale drivers, we explore the response of regional precipitation and temperature under different combined large-scale processes and circulation states. We do so by using the obtained scores of the retained PCs from the models to identify conditions of strong large-scale and/or circulation variations driving each PC. A PC is considered a “strong” driver of the regional climate when its score exceeds a threshold of plus or minus one standard deviation. This allows for the evaluation of the co-behaviour role in conditioning the regional climate response on seasonal time scales as each PC relates to the indices of large-scale processes. Composite precipitation and temperature anomalies for each of the subperiods where the threshold is exceeded are computed for each grid cell of the eight models.

For the purposes of quantifying the magnitude of association between the spatial distribution patterns of the observed co-behaviour modes and that of the models, we use Spearman's rank-order spatial correlation. This method is a non-parametric rank

statistic that measures the strength of the association between two variables (see Hauke and Kossowski 2011). It is much more robust in the presence of outliers, does not require the assumption of normality and is unbiased by non-linear relationships when compared to other methods (Endris et al. 2016).

Furthermore, we use the multi-model ensemble mean to ascertain the average model response to each co-behaviour mode. The multi-model ensemble mean is calculated by averaging the patterns of each co-behaviour mode for the respective models to obtain a single spatial pattern. We then assess the robustness of the patterns by measuring the level of agreement among models based on the condition that at least 80% of the models must agree on the sign of the anomaly with respect to the ensemble mean (see Mastrandrea et al. 2011; Pfeifer et al. 2015).

3.2 Results and discussion

3.2.1 Inter-model comparison of SOM seasonal frequencies

We objectively classify the circulation patterns over the southern African region with the SOM. Overall, we identify two distinct patterns with some transitional patterns at 700-hPa geopotential height (Figure 2.3). The SOM (Figure 2.3; nodes 4-8-12) captures disturbances in the easterly flow which develops as a result of continuous interactions between the ITCZ and the easterly wave, causing the southward migration of the semi-permanent high pressure system and thereby enhancing rainfall conditions in the interior during (austral) summer. Nodes 1-2-5-9 (Figure 2.3) represent a passing mid-latitude frontal system which brings rains over the southwestern parts of South Africa. These circulation patterns represent typical (austral) winter synoptic circulation patterns over the region.

In evaluating how the models capture the SOM node seasonal frequencies (Figure 3.2), we find most of the observed node mapping frequencies are overestimated across both summer and winter states (e.g. Figure 3.2a; nodes 11-12, Figure 3.2b; nodes 3-4-8) by the models while there are some few cases of underestimation (e.g. Figure 3.2a; nodes 4-8, Figure 2b; nodes 9-10-11).

During summer (Figure 3.2a), nodes 5 to 12 are mapped more frequently by the models. In nodes 9 to 12, models overestimate the observed, with HadGEM2-ES (39%) and IPSL-CM5A (38%) overestimating almost thrice the percentage of the observed (14%) in node 12, while MPI-ESM-LR also overestimates almost twice the observed for node 11. MIROC-ESM overestimates over three times the observed (4% and 8%) in nodes 9 (14%) and 10 (27%). However, all models underestimate in nodes 2-3-4.

In winter (Figure 3.2b), the models mapped more frequently to all nodes although frequencies in nodes 11 and 12 do not often occur. The models overestimate the observed in nodes 1 to 4 and 8, particularly in node 4; CanESM2 (17%), CNRM-CM5 (19%), GFDL-ESM2M (18%), IPSL-CM5A (16%) and MRI-CGCM3 (13%) respectively. MIROC-ESM (14%) strongly overestimates the observed (1%) in node 8. In nodes with some typical winter circulation states (Figure 3.2b; nodes 1 and 2) and also in node 7, the models do simulate fairly the frequency of occurrence. We suggest here that the overestimation (underestimation) by models to the ERA-Interim reanalysis may be as a result of models simulating associated circulation types more (less) frequently due to their inability to resolve highly complex large-scale processes (see Munday and Washington 2018; Eyring et al. 2019). This may also account for their inability to capture the seasonal variability in some nodes (e.g. Figure 3.2(4); associated wet summer circulation state).

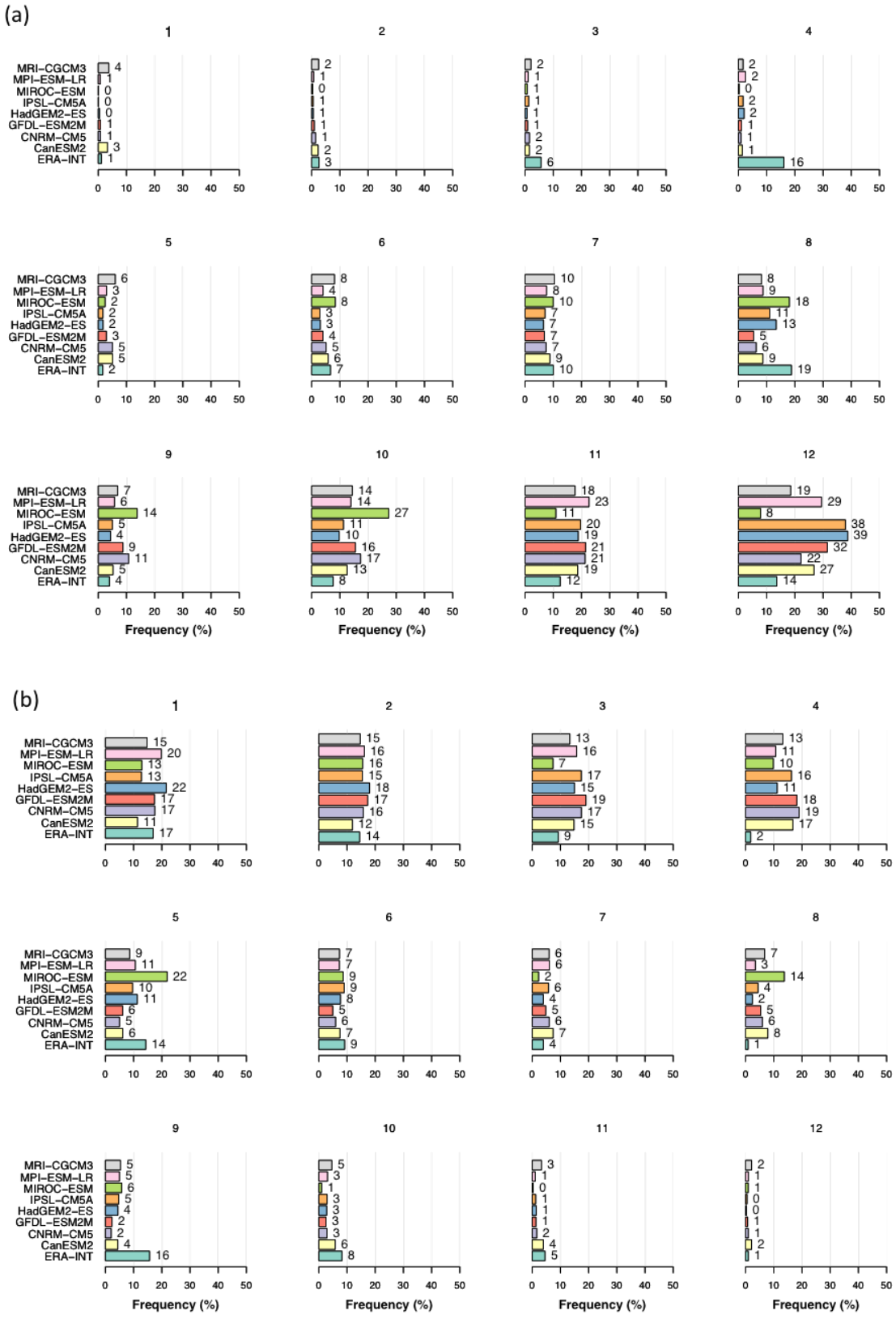

Figure 3.2: Model variability of the frequency of occurrence (%) mapped to each SOM node for the training period 1980-2013; (a) for summer (DJF) and (b) for winter (JJA) respectively. The node numbers (top center) correspond to SOM node numbers.

3.2.2 Evaluation of co-behaviour in GCMs output against observations

We use rotated PCA as a means of examining the interactions between synoptic circulation variability and large-scale climate indices. We find the first principal component (hereafter called PC1) strongly represents the seasonal cycle (SOM node frequency variance) with MEI, AAO and TRBI showing weak correlations and accounts for 30% of explained variance. The second principal component (hereafter called PC2) is largely the ENSO response with moderate and weak correlations from TRBI and AAO respectively. PC2 accounts for 19.8% of the explained variance while the third principal component (hereafter called PC3) is found to be AAO dominant with weak expressions from ENSO and TRBI and accounts for 12.6% of the explained variance. The different phases of each PCs are found to have a peculiar impact on regional precipitation and temperature response in the southern Africa region when the threshold of a “strong” driver is attained. For example, typically, an El Niño (positive phase; PC2 > 1 std) is linked to notable reduction in precipitation, and warming in central parts of the region while a negative phase (PC3 < -1 std) AAO intensifies precipitation in the southwestern parts of the region.

We assess the potential of the influence of co-behaviour on regional precipitation and temperature using eight possible combinations by mixing the alternative phases of the identified PCs from the rotated PCA. Designation for the various combinations are shown in Table 3.3 below.

Table 3.3: A list of the combinations of positive and negative phases of retained PCs where scores exceeds a threshold of plus or minus one standard deviation (co-behaviour modes (CM)).

PC1	PC2	PC3	CM
>1	<-1	<-1	1
<-1	>1	<-1	2
<-1	<-1	>1	3
>1	>1	>1	4
<-1	>1	>1	5
>1	>1	<-1	6
>1	>1	<-1	7
<-1	<-1	<-1	8

Here we present and discuss the precipitation and temperature response for four co-behaviour modes (CMs) that showed statistical significance in observed CMs for all models for a general overview of how the models represent CMs and also as a means to reducing redundancy and repetition in discussion. Results for the remaining CMs are shown in the accompanying supplementary material (Figures S3.2-3.13). We also present later the mean spatial pattern for each CM with respect to all models for precipitation and temperature.

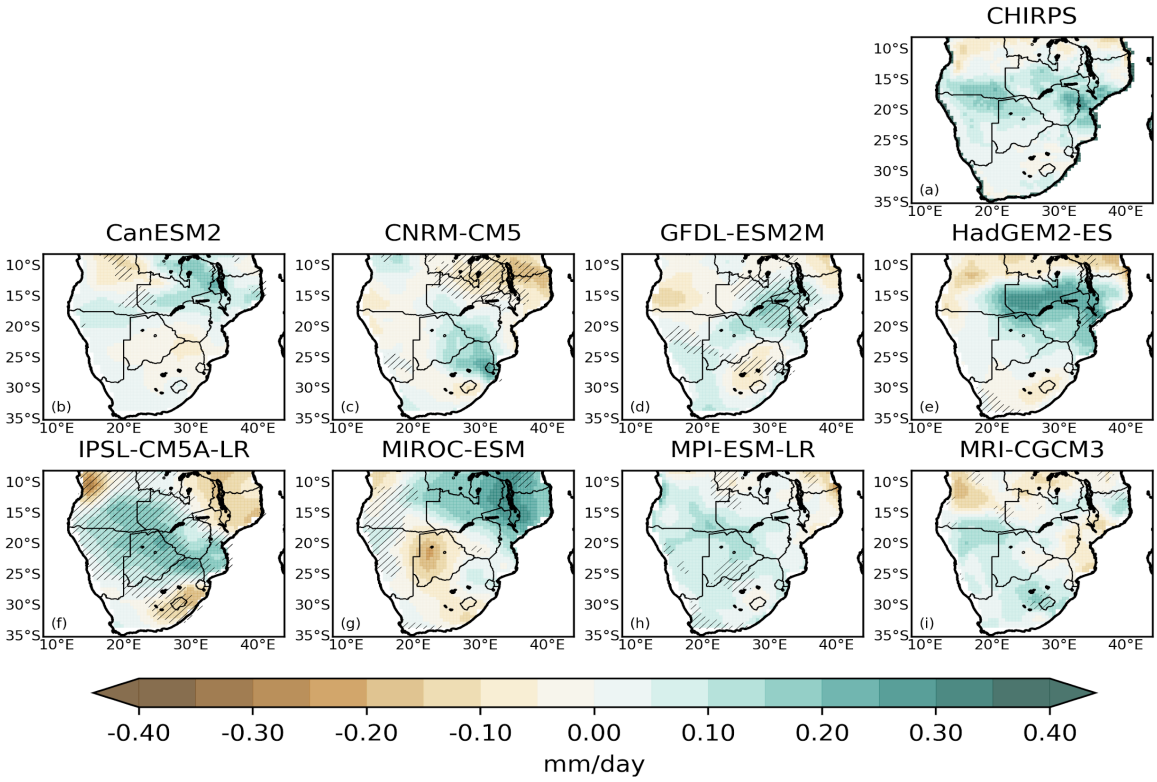

Figure 3.3: Spatial pattern of composite precipitation anomalies for observed (a) and models (b) – (i) for co-behaviour mode one (CM1; summer (PC1 > 1 std), La Niña (PC2 < -1 std) and negative phase AAO (PC3 < -1 std)). Hatching denotes grid cells not statistically significant at 95% level.

In CM1, wet summer conditions are characterised by a co-behaviour of La Niña (PC2 < -1 std), negative AAO (PC3 < -1 std) during summer (PC1 > 1std). In this mode, above 60% of models are able to fairly represent the general precipitation response and with most showing some wet bias (Figure 3.3). However, there are differences in the magnitude and location of the peak intensity across models although statistically significant. For example peak precipitation intensity is located in the north for CanESM2 (Figure 3.3b) whereas the peak is much southwards in CNRM-CM5 (Figure 3.3c). HadGEM2-ES (Figure 3.3e) best represents the response when compared with the observed (CHIRPS; Figure 3.3a).

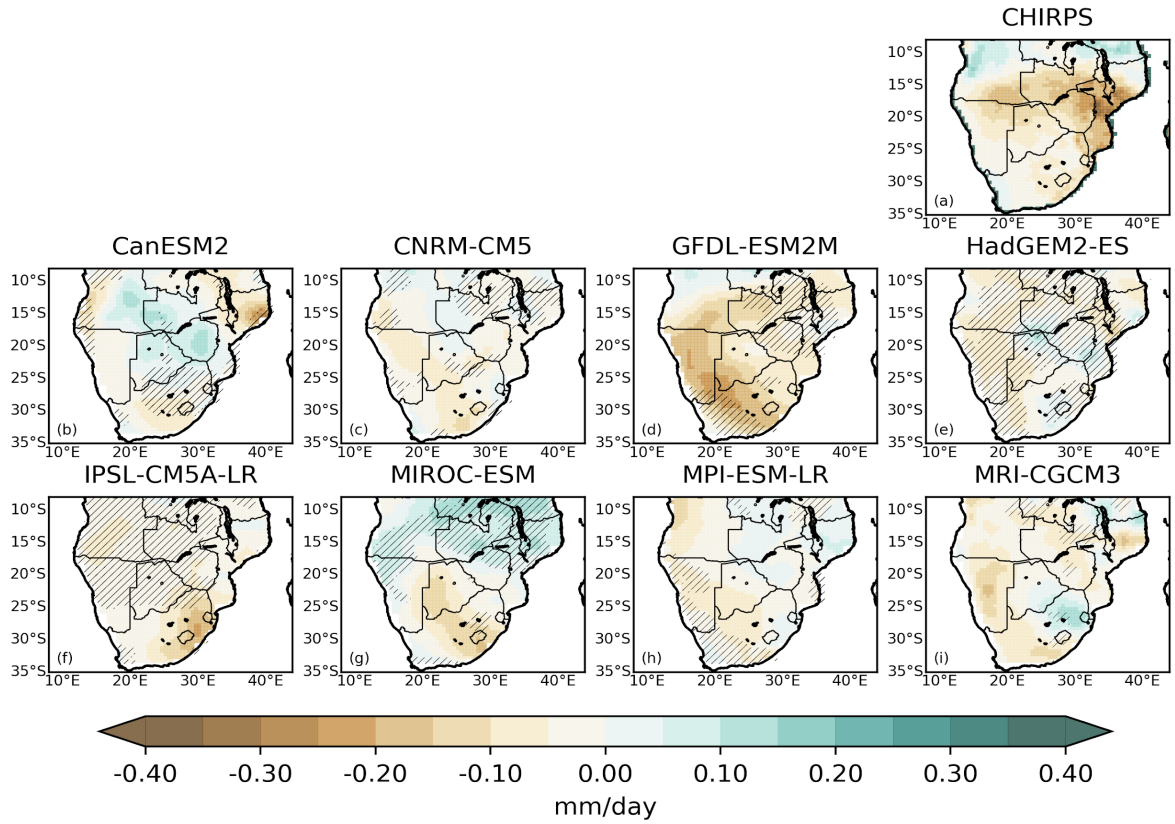

Figure 3.4: As in Figure 3.3, but for composite precipitation anomalies for co-behaviour mode four (CM4; summer (PC1 > 1 std), El Niño (PC2 > 1 std) and positive phase AAO (PC3 > 1 std)).

Similarly, during summer (PC1 > 1 std), El Niño (PC2 > 1 std) and positive AAO (PC3 > 1 std) co-behaving characterises dry summer conditions. We find a mixed representation of precipitation response across the region (CM4; Figure 3.4). However, many models fail to produce statistically strong response signals under these forcing conditions which is concerning as this is a very important drought pattern for the region. For instance, while MIROC-ESM (Figure 3.4g) captures peak intensity south of the region, in GFDL-ESM2M (Figure 3.4d), peak intensity is further southwest. Also, CanESM2 (Figure 3.4b) and MIROC-ESM (Figure 3.4g) show a wet bias relative to the observed (Figure 3.4a).

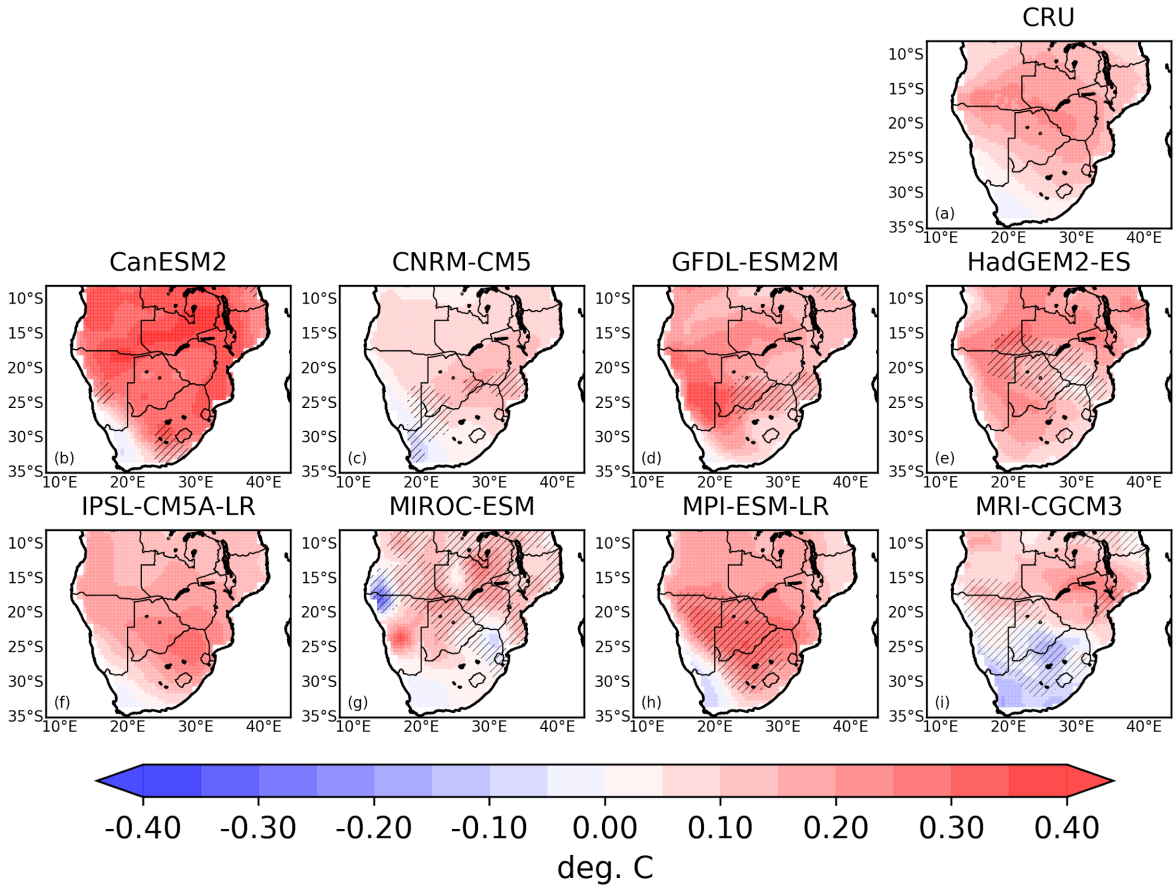

Figure 3.5: Spatial pattern of composite temperature anomalies for observed (a) and models (b) – (i) for co-behaviour mode four (CM4; summer (PC1 > 1 std), El Niño (PC2 > 1 std) and positive phase AAO (PC3 > 1 std)). Hatching denotes grid cells not statistically significant at 95% level.

Focusing on warm conditions (CM4; Figure 3.5) characterised by El Niño (PC2 > 1 std) co-behaving with positive AAO (PC3 > 1 std) during summer (PC1 > 1 std), over 75% of models are able to represent the significant warming found in CRU (Figure 3.5a) although a few overestimate its intensity, e.g. CanESM2 (Figure 3.5b). On the other hand, the models do well to capture the cooling around the southwestern part of the region with the exception being HadGEM2-ES (Figure 3.5e).

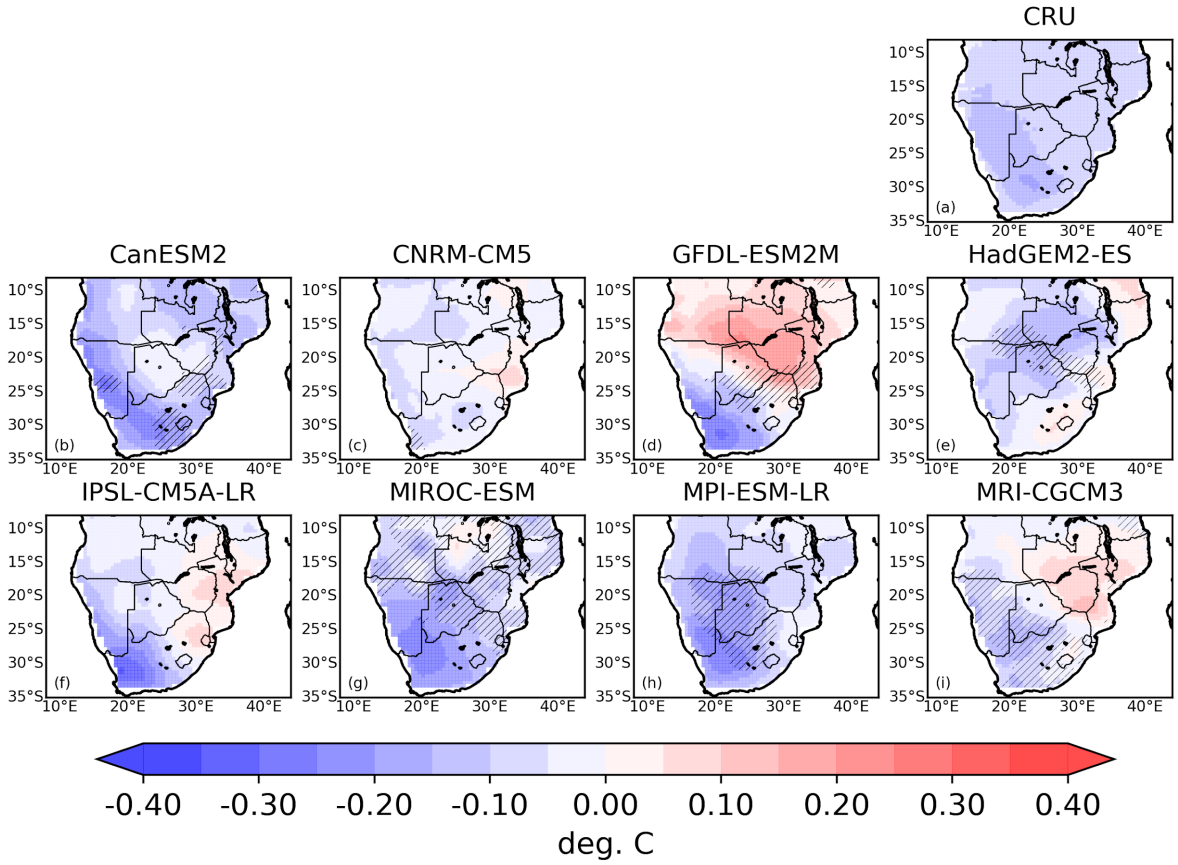

Figure 3.6: As in Figure 3.5, but for composite temperature anomalies for co-behaviour mode three (CM3; winter (PC1 < -1 std), La Niña (PC2 < -1 std) and positive phase AAO (PC3 > 1 std)).

Similarly, when La Niña (PC2 < -1 std) co-behaves with a positive AAO (PC3 > 1 std) under winter conditions (PC1 < -1 std), about 70% of the models are able to capture the cold conditions across most parts of the region, especially over South Africa and along the Atlantic coast (CM3; Figure 3.6). A few models, GFDL-ESM2M (Figure 3.6d), IPSL-CM5A-LR (Figure 3.6f) and MRI-CGCM3 (Figure 3.6i), predict warming in the north/central parts of the region.

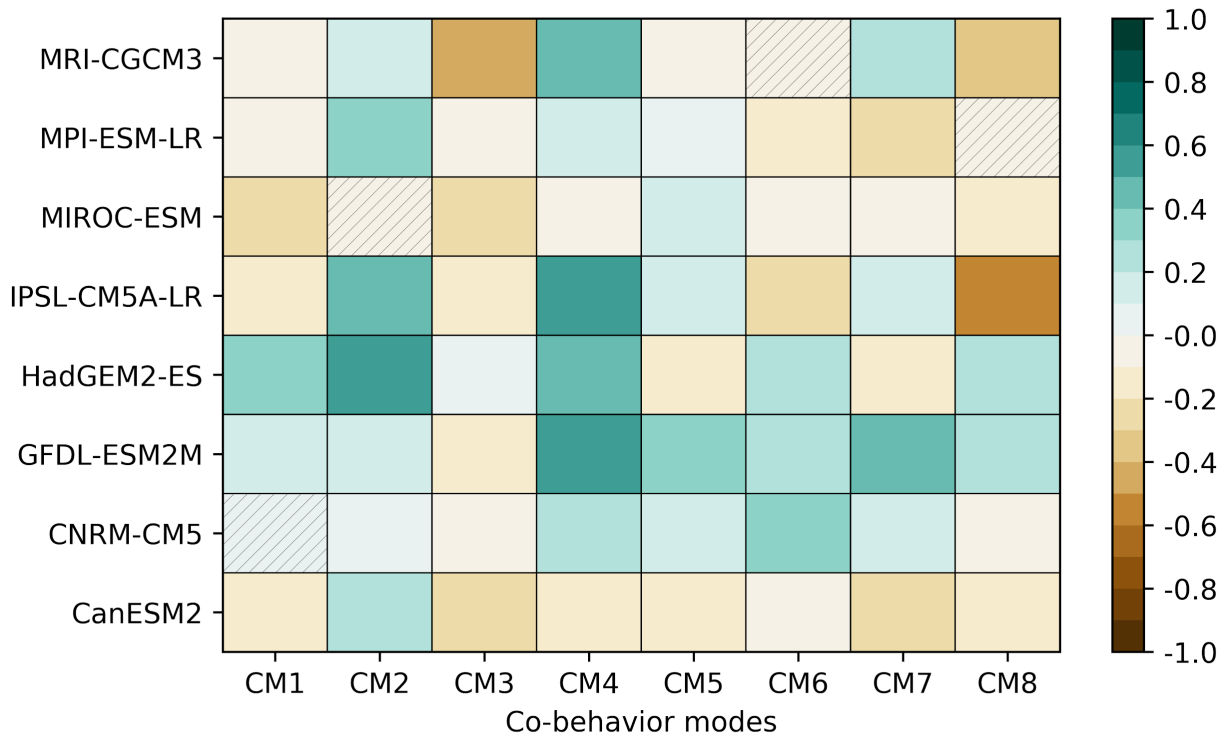

Figure 3.7: Correlations of models (listed on the left) versus observed co-behaviour modes (CMs) for composite precipitation based on Spearman rank-order spatial correlation expressed as a heatmap. Hatched boxes denote CMs where correlations are not statistically significant at 95% level.

Figure 3.7 shows spatial correlations between model composite response spatial patterns and observed composite response spatial patterns across CMs for precipitation. Here, we find no consistent patterns among models in representing CMs as we generally find weak correlations although significant. A possible reason for this to occur is when the sample size (number of months used in the composite) for a model for a particular CM differs significantly from that of the reanalysis (e.g. Faber and Fonseca 2014; Leppink et al. 2016). In contrast, the models show coherence in representing CMs for temperature (Figure 3.8) as they show strong and significant correlations with observed CMs.

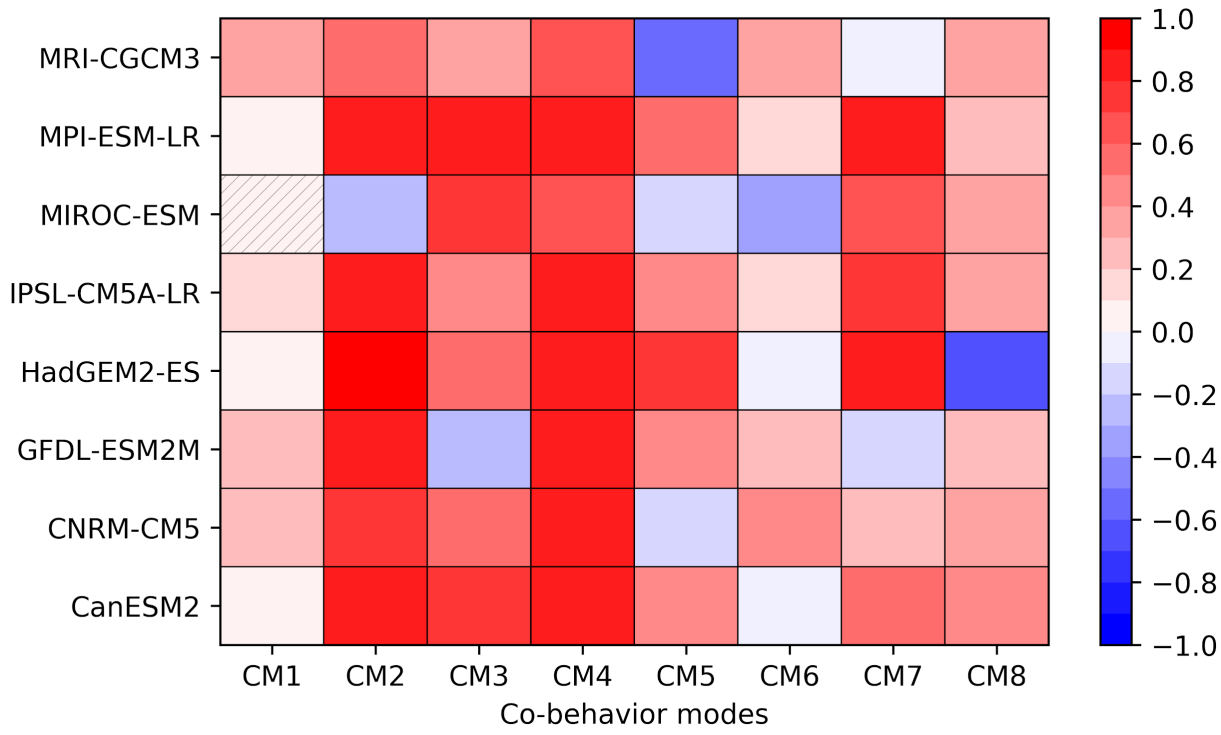

Figure 3.8: As in Figure 3.7, but for composite temperature.

Furthermore, we examined the model agreement and ensemble mean response for each combination with respect to all models for precipitation (Figure 3.9) and temperature (Figure 3.10) showing areas where at least 80% of models agree on the sign of response as hatches. For precipitation (Figure 3.9), the general circulation states of the multi-model ensemble mean of the GCMs are fairly consistent with the observed CMs (see Figures S3.2a-3.13a), however, there is not a strong agreement on the sign of the response under certain CMs and there are also differences in intensity and location. For instance, although the ensemble mean (Figure 3.9a) under the co-behaviour of La Niña (PC2 < -1 std) and negative AAO (PC3 < -1 std) during summers (PC1 > 1 std) captures intense wet conditions over central (southern Zambia, western Zimbabwe and northern Botswana) and western (Angola and Botswana coast) parts of the region and show strong model agreement on the sign of response, the magnitude is much lower and the location of the peak is not much spread about as noted in the observed (see Figure 3.3a).

Similarly, the intensity of peak dry conditions is much lower and located southwards, specifically central to southern parts of South Africa (Figure 3.9d) when El Niño (PC2 > 1 std) co-behaves with positive AAO (PC3 > 1 std) during summers (PC1 > 1 std). In the observed, intensity is higher and located to the northeast of the region; around Mozambique spreading towards Zimbabwe, Zambia and Angola (see Figure 3.4a). About 63% (~5 out of 8) of models represent the peak intensity much southward than the observed (not shown). We suggest that this southward shift of the peak intensity may be as a result of the models exaggerating the extent of the south Indian ocean convergence zone (SIOCZ) which brings precipitation to the region (see Grimm and Reason 2015; Tang et al. 2019).

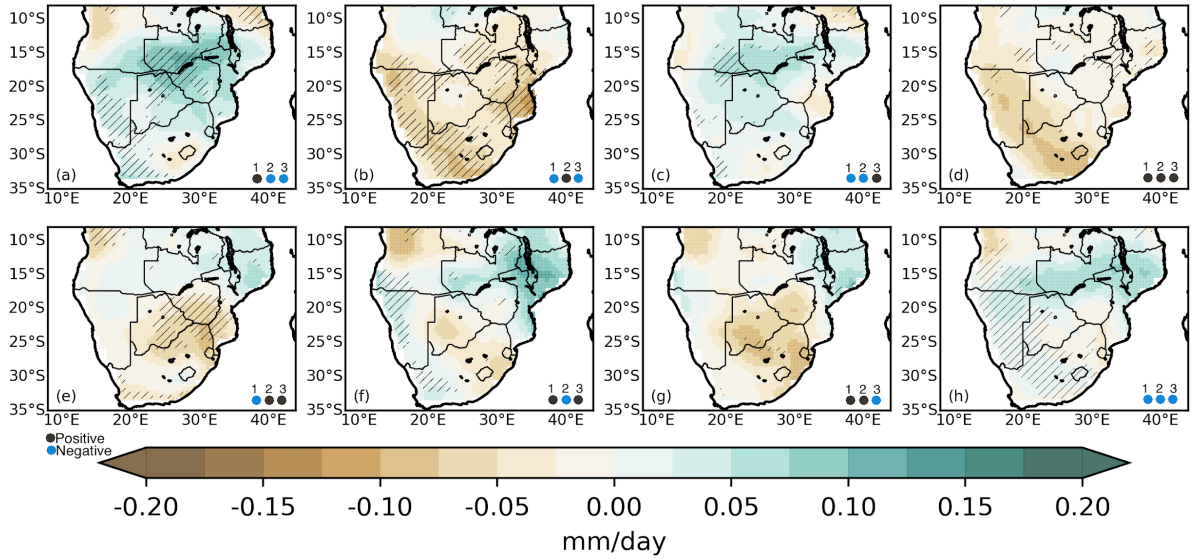

Figure 3.9: Multi-model mean spatial pattern for the combination of positive and negative phases of retained PCs (co-behaviour modes; CMs) for composite precipitation anomalies. Numbers on bottom right corner denote retained PCs (1)-(3) with colours showing positive (black) and negative (blue) phases. Hatching denotes grid-cells where at least 80% of models agree with the ensemble mean on the sign of the anomaly.

Focusing on temperature (Figure 3.10), there is also generally a good model agreement of sign of response under the CMs with the exception of CM7 when El Niño (PC2 > 1std) co-behaves with negative AAO (PC3 < -1 std) during summer (PC1 > 1

std) where models agree to the sign of the anomaly over a small area in the northern part of South Africa and southern Botswana (Figure 3.10g). Additionally, when AAO shifts to positive (Figure 3.10d), the peak of the warming is not centered but much more spread around the region when compared to the observed (Figure S3.12a). The models (Figure 3.10b) do not capture the longitudinal shift as noted in the observed (Figure S3.9a).

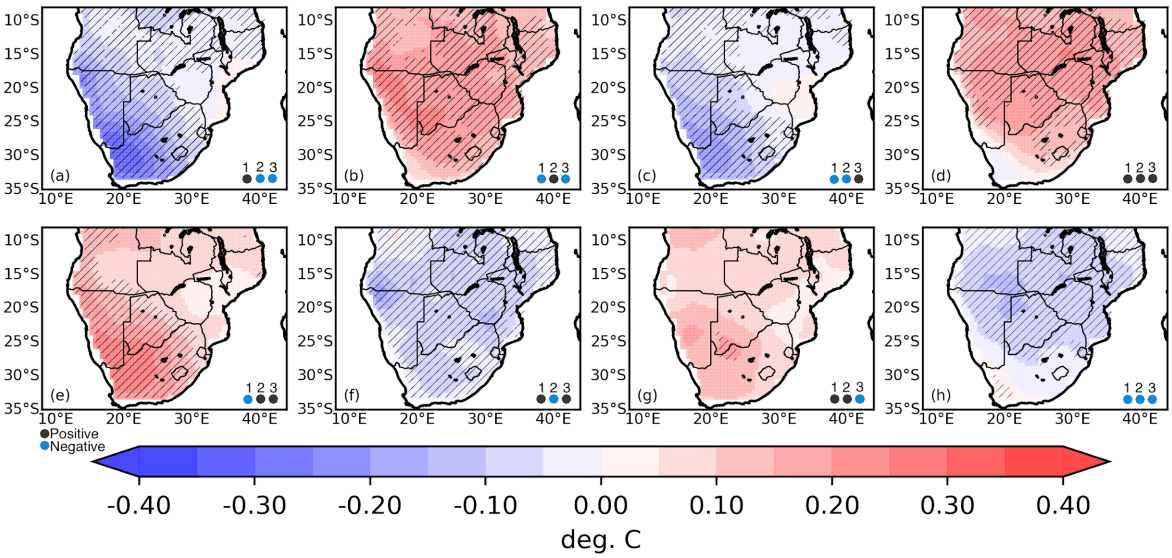

Figure 3.10: As in Figure. 3.9, but for composite temperature anomaly.

3.3 Summary and Conclusion

We assesses how CMIP5 GCMs are able to represent already identified co-behaviour modes in observation datasets and the nature of the variability. Precipitation and temperature datasets for eight GCMs under eight co-behaviour modes (CMs) are analysed in this study.

As a means to establish the relationship between surface expressions and large-scale processes we first identified the synoptic circulation states over the region using SOM. The seasonal frequency of occurrence for each SOM node with respect to each individual model is examined. An evaluation of the ERA-Interim reanalysis and the GCMs show the models are fairly consistent with the reanalysis in representing the

seasonal variability although in some nodes there are overestimations and in others underestimations.

For the purpose of identifying co-behaviour representation in models, we analyze how individual models and their ensemble mean represent co-behaviour modes as captured in precipitation and temperature observations. Results show the individual models reasonably simulate precipitation over southern Africa and is fairly consistent with observations. However, the models tend to overestimate precipitation maxima and its location, especially in northern to central parts of the region. For instance, when El Niño (PC2 > 1 std) co-behaves with positive AAO (PC3 > 1 std) during summer (PC1 > 1 std), some models show a wet bias north of the region while precipitation maxima in other models are further south when compared with the observed in co-behaviour mode four. This mode depicts an important drought pattern for the region and most models fail to produce statistically strong response signals.

We demonstrate that individual models fairly simulate the temperature response and are consistent with the observed over most parts of southern Africa for all co-behaviour modes. Most models are able to represent the maxima locations although the intensity is overestimated. The models do well to represent the temperature response when La Niña (PC2 < -1 std) co-behaves with a positive AAO (PC3 > 1 std) under winter conditions (PC1 < -1 std) where about 70% of the models accurately simulate the response. However, in some instances some models show a warm bias over some areas (north/central parts) of cooling in the observed but does well in representing the maxima and its location. Again, over 75% of models are able to adequately simulate the temperature response when El Niño (PC2 > 1 std) co-behaves with positive AAO (PC3 > 1 std) during summer (PC1 > 1 std).

Furthermore, we show that there are generally significant weak correlations for precipitation for most model co-behaviour modes when compared with observation. However, some individual models show significant positive correlations on specific co-behaviour modes. Similarly, correlations in temperature is widespread with most models showing significant strong correlations on most co-behaviour modes. Thus we generally find coherent temperature responses in models as opposed to a not so

coherent response in precipitation across the models to large-scale co-behaving processes.

On the other hand, the multi-model ensemble mean shows a good representation of observed co-behaviour modes with a larger spread in precipitation maxima when compared with the individual GCMs and the observation. However, differences in characteristics such as the location and intensity of the maxima to observation as a result of biases in individual models persists (see Eyring et al. 2019). This may account for the low number of grid-cells where models agree to the sign of the anomaly of the ensemble mean. For temperature response, the multi-model ensemble mean is consistent with observation. There is a strong model agreement on most co-behaviour modes with the exception of a co-behaviour of El Niño (PC2 > 1 std) and negative AAO (PC3 < -1 std) during summer (PC1 > 1 std) where most models do not agree.

We assert that evaluating the co-behaviour of processes in GCMs can provide a rich source of information for how models represent large-scale processes. This may also be useful for climate model evaluation as it is important that models adequately represent the interactions amongst climate processes over southern Africa or any region without singular circulation control for that matter. As models become more successful in simulating these climate process interactions, climate scientists will have greater confidence in making future projections.

Acknowledgements

This work was conducted under the Future Resilience for African CiTies and Lands (FRACTAL) project (Grant NE/M020347/1), which is part of Future Climate for Africa (FCFA) program funded by the U.K. Department for International Development (DFID) and Natural Environment Research Council (NERC). The authors are grateful to Grigory Nikulin at Rossby Centre, Swedish Meteorological and Hydrological Institute, Sweden, for the provision and use of the Tropical Rainbelt index. The first author is grateful to the University of Cape Town for funding assistance. Additionally, the first author is thankful to African Climate and Development Initiative (ACDI) of University of Cape Town, Tyndall Centre for Climate Change and Climatic Research Unit (CRU)

under the Newton PhD Partnering Scheme funded by Research Councils UK (RCUK) and the National Research Foundation (NRF) of South Africa. We acknowledge the World Climate Research Programme's Working Group on Coupled Modelling, which is responsible for Coupled Model Intercomparison Project (CMIP), and we thank the climate modelling groups (listed in Table 3.1 of this paper) for producing and making available their model output. We are grateful for helpful comments and suggestions by the anonymous reviewers towards improving the manuscript.

Chapter 4

Process-Based Model Evaluation of the Co-Behavior of Regional Climate Drivers over Southern Africa

What are the possible mechanisms responsible for how the models are representing co-behaviour?

Specific Questions?

- What are the likely sources of variability in model representation of co-behaviour drivers?

Abstract

This paper evaluates Global Climate Model (GCM) representation of the influence of multiple process interactions on regional climates, and is the third of a series of papers exploring the combinatory influence of large-scale processes over southern African climate. GCM plausibility for future projections is in part dependent on the models skill in capturing the joint behavior of the processes governing regional climate. Such a process-based evaluation provides a more holistic approach to examine the mechanisms driving regional climate responses to climate change. In this study, a previously developed methodology is applied to examine the interacting influence of large-scale atmospheric processes (co-behavior) in order to evaluate GCM historical simulations representations for southern Africa. The results show that the evaluated GCMs generally represent the co-behavior of El Niño-Southern Oscillation (ENSO) and Antarctic Oscillation (AAO) large-scale processes in relation to the regional circulation processes. However, in representing the variability and co-behavior of the Inter-tropical Convergence Zone (ITCZ) the GCMs show notable differences compared to the reanalysis data.

A paper based on this part is to be submitted to a journal:

"Process-Based Evaluation of the Co-Behavior of Regional Climate Drivers over Southern Africa"

K. A. Quagraine, *C. Jack, B. Hewitson, P. Wolski, I. Pinto and C. Lennard*

4. Introduction

Global Climate Model (GCM) ensembles from the Coupled Model Intercomparison Project Phase 5 (CMIP5; Taylor et al. 2012) and Phase 6 (CMIP6; Eyring et al. 2016) are routinely and extensively used, either directly, or in conjunction with various downscaling methods, to project future climate change at spatial scales relevant to society.

Multi-model ensembles may be used to approximate model structural uncertainty, a primary source of overall uncertainty (Hawkins and Sutton 2011), by analysing ensemble spread in projected variables. Model democracy (e.g. Knutti 2010), where all members of the ensemble are treated equally regardless of relative or absolute model performance, remains a common practice. The consequence of this is that unrealistic models that are also outliers in projected changes can result in an increase in the ensemble range of projected change, the most common characterisation of model uncertainty.

To constrain uncertainty, poorly performing models may be excluded, or their contribution to ensemble statistics (e.g. ensemble mean) down-weighted. Increasingly, where regional scale climate projections are being developed, models are evaluated based on their ability to represent relevant regional climate characteristics (e.g. McSweeney et al. 2015; James et al. 2015; Tamoffo et al. 2019). Even in cases where the objective is not an estimate of projected changes to inform decision making, but rather an understanding of future climate dynamics, evaluation of model realism or performance is valuable.

When evaluating the models, a key decision is the selection of performance metric(s) that are most relevant to the region. Africa, a region which is recognized to be highly vulnerable to the effects of climate change (Niang et al. 2014) has historically not been a region of focus of GCM improvements (James et al. 2015, 2018). While programs such as CORDEX (COrdinated Regional Downscaling EXperiment, Giorgi et al. 2009) have placed focus on Regional Climate Model (RCM) and their performance for specific regions, RCM performance remains dependent on the realism of the driving GCMs (Dosio 2017; Pinto et al. 2018; Tang et al. 2019).

Some examples of climate features relevant to Africa but poorly represented by many GCMs include mesoscale convective systems and the sharp temperature and aridity gradients in the Sahel (James et al. 2018). Others (e.g. Samanta et al. 2019; Yang et al. 2015) report cold equatorial sea surface temperature (SST) biases in GCMs affect how models position the ITCZ. Likewise other studies highlight the challenges GCMs have in representing the inter-annual variability of rainfall and their ability to capture the west African monsoon (McSweeney et al. 2015).

GCMs are often evaluated by comparing their simulations of historical surface variables (temperate and rainfall) to historical observations of surface variables (bias evaluation) because these are the variables that are commonly important to societal decision making and are often used to drive impacts models such as hydrology models. However, the representation of surface variables, particularly at smaller spatial scales, is arguably the weakest characteristic of GCMs. This is because the associated processes of convection, orographic rainfall, and local land surface and topography, are generally parameterized estimations or coarse scale representations.

It is plausible that a GCM might realistically represent regional climate dynamics, but fail to represent the local scale processes and so be excluded through a bias evaluation. There is no certainty that models excluded based on bias evaluation are not able to generate plausible future projections (Knutti 2010; McSweeney et al. 2015) or that models which are included through such an analysis are more robust for future projections. A process-based model evaluation provides a means to assess model skill by investigating the underlying physical mechanisms and potential drivers of future climate change projections (James et al. 2015; McSweeney et al. 2015). This is arguably more defensible and robust as models are evaluated based on their representation of fundamental dynamical processes (e.g. James et al. 2015; Pinto et al. 2018). For example, some recent process-based model evaluation studies over southern Africa (e.g. Pinto et al. 2018) focused on changes in precipitation and the circulation processes driving those projected changes as well as agreement between RCM and parent GCMs. Munday and Washington (2018) assessed reliability of rainfall estimates by exploring the individual climate processes associated with rainfall bias. Dieppois et al. (2015) examined ENSO impact on southern African rainfall while a

study by Munday and Washington (2017) explored the role of the Angola low in southern African precipitation in coupled models.

Regional climate variability is a result of interactions between multiple climate drivers and processes (Daron et al. 2019) and these interactions cannot be assumed to be simply linear and or additive. The development of methods that examine the combined influence and co-behavior of drivers and processes such as ENSO, ITCZ, or AAO may offer new insights into regional climate variability and change, and may provide more comprehensive and robust model evaluations.

Using the ERA-Interim reanalysis (Dee et al. 2011), Quagraine et al. (2019) (hereafter Q19) developed a methodology to examine the co-behavior of ENSO, ITCZ, and AAO and their influence on precipitation and temperature over southern Africa. Quagraine et al. (2020) (hereafter Q20) assessed the performance of eight models from the CMIP5 experiment in representing precipitation and temperature responses to different driving process co-behavior modes. In this paper the approach is developed further in order to examine how the same set of CMIP5 models represent variability and co-behavior of the driving processes and so provide a process-based analysis of the GCM performance.

4.1 Data and methods

4.1.1 Data

To represent observed circulation and regional to global scale climate indices the daily ERA-Interim (Dee et al. 2011) are used with a grid resolution of 0.75° latitude/longitude. It is assumed that the reanalysis fields are acceptable approximations of reality with respect to regional scale circulation states and large-scale climate indices (e.g. Brands et al. 2013; Dee et al. 2011; Zhang et al. 2013).

Eight models from the CMIP5 GCMs (Table 1) are used in the study. These were selected based on the availability of variables needed for the study at the time of analysis, specifically daily geopotential height at 700-hPa, surface pressure, precipitation, and monthly SSTs. Geopotential height at the 700-hPa level is used in

order to represent tropical through to mid-latitude synoptic weather systems which encapsulates subtropical high pressures, continental low pressures, easterly and westerly waves. Prior to analysis, all GCM fields are re-gridded to the same resolution as the ERA-Interim reanalysis (0.75°) using nearest neighbour interpolation (Accadia et al. 2003). We recognise the ERA-Interim resolution is finer than all the GCMs native resolutions and would therefore expect the resultant GCM fields to have lower spatial and temporal variance than the ERA-interim at the grid scale. However, the analysis approach is not strongly sensitive to grid scale variance.

4.1.2 Methods

The co-behavior methodology is described in detail in Q19. In brief the method identifies correlated modes of variability across multiple potential drivers of local climate responses which range from global scale drivers such as ENSO, through to synoptic scale circulation states. The drivers are collated into a matrix of index variables (e.g. Niño 3.4 index values) through time. Principal Component Analysis (PCA; Lever et al. 2017; Jolliffe and Cadima 2016) is then used to identify orthogonal modes of variability within this matrix where each particular mode of variability represents combinations (co-behavior) of the original drivers. The analysis of local surface responses of temperature and precipitation to the newly identified modes of variability is then used to identify the role of co-behaving drivers in local scale surface (e.g. rainfall and temperature) climate variability as detailed in Q19.

Based on the prior work (Q19, Q20) three indices are used to characterise the large-scale drivers of the southern Africa region. These indices capture the ITCZ (represented by the Tropical Rain Belt Index; TRBI: Nikulin and Hewitson 2019), the AAO, and ENSO. As before PCA is used to identify dominant modes of co-variability of these indices. The AAO index is calculated using the leading mode of the Empirical Orthogonal Function (EOF) for daily 700-hPa geopotential height anomalies poleward of 20^{o} S (Thompson and Wallace 2000b). The TRBI uses cross-sectional (zonal mean) precipitation over 25^{o}N to 25^{o}S latitudinal belt to fit a gaussian distribution with parameters representing the width, latitudinal location, and peak intensity of the TRB. TRBI is preferred to other indices of the ITCZ because of its simplicity and efficiency in describing the temporal-spatial characteristics of the ITCZ over Africa (Nikulin and

Hewitson 2019). In this study we only use the intensity part of the index. The ENSO index uses the SST anomalies averaged over 5^{o} N to 5^{o} S, 170^{o} W to 120^{o} W (Niño 3.4 region).

The three process indices represent the important large-scale processes that condition the southern African regional climate and their individual influence are well understood (e.g. Engelbrecht et al. 2013; Meque and Abiodun 2015; Nicholson 2000; Reason and Rouault 2005; Suzuki 2011; Weldon and Reason 2014).

While large-scale processes such as the ones described above play an important role in conditioning regional climate variability ultimately it is the response of the regional synoptic scale circulation interacting with local scale features such as topography that give rise to the local scale climate (e.g. Wolski et al. 2018).

In order to capture the role of synoptic scale circulation the synoptic patterns are characterised with generalised archetypical synoptic circulation states using Self Organizing Maps (SOMs; Kohonen 2001; Hewitson and Crane 2002). Following prior work, a 12-node SOM is trained using daily standardised anomaly fields of 700-hPa ERA-Interim geopotential height over the period, 1980-2013 (Figure 4.1a(i)). The standardization is done in order to avoid areas of high variance dominating the total variance represented by the SOM.

Each day in the timeseries of 700-hPa geopotential height anomalies is then mapped onto one of the 12 archetype synoptic circulation patterns of the SOM to create a time series index of synoptic states.

The GCM 700-hPa fields are mapped onto the reanalysis trained-SOM space (Figure 4.1a(ii)) to create comparable index time series of synoptic states. We note that mapping GCM circulation fields, that may contain significant magnitude and pattern biases, onto a SOM trained with reanalysis fields could manifest in anomalously large frequencies of synoptic states that are on the tails of the distribution found in the ERA data. However, a comparison of the mean mapping distance of each GCMs daily circulation pattern to the SOM nodes (not shown) reveals that in most cases, the GCMs have mapping distances smaller than the reanalysis, likely reflecting the

reduced variance of the GCM compared to the real atmosphere as represented by the ERA-Interim data.

The time series index of synoptic patterns is then low-pass filtered with a 3-month moving average filter to remove high frequency variability in order to focus on lower frequency variability. Using the ERA-based time series of synoptic patterns, this is then combined with the equivalent monthly indices of ENSO, AAO and TRBI. A PCA is then used to identify dominant modes of co-variability. As in the prior work, the PCA uses a correlation matrix with varimax rotation of the principal components (e.g. Jolliffe and Cadima 2016). Three of the principal components (PCs) are retained at 90% significance level determined using the N-Rule stopping rule (Peres-Neto et al. 2005). The PC score time series then represents the three co-behavior modes of the large-scale indices in conjunction with the regional synoptic patterns.

To create the equivalent PC score time series for the GCMs, each GCM's data time series of ENSO, AAO and TRBI and their synoptic pattern index are projected onto the eigenvectors of the ERA-based PCA (Figure 4.1b(ii)). Projecting the GCM data onto the ERA-based PCA eigenvectors enables comparison of the variance of each mode of variability produced by each GCM in relation to that seen in ERA. This allows examination of the differences and similarities in how the GCMs are representing the underlying co-behavior of processes.

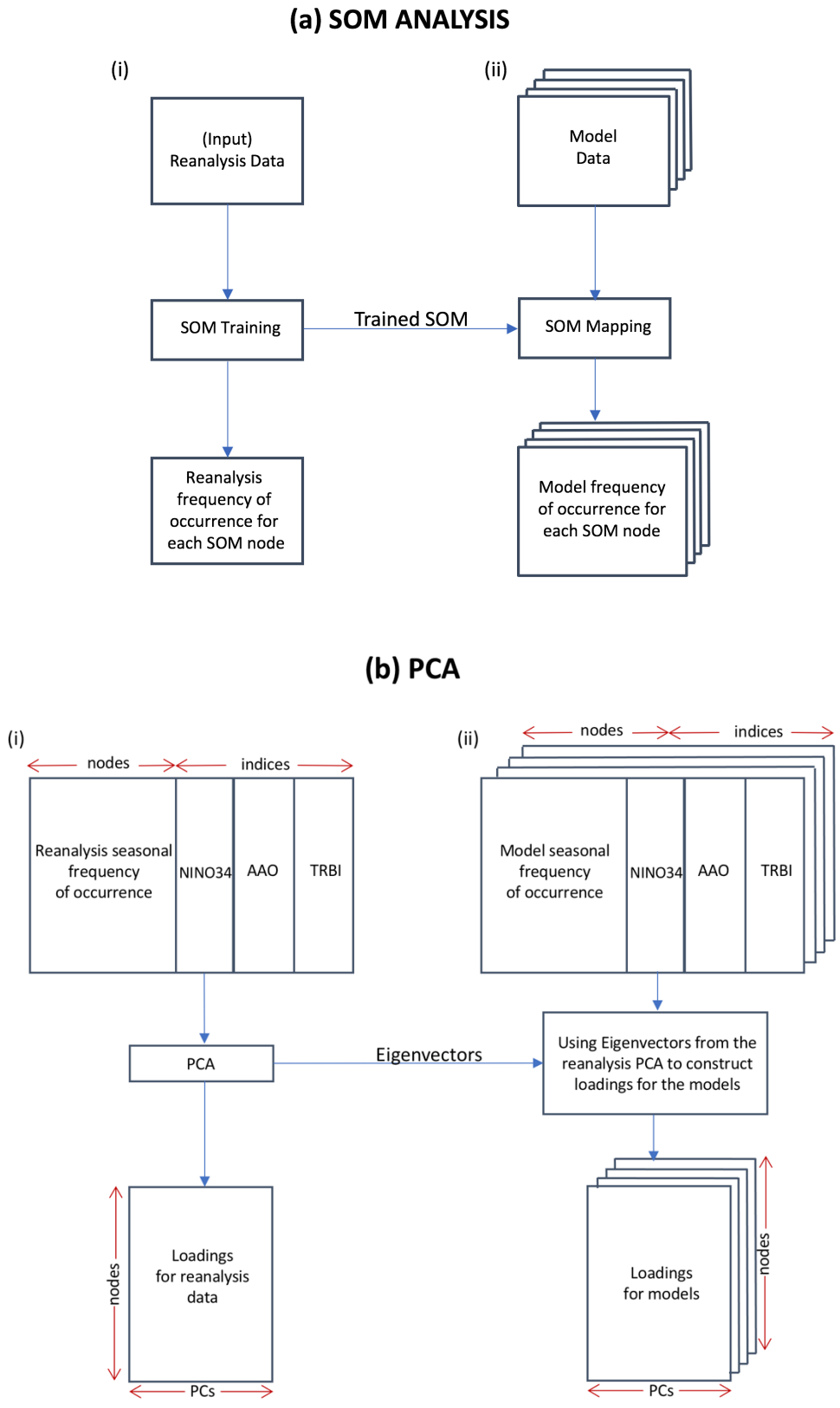

Figure 4.1: A schematic representation of the implementation of the (a) Self-Organizing Map (SOM) and (b) Principal Component Analysis (PCA; modified after Quagraine et al. 2019).

4.2 Results and discussions

In this section the results are described and discussed. Before co-behavior is discussed, the preliminary analyses of SOM node mappings and climate indices are unpacked and discussed as these provide important background to the co-behavior analysis.

4.2.1 SOM node mapping of 700 hPa geopotential height anomalies and frequency distribution

Figure 4.2 shows the characteristic synoptic patterns of the 700-hPa geopotential height anomaly circulation over southern Africa. The circulation states typically associated with winter (and a dry continental interior) are most represented by nodes 1, 2, 5, and 9 (inset in Figure 4.2). Nodes 1 and 2 represent mid-latitude westerlies in their northerly position whereas patterns in nodes 5 and 9 are typically subtropical highs. Under winter conditions, the subtropical high pressure system migrates equatorward with the continental high pressure systems now intensified and, coupled with reduced surface heating, suppressing convection in the continental interior. The passing mid-latitude cyclonic disturbances with associated cold fronts are primarily responsible for precipitation along the southwestern coast of South Africa during the winter season.

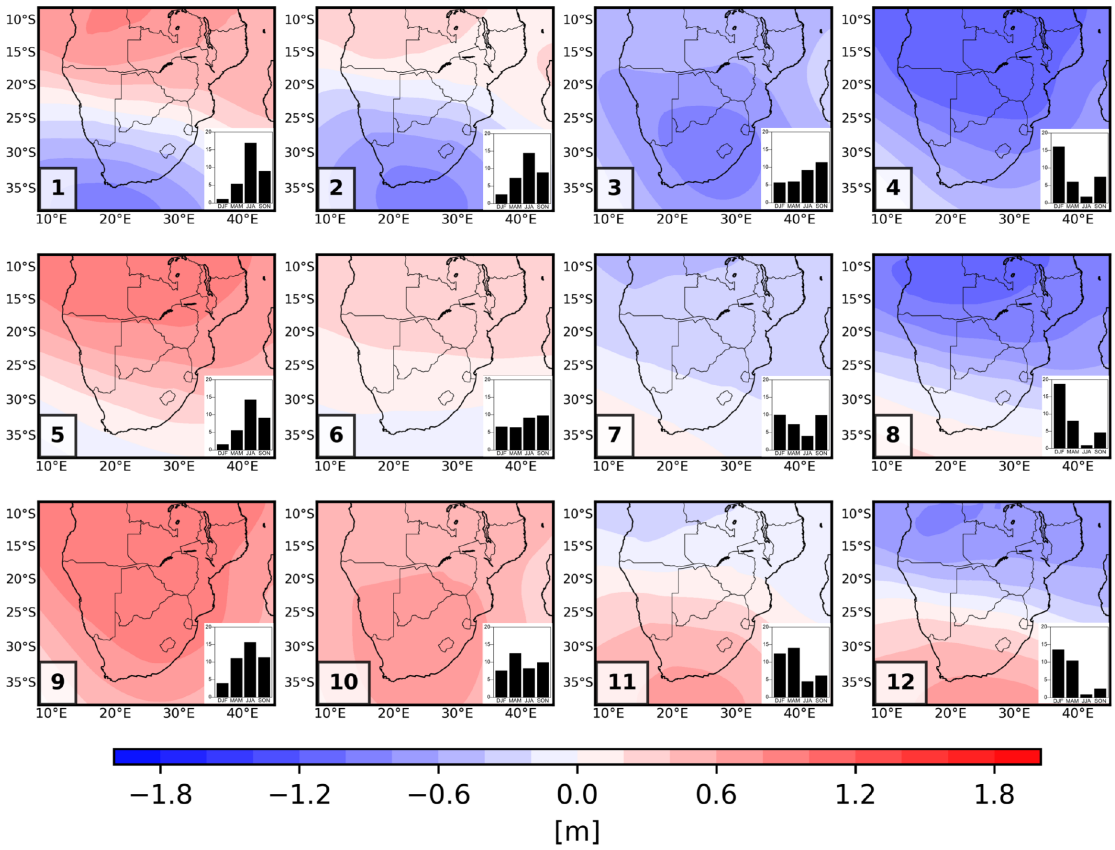

Figure 4.2: The 4x3 SOM using daily ERA-Interim geopotential height (Z) anomalies at 700-hPa for southern Africa for the period 1980-2013. Bar graph inset shows SOM per-node seasonal frequency variation; DJF (Summer), MAM (Autumn), JJA (Winter) and SON (Spring). Node numbers are shown on the bottom left.

SOM nodes 4, 8, and 12 occur most frequently during summer months (inset Figure 4.2) and represent continental low pressure systems which are typical of summer (wet) conditions in the interior. Here, the mid-latitude low pressure systems are not as apparent and instead the sub-continent is dominated by a weakened high pressure or (in node 4) a tropical easterly low pressure pattern. Frontal systems are displaced poleward leading to drier conditions over the southwestern coast of South Africa due to the presence of a high pressure system located southwest of the domain. Collectively, the SOM nodes represent the range of generalised synoptic events across the seasons, including characteristic intermediate synoptic states in nodes 3, 6, 7, 10 and 11.

In Figure 4.3 we map the frequency of synoptic states represented by each SOM node for the ERA-Interim reanalysis and for each of the eight GCMs over the common evaluation period (1980 - 2013) for austral summer (DJF, Figure 4.3a) and austral winter (JJA, Figure 4.3b). We find that the models tend to overestimate the frequency of some summer synoptic states (e.g. Figure 4.3a; nodes 11 and 12) and winter states (e.g. Figure 4.3b; nodes 3-4-8). For instance, all the models, except MIROC-ESM, overestimate, the frequency of summer state circulation on node 12 (Figure 4.3a), and that overestimation is particularly large for HadGEM2-ES and IPSL-CM5A GCMs. This deviation from the reanalysis frequencies is not peculiar to this node, but is observed across most SOM nodes in both summer and winter states. Thus we can infer that models may be representing a reduced regional circulation variability and failing to adequately represent the full range of synoptic variability, thus under-representing some states while over-representing others, e.g. Figure 4.3a; node 4 and Figure 4.3b; node 4. While in general this is likely due to the reduced variability of a model compared to reality, some studies (e.g. Munday and Washington 2018; Eyring et al. 2019) have also attributed this to the difficulty in resolving particular regional synoptic processes such as tropical/mid-latitude interactions. The consequence of models underestimating say, node 4 and overestimating say node 12 implies models fail to produce the identified reanalysis circulation pattern in node 4, but rather they simulate often the circulation pattern associated with node 12.

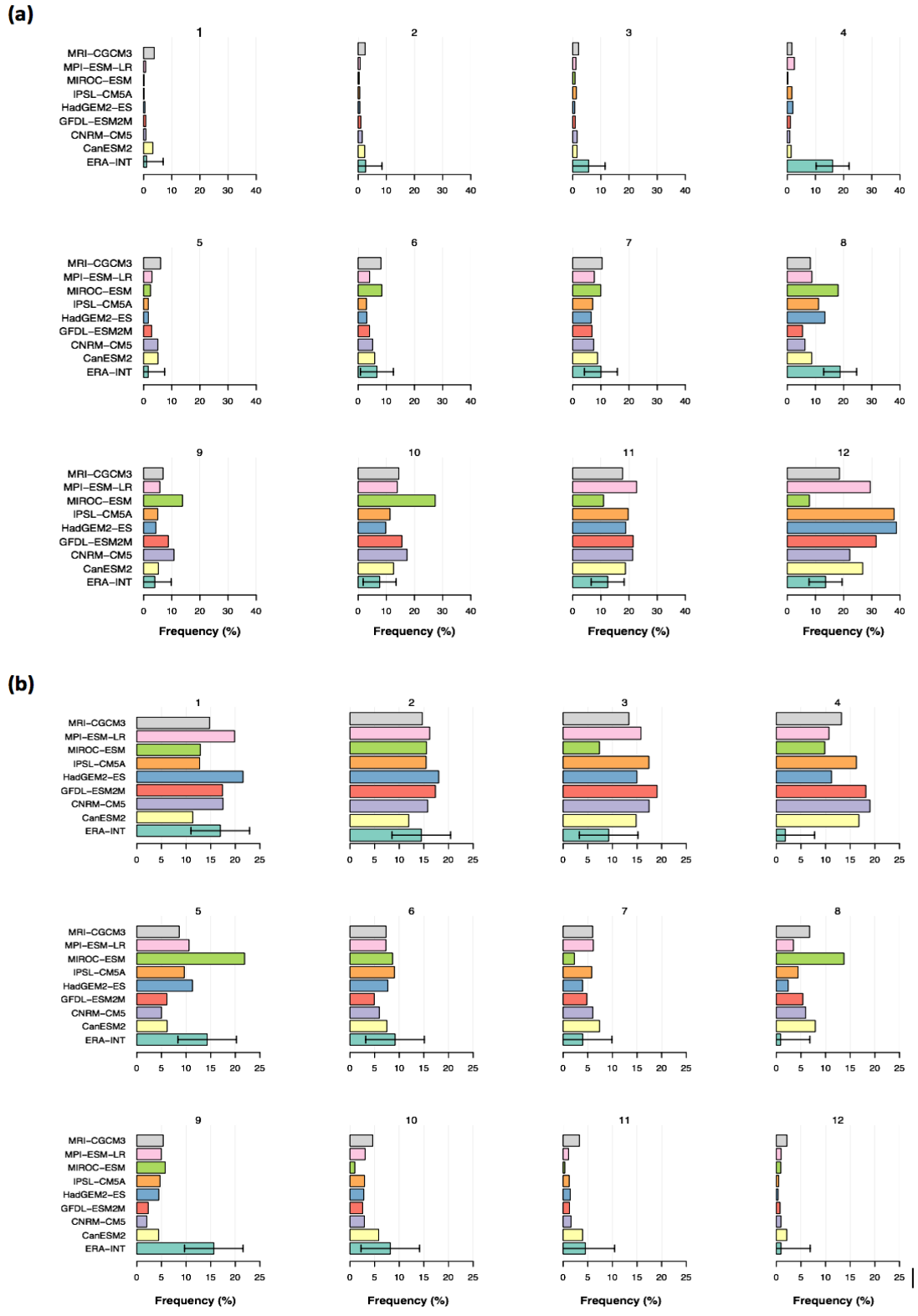

Figure 4.3: Model variability of the frequency of occurrence (%) mapped to each SOM node for the training period 1980-2013; (a) for summer (DJF) and (b) for winter (JJA) respectively. The error bars on the reanalysis shows the uncertainty range at 95% confidence level. The node numbers (top center) correspond to SOM node numbers in Figure 4.2.

4.2.2 Internal state variability across GCMs in representation of climate indices

The next step in the comparison between GCMs and reanalysis is to compare the variances of the three standard climate indices (TRBI, ENSO, and AAO) across the GCMs and reanalysis. This allows the evaluation of the magnitude of variability of these indices within each model with respect to the reanalysis and provides a basis for further analysis of co-behavior in the next section.

The ITCZ intensity is represented by the TRBI. The models have a higher variance with a large spread when compared with the reanalysis (Figure 4.4). Earlier studies (e.g. O'Gorman and Singh 2013; Yang et al. 2015; Cook and Vizy 2016; Lazenby et al. 2016; Pinto et al. 2018; Eyring et al. 2019; Quagraine et al. 2020; Samanta et al. 2019) have shown most models overestimate tropical precipitation with a large range in magnitude over this region, and thus would be reflected in the higher variance of the TRBI. These studies have asserted that this bias and spread may be as a result of the different precipitation parameterization schemes and their interaction with model dynamics and thus represent a measure of the uncertainty in the models tropical rainfall precipitation estimation.

The inability of models to accurately represent tropical precipitation has been suggested to be due convective precipitation parameterization. The presence of different dynamics within models over land and ocean, and their representation of moisture convergence flux has been identified as a major contributor to this error (Lazenby et al. 2016). Previous work (Q19) has identified the TRBI as a proxy for an important regional process driver (ITCZ). The diverse representation of TRBI variance in CMIP5 GCMs suggests TRBI variance is a useful measure of GCM performance in southern Africa.

The analysis of the variance in ENSO and AAO indices reveals both indices have lower inter-model spread and difference between model and the ERA reanalysis (Figure 4.4). The spread in models representing ENSO has been attributed to the challenge of simulating the sea-air interactions that are responsible for distinguishing phase transitions (e.g. Lu et al. 2018). Our findings also support earlier study by Kim

and Yu (2012) who also found that CMIP5 GCMs fairly represent the ENSO teleconnection and in some cases over-estimate ENSO variability.

For AAO, there is very little inter-model differences as well as very little difference between the models and the ERA reanalysis which suggests the GCMs are representing the magnitude of AAO variance realistically. Even so, this does not imply that the GCMs are correctly simulating any of the underlying processes, but merely that the variance of this particular indices, which provides some level of diagnostic of the underlying processes, are realistic.

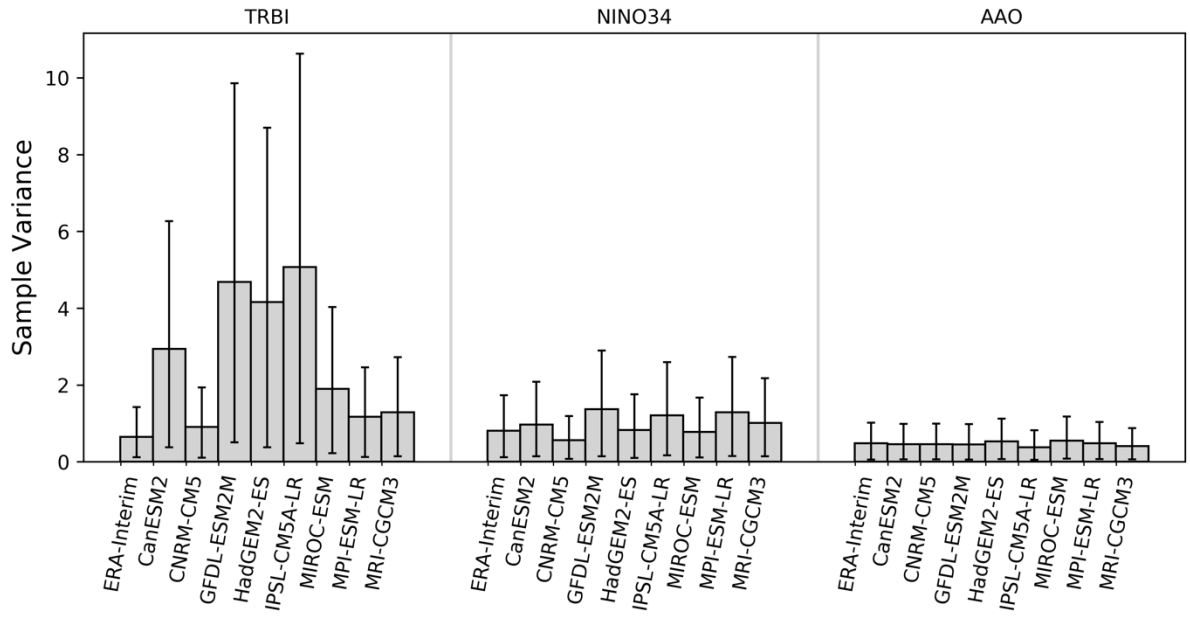

Figure 4.4: Sample variance across process indices developed from ERA-Interim reanalysis and a set of CMIP5 GCMs.

4.2.3 Process co-behaviour analysis

As noted in the introduction, regional synoptic circulation variability is expected to partially correlate with the regionally relevant large-scale climate indices. For example, one would expect that southern African regional circulation would correlate to some extent with the Niño 3.4 index. This is because the process link between Pacific Ocean variability and southern African rainfall, and temperature variability manifests through circulation anomalies (e.g. Reason and Jagadheesha 2005).

To explore the relationships between synoptic circulation states and climate indices, we calculate the non-parametric correlation between the frequency of synoptic circulation states and the large-scale conditioning process indices for each GCM. The correlations are then compared to those derived from the reanalysis data (Figure 4.5). Ideally the GCMs would demonstrate similar correlations to those in the reanalysis if they are realistically representing the underlying physical processes that translate large-scale variability to regional variability. The core winter and summer SOM circulation states correlated with the conditioning large-scale process indices is shown in Figure 4.5.

In general, ERA-Interim shows a statistically significant but weak negative correlation of TRBI with winter state variability, e.g. TRBI versus W1, W2, and W5 (Figure 4.5a). This is physically interpretable as a weak ITCZ being associated with drier summer states and/or dominance of winter states. The weak ITCZ influence on winter and transition states can be attributed to the fact that these states are mostly dominated by mid-latitude circulation systems, and weak continental lows and highs respectively. The models (Figure 4.5b-i) generally fail to reproduce the same correlation structure for TRBI.

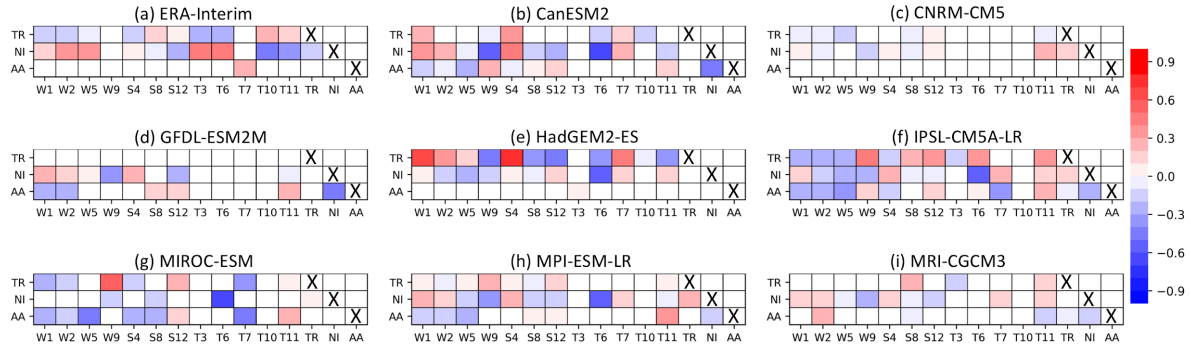

Figure 4.5: Correlation matrix of some selected SOM circulation states and climate process indices showing pattern of relationships for ERA-Interim reanalysis and a set of CMIP5 GCMs. For the set of CMIP5 GCMs we show their biases from the ERA-Interim. All winter states in the SOM are denoted by W, summer states by S and transition states by T. Boxes marked 'X' denote perfect correlations. All numbers that follow represent SOM node numbers. Climate indices are denoted by TR=TRBI, NI=NINO3.4 and AA=AAO. White boxes show differences that are not statistically significant at 95% level.

Similarly, there is significant positive correlation between the TRBI and circulations associated with summer states which are typically dominated by strong continental lows (e.g. S8) and transition states (e.g. T10, T11) with weak continental highs. This is consistent with southern African climate and is one of the key mechanisms for rainfall over the region during summer. During summer, the ITCZ extends towards 10^0 S to 20^0 S inducing convergence over Congo and Angola while interacting with the inter-ocean convergence zone troughs over the region thereby producing strong continental lows to yield rain-bearing synoptic systems. Further analysis may be needed to understand the strong correlation of TRBI with transition states. However, one explanation may be that during transition states, synoptic circulations typical of either summer can occur, and such circulation may be influenced by the ITCZ.

In the reanalysis, the Niño 3.4 index correlates strongly with the frequency of winter states, (Figure 4.5a) e.g. W1, W2 and W5 (typical mid-latitude circulation and tropical high pressure systems), and some transition states, e.g. T3 and T6 (weak continental low and high respectively) while showing a weak negative correlation with the frequency of summer states (e.g. S8, S12) and other transition states (e.g. T10 and T11). In some models this relationship is stronger (Figure 4.5b, d and h), while for others, it is weak (Figure 4.5c, e and g). Thus to some extent, ENSO does impact mid-latitude systems as well as continental highs and lows over the region although the models do not consistently replicate that pattern. The models show weak correlations with the frequency of winter nodes e.g. W1 and W2, for AAO, which is contrary to the reanalysis, where such correlation is not present. In the reanalysis, AAO correlates strongly with a transition node (T7) which is circulation dominated by a weak continental low.

4.2.4 Additional explanatory analysis for co-behavior representation in GCMs

We use the PC analysis to gain an understanding on how each model relates the circulation states identified and the process indices to capture co-behavior.

For all models, PC1 captures a smaller proportion of the total variance of the analysed variables compared to that in the reanalysis (Figure 4.6). For instance, the highest proportion of total variance captured by PC1 in a model is 20.5% (MPI-ESM-LR) while

in the reanalysis, PC1 captures 30% of total variance. This suggests that the GCMs are under-representing regional circulation variance which agrees with the analysis of SOM node frequencies and the models failure to represent particular circulation states. In general, it appears the GCMs have a constrained regional circulation variance when considered through these analyses though further analysis would be required to better understand this issue.

On the other hand PC2 (Figure 4.6) shows a stronger contribution to the total variance explained for 4 out of 8 of models when compared to the reanalysis. Here, we find specifically the explained variance in CNRM-CM5 (23.3%), GFDL-ESM2M (20.8%), MIROC-ESM (24.3%) and MRI-CGCM3 (22.8%) models to be above that of the reanalysis (19.8%).

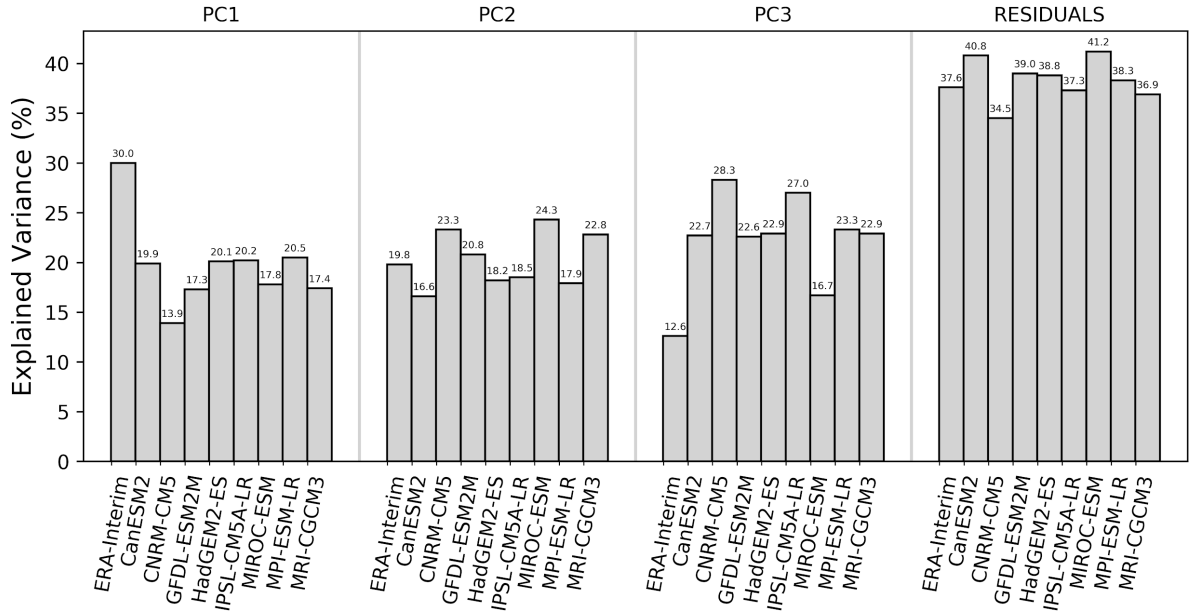

Figure 4.6: Variance-based sensitivity analysis for retained PCs for ERA-Interim reanalysis and a set of CMIP5 GCMs.

Similarly, results show PC3 accounts for much of the explained variance in models when compared to the reanalysis (12.6%). The CNRM-CM5 model recorded the maximum variance (28.3%) for this PC, while we find 27.0% and 23.3% variance in IPSL-CM5A-LR and MPI-ESM-LR respectively. MIROC-ESM model shows the least variance for the models in PC3 although greater than reanalysis.

4.3 Conclusions

Applying a previously developed method for analysing process co-behavior and regional climate variability, we have investigated the representation of co-behavior of large-scale conditioning drivers and the regional synoptic circulation patterns in a set of CMIP5 GCMs, and compared this to the relationships as seen in the ERA reanalysis.

To identify and classify the characteristic variability of daily patterns of synoptic circulation states over the region, we use a SOM to identify archetype circulation patterns in 700-hPa ERA-Interim geopotential height anomalies over the region. SOM state frequency distributions are calculated for the summer and winter seasons. The GCMs are evaluated by mapping the GCM geopotential height standardized anomaly fields through the reanalysis SOM to generate state frequency maps comparable with the ERA-Interim state frequency maps. Most GCMs are able to reproduce the overall frequency distribution associated with the SOM nodes as well as the seasonal variability in frequency distributions. However, there are particular circulation states where the GCM frequencies are markedly different relative to the reanalysis. In particular, synoptic conditions associated with strong tropical circulation anomalies are strongly underrepresented in all GCM circulation frequency maps in the summer season. As mentioned earlier, some studies (e.g. Munday and Washington 2018; Eyring et al. 2019) attribute the differences in representing synoptic variability to the challenge of models resolving particular transient synoptic conditions and tropical convection processes.

Generally, GCMs tend to have strong precipitation biases in tropical Africa (e.g. Dai 2006; Yang et al. 2015) which relates to the parameterization of tropical convection in the models (Pathak et al. 2019). Our analysis identifies large inter-model spread in the representation of the process index for ITCZ when compared with the ERA-Interim reanalysis which similarly suggests the CMIP5 GCMs struggle to represent tropical convection over Africa. In contrast, the inter-model spread is minimal for the ENSO and AAO process indices and GCMs compare well to the reanalysis. This shows the models are more realistically representing these two processes.

Models accurately represent ENSO correlations. They show good correlations on circulation states and the ENSO index similar to the reanalysis over the region. The models however diverge on a robust conclusion on ENSO impact on mid-latitude systems as well as continental highs and lows over the region as asserted by earlier studies by Dieppois et al. (2015).

A greater number of models exhibit strongly different internal correlations compared to the reanalysis for the ITCZ and AAO process indices and circulation states. Thus a model may represent a large-scale process index variance (in this case, AAO index) well but may correlate poorly with other co-behavior indices and circulation states.

For the drivers of co-behavior, the results show that the first PC as identified through the ERA-Interim reanalysis, does not necessarily correspond to the largest variance in all models. As this PC reflects mostly the synoptic variability response, we suggest here that the weak representation of synoptic variability in the models may contribute to the reduced explained variance with respect to the reanalysis. In 4 out of 8 models, the explained variance in PC2 was higher than that of the reanalysis and the source of variability was largely a co-behavior of ENSO response with moderate and weak responses from TRBI and AAO. Notably, all models showed a higher explained variance on PC3, which is dominated by a co-behavior of AAO response with weak expressions of TRBI and ENSO, with respect to the reanalysis.

As co-behavior of multiple processes is a strong determinant of regional precipitation and temperature variability over southern Africa (as shown in Q19 and Q20), the evaluation of the drivers of co-behavior is of the essence in understanding regional climate variability and change and evaluating models ability to represent regional climate dynamics.

While beyond the scope of this analysis which primarily focused on applying this particular methodology to GCMs, the evaluation of reanalysis uncertainty through the analysis of multiple reanalyses would be an important next step in future work.

Acknowledgements

This work was conducted under the Future Resilience for African CiTies and Lands (FRACTAL) project (Grant NE/M020347/1), which is part of Future Climate for Africa (FCFA) program funded by the U.K. Department for International Development (DFID) and Natural Environment Research Council (NERC). The authors are grateful to Grigory Nikulin at Rossby Centre, Swedish Meteorological and Hydrological Institute, Sweden, for the provision and use of the Tropical Rain belt index. Thanks to Philip Mukwenha for the numerous discussion on optimisation and also for setting up my working environment. The first author is grateful to the University of Cape Town for funding assistance. Additionally, the first author is thankful to African Climate and Development Initiative (ACDI) of University of Cape Town, Tyndall Centre for Climate Change and Climatic Research Unit (CRU) under the Newton PhD Partnering Scheme funded by Research Councils UK (RCUK) and the National Research Foundation (NRF) of South Africa. We acknowledge the World Climate Research Programme's Working Group on Coupled Modelling, which is responsible for Coupled Model Intercomparison Project (CMIP), and we thank the climate modelling groups (listed in Table 3.1) for producing and making available their model output.

Chapter 5

5 Synthesis

This dissertation presents a pioneering methodology of investigating the co-behaviour of large-scale processes over southern Africa. This work serves to underpin future work to advance understanding of the co-behaviour of synoptic to global-scale climate processes as a driver of regional climate variability and change. Overall, the dissertation was centered around three specific questions:

1. *What is the co-behaviour of key climate processes and how do we assess their impact over southern Africa?*
2. *How well do climate models capture co-behaviour as identified in reanalysis datasets?*
3. *What are the possible mechanisms responsible for how the models are representing co-behaviour?*

The thesis pursued the answers to these questions and addressed the overarching aim through the following:

1. *Development of an experimental new methodology designed to allow the characterisation and evaluation of co-behaviour in regional climate processes.*
2. *Through applying the methodology to the southern African climate system, address questions (1 and 2) above as well as evaluate the effectiveness of the methodology.*
3. *Apply the methodology to the evaluation of GCMs in order to address question (3) above.*

These questions have been explored throughout the dissertation, for which the framing and findings are summarized in the sections below.

5.1 Theoretical framing

As mentioned earlier in this thesis, the influence of individual large-scale processes to some extent have been well addressed in literature to understand the roles they play in driving regional climate variability and change. For instance, the impact teleconnective drivers have on the southern African climate includes for example, increasing dryness and warming in the summer rainfall region under ENSO influence (e.g. Meque and Abiodun 2015), likewise negative phase AAO influences winter rainfall in the winter rainfall region of southern Africa as identified by Reason and Rouault (2005). Nonetheless, these large-scale processes overlap in time and space so interact and the co-behaviour between these processes and their impact on the synoptic environment remains relatively unexplored. Although few earlier studies (e.g. Fauchereau et al. 2009; Pascale et al. 2019; Hoell et al. 2017a; Hart et al. 2018; Pohl et al. 2018; Meehl et al. 2001; Pohl et al. 2010) have attempted to develop an understanding for large-scale processes interactions, they fall short of developing a methodology for investigating large-scale process interactions.

The exploration of the nature of co-behaviour influence and possible impact on regional climate variability and change is paramount to accurately present the regional climate information and as a result contribute to addressing regional climate change. Critical to this is the development of methodologies to quantify this phenomena and as earlier established throughout this thesis, to accommodate the fact that regional climate variability is an outcome of multiple, possibly interacting large-scale processes.

The research evaluates the co-behaviour as a driver of regional climate variability in terms of precipitation and temperature responses. Across southern African sub-region, the study finds that co-behaviour response varies with respect to the established rainfall regimes of the region and is dependent on how the processes interact at any given time. In that, co-behaviour does modulate the distribution and impact of the large-scale processes over the region and thus contribute to regional climate variability.

Co-behaviour further presents the opportunity to evaluate the performance of GCMs and their ability to reasonably replicate identified co-behaviour influence on precipitation and temperature as captured by observations. This presents a new perspective of how models might be assessed and weighted. For instance, the ability of a model to reasonably simulate co-behaviour improves confidence in the future projections made using that model. We present the key findings in the section that follows.

5.2 Key findings

What is the co-behaviour of key climate processes and how do we assess the impact over southern Africa?

A concept and methodology is developed through the combination of well-established methods. Regional synoptic circulation types are first characterised using a 12-node SOM. The SOM develops 12 exemplar circulation types over the region as discussed in Chapters 2 and 4 of the dissertation. The PCA is used to relate combined teleconnection drivers with the identified synoptic circulation types. Results from the PCA shows the first of three retained PCs to represent:

1. predominantly a seasonal variability response,
2. a co-behaviour of ENSO response with moderate TRBI (a measure of ITCZ), and weak AAO responses,
3. a co-behaviour of AAO response with weak expressions of the TRBI and ENSO

This result forms the foundational characterization of regional co-behaviour as well as demonstrating the strength of the concept and methodology. The results showed the fundamental roles of large-scale processes interacting with each other and with regional circulation variability and addressed in part, the first objective of the dissertation.

In tackling the remaining part of the objective, precipitation and temperature responses were evaluated under eight identified modes of co-behaviour characterised as

combinations of positive and negative states of each of the three PCs. Each mode is found to have varying impacts on precipitation and temperature of the three main rainfall regions: summer, winter and all-year rainfall regions of southern Africa. The impact of co-behaviour is particularly strong in the summer rainfall region with moderate impacts on the winter and all-year rainfall regions. For instance, in summer, when El Niño co-behaves with positive phase AAO, it results in dry and warm conditions in the summer rainfall region; negative phase AAO drives these conditions north-west. Likewise during winter, interactions between La Niña and positive phase AAO causes the summer and all-year rainfall region to be cold with the winter rainfall region both wet and cold.

The above insight is particularly useful when trying to understand the sources of climate variability and change for the region as well as understanding future climate dynamics as it shows how the various rainfall regions are being impacted by the interacting large-scale processes.

How well do climate models capture co-behaviour as identified in reanalysis datasets?

With the fundamental influence of co-behaviour established, the question was asked of how well do climate models represent already identified co-behaviour in reanalysis datasets? As global climate models are our primary tools for understanding past and future climates, the idea was to evaluate the ability of these models to simulate co-behaviour. To address this, the co-behaviour methodology was applied to eight GCMs from eight different modelling groups participating in the CMIP5 project (Chapter 3). The methodology is modified to allow for the comparison of SOM node frequencies across the GCMs as well as providing comparable inputs to the PCA.

Results suggest that although models reasonably simulate the general mean precipitation response compared to the observed one, the response under different co-behaviour modes is widely varied across models, particularly in location and magnitude. For instance, over 60% of models used in the study represent the general

circulation response with wet bias under wet summer conditions characterised by a co-behaviour of La Niña (PC2 < -1 std), negative AAO (PC3 < -1 std) during summer (PC1 > 1std). However, the HadGEM2-ES model best represents the response in terms of its spatial distribution and to a lesser extent the magnitude under this co-behaviour mode when compared with CHIRPS. About 80% of the models also fail to show statistically significant response signals for El Niño co-behaving with positive AAO during summer which is an important drought pattern for the region.

On the other hand, the models are consistent in representing temperature response across the region with at least 80% of models tending to agree on the sign of response relative to the observed. The same cannot be said for precipitation as models have less agreement on the sign of response. It is likely that the cause of this disagreement may be how the models parameterize precipitation hence modelers may need to focus their attention on adapting a coherent parameterization scheme or generating convective permitting models for future use.

What are the possible mechanisms responsible for how the models are representing co-behaviour?

The final objective of this dissertation is addressed by applying a process-based evaluation of the underlying mechanisms responsible for how models represent co-behaviour (Chapter 4). Here, the same set of GCMs are examined on their representation of large-scale processes: ENSO, AAO and ITCZ that drive co-behaviour response relative to the observed. The analysis revealed a coherent representation of the ENSO and AAO processes across models when compared with the observed. Thus these two processes are relatively well represented across models. However, the models show a large spread in representing the ITCZ. It is understandable to some extent why this occurs, as the parameter used in representing the ITCZ (rainfall) largely depends on its intensity which invariably relies heavily on the parameterization schemes employed in simulations by the different modelling groups in the CMIP5 experiment. To an extent, this may possibly explain why there is so much variability in the ability of the models to reproduce co-behaviour influence on

precipitation and their inability to produce statistically significant response signals to the drought pattern of the region.

In summary, while the models are able to reproduce co-behaviour influence on temperature which is consistent with our earlier findings, they diverge on precipitation response as they appear to be limited to an extent by precipitation parameterizations. This has broader implications for future climate change projections as it is expected that models respond realistically to climate forcings when simulating climate processes and their interactions across space and time. However, failure to accurately simulate these underlying process interactions may possibly lead to unrealistic projections. A possible way to tackle this challenge may be to resort to high resolution model simulations e.g. convective-permitting model for Africa (CP4A; Kendon et al. 2019) and other models that explicitly resolve precipitation.

5.3 Conclusions

The intent of this section is to draw together some conclusions in assessing co-behaviour as a factor in understanding regional climate variability and change, especially in Africa, a region susceptible to climate change.

The thesis through a series of scientific questions has addressed the co-behaviour of selected large-scale processes that influence southern African climate through their control of synoptic features as a means to addressing the knowledge gap in understanding regional climate variability and change. To this end, the three objectives as mentioned in chapter one were tested and the following conclusions can be drawn:

- The influence of co-behaviour varies across the three main rainfall regions of southern Africa with particularly strong influence in the summer rainfall region with moderate impacts in winter and all-year rainfall regions.
- The spatial distribution and magnitude of surface responses under co-behaviour differs when compared to the individual independent responses for each process.

- The AAO teleconnection modulates ENSO teleconnection impacts across all rainfall regions under moderate influence of the ITCZ.
- The models represent regional patterns of response to different co-behaviour modes well when compared to observed responses, however they tend to represent responses of greater magnitude.
- Model representation of precipitation responses under different modes of co-behaviour are much more mixed with some models producing patterns of response close to observed patterns while others fail to reproduce observed responses, particularly at local scales.
- Most models used in the study fail to produce statistically significant strong response signal to the drought pattern of the region under co-behaviour modes.
- Models simulate ENSO and AAO teleconnective processes much better than the ITCZ.
- Care needs to be taken when developing an effective adaptation decision-making using models, especially when considering precipitation, as there is a wide uncertainty range. However, co-behaviour helps to reduce this uncertainty by eliminating models that do not realistically represent the regional climate information.
- The methodology developed can be applied to any particular region through an informed configuration of the methodology.

Overall, the concept of co-behaviour complements the existing understanding of regional climate as well as helps explain the sources of variability of the regional climate of southern Africa. The methodology developed provides a novel approach to better understand the influence of the different combining mechanisms driving the regional climate of southern Africa as this establishes the environment for responses such as precipitation and temperature. Furthermore, the concept provides an alternative way of evaluating models with respect to how they represent key processes relevant to any region. This work clearly brings added value to the broader discourse of climate variability in Africa, which is largely vulnerable to climate change impacts.

5.4 Caveats and Future Work

As with any methodology development and model evaluation study, one should consider the caveats and assumptions when interpreting the results. In this study, a few caveats and assumptions are made, consequently they are discussed in this section.

First, the methodology may be improved by incorporating other processes (e.g. Angola Low, Botswana High, high pressure systems) to ascertain whether these bring additional independent influence in modulating the regional climate.

Second, the representation of synoptic variance is impacted by models with large SOM node frequency bias. Although the study standardises the inputs of the PCA, the variance structure of reach GCM which is mapped through the SOM will be a combination of the synoptic state variance, and the underlying synoptic state bias. Thus a GCM can have a realistic synoptic state variance but with a systematic 700-hPa bias which will result in an unrealistic variance structure as an input into the PCA. Such a GCM will then be evaluated poorly.

The selection of the domain size has implications on the sub-regional differences which is a limitation of the study. In that the size of the domain chosen for the study is a trade-off with discriminating sub-regional differences but the study considers the response of the region as a collective whole.

Also, the use of eight GCMs out of the 39 CMIP5 model stack is a limitation as the present study is unable to completely sample the uncertainty space of the CMIP5 GCMs in relation to how they reproduce co-behaviour influence. However with the introduction of CMIP6 models which will be archiving additional variables (for instance geopotential height at 700-hpa), future studies may explore the complete uncertainty space of the models in representing co-behaviour. Furthermore, the present study has explored co-behaviour in observation, reanalysis and GCM datasets for the historical period, however, future work into GCM projection of co-behaviour and the nature of those interactions may be beneficial.

In addition, the results obtained are dependent on the characterization of the ITCZ by the models, in that, how a model parameterizes precipitation plays a crucial role in how co-behaviour is represented by that model. Nonetheless, future work may explore how the new CMIP6 models with improved parameterization schemes and a better representation of tropical convection may characterise the ITCZ and subsequently co-behaviour.

In conclusion, there are clear avenues of potential value for future work to further examine co-behaviour influence on the regional precipitation and temperature of southern Africa, and to constrain multi-model uncertainty in climate projections. As alluded to above, examining co-behaviour in future projections may establish whether these identified relationships remain unchanged or may change into the future.

Further development and improvement of this methodology would additionally improve the understanding of regional climate variability and change. For instance, alternative weighting techniques may be explored when filtering the monthly time-series to ascertain whether they bring any significant changes in the results. Also, the inclusion of more large-scale processes to the augmented matrix going into the PCA may lead to an further understanding of how those processes contribute to the variability of the regional climate.

References

Abdi, H., and L. L. J. Williams, 2010: Principal component analysis. *Wiley Interdiscip. Rev. Comput. Stat.*, **2**, 433–459, doi:10.1002/wics.101.

Abiodun, B. J., N. Makhanya, B. Petja, A. A. Abatan, and P. G. Oguntunde, 2018: Future projection of droughts over major river basins in Southern Africa at specific global warming levels. *Theor. Appl. Climatol.*, 1–15, doi:10.1007/s00704-018-2693-0.

Accadia, C., S. Mariani, M. Casaioli, A. Lavagnini, and A. Speranza, 2003: Sensitivity of precipitation forecast skill scores to bilinear interpolation and a simple nearest-neighbor average method on high-resolution verification grids. *Weather Forecast.*, **18**, 918–932, doi:10.1175/1520-0434(2003)018<0918:SOPFSS>2.0.CO;2.

Arora, V. K., and Coauthors, 2011: Carbon emission limits required to satisfy future representative concentration pathways of greenhouse gases. *Geophys. Res. Lett.*, **38**, n/a-n/a, doi:10.1029/2010GL046270.

Bartman, A. G., W. A. Landman, and C. J. D. W. Rautenbach, 2003: Recalibration of general circulation model output to austral summer rainfall over southern Africa. *Int. J. Climatol.*, **23**, 1407–1419, doi:10.1002/joc.954.

Blamey, R. C., S. R. Kolusu, P. Mahlalela, M. C. Todd, and C. J. C. Reason, 2018: The role of regional circulation features in regulating El Niño climate impacts over southern Africa: A comparison of the 2015/2016 drought with previous events. *Int. J. Climatol.*, 1–20, doi:10.1002/JOC.5668.

Boulard, D., B. Pohl, J. Crétat, N. Vigaud, and T. Pham-Xuan, 2013: Downscaling large-scale climate variability using a regional climate model: The case of ENSO over Southern Africa. *Clim. Dyn.*, **40**, 1141–1168, doi:10.1007/s00382-012-1400-6.

Brands, S., S. Herrera, J. Fernández, and J. M. Gutiérrez, 2013: How well do CMIP5 Earth System Models simulate present climate conditions in Europe and Africa?: A performance comparison for the downscaling community. *Clim. Dyn.*, **41**, 803–817, doi:10.1007/s00382-013-1742-8.

Brown, S. J., 2017: The drivers of variability in UK extreme rainfall. *Int. J. Climatol.*, **38**, e119–e130, doi:10.1002/joc.5356.

Buckle, C., 1996a: *Weather and climate in Africa*. Longman, 312 pp.

——, 1996b: *Weather and Climate in Africa*. Longman, Harlow, 312 pp.

Camberlin, P., S. Janicot, and I. Poccard, 2001: Seasonality and atmospheric dynamics of the teleconnection between African rainfall and tropical sea-surface temperature: Atlantic vs. ENSO. *Int. J. Climatol.*, **21**, 973–1005, doi:10.1002/joc.673.

Cassano, E. N., J. M. Glisan, J. J. Cassano, W. J. Gutowski, and M. W. Seefeldt, 2015: Self-organizing map analysis of widespread temperature extremes in Alaska and Canada. *Clim. Res.*, **62**, 199–218, doi:10.3354/cr01274.

Chase, B., and M. Meadows, 2007: Late Quaternary dynamics of southern Africa's winter rainfall zone. *Earth-Science Rev.*, **84**, 103–138, doi:10.1016/j.earscirev.2007.06.002.

Collins, W. J., and Coauthors, 2011: Geoscientific Model Development Development and evaluation of an Earth-System model-HadGEM2. *Geosci. Model Dev*, **4**, 1051–1075, doi:10.5194/gmd-4-1051-2011.

Cook, K. H., 2000: The South Indian convergence zone and interannual rainfall variability over Southern Africa. *J. Clim.*, **13**, 3789–3804, doi:10.1175/1520-0442(2000)013<3789:TSICZA>2.0.CO;2.

Cook, K. H., and E. K. Vizy, 2016: The Congo Basin Walker circulation: dynamics and connections to precipitation. *Clim. Dyn.*, **47**, 697–717, doi:10.1007/s00382-015-2864-y.

D'Abreton, P. C., and J. A. Lindesay, 1993: Water Vapour Transport Over Southern Africa. *Int. J. Climatol.*, **13**, 151–170.

Dai, A., 2006: Precipitation Characteristics in Eighteen Coupled Climate Models. *J. Clim.*, **19**, 4605–4630, doi:https://doi.org/10.1175/JCLI3884.1.

Daron, J., L. Burgin, T. Janes, R. G. Jones, and C. Jack, 2019: Climate process chains: examples from Southern Africa. *Int. J. Climatol.*, 1–14, doi:10.1002/joc.6106.

Daron, J. D., 2014: *Regional Climate Messages for Southern Africa About ASSAR Working Papers*. 1–30 pp.

DeBlander, E., and J. Shaman, 2017: Teleconnection between the South Atlantic convergence zone and the southern Indian Ocean: Implications for tropical cyclone activity. *J. Geophys. Res. Atmos.*, **122**, 728–740, doi:10.1002/2016JD025373.

Dee, D. P., and Coauthors, 2011: The ERA-Interim reanalysis: configuration and

performance of the data assimilation system. *Q. J. R. Meteorol. Soc.*, **137**, 553–597, doi:10.1002/qj.828.

Dieppois, B., M. Rouault, and M. New, 2015: The impact of ENSO on Southern African rainfall in CMIP5 ocean atmosphere coupled climate models. *Clim. Dyn.*, **45**, 2425–2442, doi:10.1007/s00382-015-2480-x.

——, B. Pohl, J. Crétat, J. Eden, M. Sidibe, M. New, M. Rouault, and D. Lawler, 2019: Southern African summer-rainfall variability, and its teleconnections, on interannual to interdecadal timescales in CMIP5 models. *Clim. Dyn.*, **53**, 3505–3527, doi:10.1007/s00382-019-04720-5.

Dike, V. N., M. H. Shimizu, M. Diallo, Z. Lin, O. K. Nwofor, and T. C. Chineke, 2015: Modelling present and future African climate using CMIP5 scenarios in HadGEM2-ES. *Int. J. Climatol.*, **35**, 1784–1799, doi:10.1002/joc.4084.

Dosio, A., 2017: Projection of temperature and heat waves for Africa with an ensemble of CORDEX Regional Climate Models. *Clim. Dyn.*, **49**, 493–519, doi:10.1007/s00382-016-3355-5.

Dufresne, J. L., and Coauthors, 2013: *Climate change projections using the IPSL-CM5 Earth System Model: From CMIP3 to CMIP5*. 2123–2165 pp.

Dunne, J. P., and Coauthors, 2012: GFDL's ESM2 global coupled climate-carbon earth system models. Part I: Physical formulation and baseline simulation characteristics. *J. Clim.*, **25**, 6646–6665, doi:10.1175/JCLI-D-11-00560.1.

Dunning, C. M., E. C. L. Black, and R. P. Allan, 2016: The onset and cessation of seasonal rainfall over Africa. *J. Geophys. Res.*, **121**, 11405–11424, doi:10.1002/2016JD025428.

Efron, B., and R. Tibshirani, 1994: *An introduction to the bootstrap*. Chapman & Hall, 436 pp.

Endris, H. S., C. Lennard, B. Hewitson, A. Dosio, G. Nikulin, and H. J. Panitz, 2016: Teleconnection responses in multi-GCM driven CORDEX RCMs over Eastern Africa. *Clim. Dyn.*, **46**, 2821–2846, doi:10.1007/s00382-015-2734-7.

Engelbrecht, C. J., F. A. Engelbrecht, and L. L. Dyson, 2013: High-resolution model-projected changes in mid-tropospheric closed-lows and extreme rainfall events over southern Africa. *Int. J. Climatol.*, **33**, 173–187, doi:10.1002/joc.3420.

Eyring, V., S. Bony, G. A. Meehl, C. A. Senior, B. Stevens, R. J. Stouffer, and K. E. Taylor, 2016: Overview of the Coupled Model Intercomparison Project Phase 6 (CMIP6) experimental design and organization. *Geosci. Model Dev.*, **9**, 1937–

1958, doi:10.5194/gmd-9-1937-2016.

——, and Coauthors, 2019: Taking climate model evaluation to the next level. *Nat. Clim. Chang.*, **9**, 102–110, doi:10.1038/s41558-018-0355-y.

Faber, J., and L. M. Fonseca, 2014: How sample size influences research outcomes. *Dental Press J. Orthod.*, **19**, 27–29, doi:10.1590/2176-9451.19.4.027-029.ebo.

Fauchereau, N., S. Trzaska, M. Rouault, and Y. Richard, 2003: Rainfall Variability and Changes in Southern Africa during the 20th Century in the Global Warming Context. *Nat. Hazards*, **29**, 139–154, doi:10.1023/A:1023630924100.

Fauchereau, N., B. Pohl, C. J. C. Reason, M. Rouault, and Y. Richard, 2009: Recurrent daily OLR patterns in the Southern Africa/Southwest Indian ocean region, implications for South African rainfall and teleconnections. *Clim. Dyn.*, **32**, 575–591, doi:10.1007/s00382-008-0426-2.

Fogt, R. L., D. H. Bromwich, R. L. Fogt, and D. H. Bromwich, 2006: Decadal variability of the ENSO teleconnection to the high-latitude south pacific governed by coupling with the Southern Annular mode. *J. Clim.*, **19**, 979–997, doi:10.1175/JCLI3671.1.

Frame, D. J., and D. A. Stone, 2013: Assessment of the first consensus prediction on climate change. *Nat. Clim. Chang.*, **3**, 357–359, doi:10.1038/nclimate1763.

Frei, C., R. Schöll, S. Fukutome, J. Schmidli, and P. L. Vidale, 2006: Future change of precipitation extremes in Europe: Intercomparison of scenarios from regional climate models. *J. Geophys. Res.*, **111**, D06105, doi:10.1029/2005JD005965.

Funk, C., and Coauthors, 2015: The climate hazards infrared precipitation with stations—a new environmental record for monitoring extremes. *Sci. Data*, **2**, 150066, doi:10.1038/sdata.2015.66.

Garreaud, R. D., M. Vuille, R. Compagnucci, and J. Marengo, 2008: Present day South America climate. *Palaeogeogr. Palaeoclimatol. Palaeoecol.*, 1–16, doi::10.1016/j.palaeo.2007.10.032.

Gibson, P. B., S. E. Perkins-Kirkpatrick, P. Uotila, A. S. Pepler, and L. V. Alexander, 2017: On the use of self-organizing maps for studying climate extremes. *J. Geophys. Res.*, **122**, 3891–3903, doi:10.1002/2016JD026256.

Giorgi, F., C. Jones, and G. Asrar, 2009: Addressing climate information needs at the regional level: the CORDEX framework. *Organ. Bull.*, **58**, 175–183.

Grimm, A. M., and C. J. C. Reason, 2015: Intraseasonal teleconnections between South America and South Africa. *J. Clim.*, **28**, 9489–9497, doi:10.1175/JCLI-D-

15-0116.1.

Harris, I., P. D. Jones, T. J. Osborn, and D. H. Lister, 2014: Updated high-resolution grids of monthly climatic observations - the CRU TS3.10 Dataset. *Int. J. Climatol.*, **34**, 623–642, doi:10.1002/joc.3711.

Hart, N. C. G., C. J. C. Reason, and N. Fauchereau, 2010: Tropical–Extratropical Interactions over Southern Africa: Three Cases of Heavy Summer Season Rainfall. *Mon. Weather Rev.*, **138**, 2608–2623, doi:10.1175/2010MWR3070.1.

——, R. Washington, and C. J. C. Reason, 2018: On the likelihood of tropical-extratropical cloud bands in the South Indian convergence zone during ENSO events. *J. Clim.*, **31**, 2797–2817, doi:10.1175/JCLI-D-17-0221.1.

——, R. Blamey, R. James, & FCFA UMFULA Climate Research team (2016): Southern Africa Regional Overview: Studying Variability and Future Change, in *Africa's climate: Helping decision-makers make sense of climate information*, Future Climate for Africa, NERC/DfID Programme, United Kingdom.

Hauke, J., and T. Kossowski, 2011: Comparison of Values of Pearson's and Spearman's Correlation Coefficients on the Same Sets of Data. *Quaest. Geogr.*, **30**, 87–93, doi:10.2478/v10117-011-0021-1.

Hawkins, E., and R. Sutton, 2011: The potential to narrow uncertainty in projections of regional precipitation change. *Clim. Dyn.*, **37**, 407–418, doi:10.1007/s00382-010-0810-6.

Hewitson, B., and R. Crane, 1996: Climate downscaling: techniques and application. *Clim. Res.*, **7**, 85–95, doi:10.3354/cr007085.

Hewitson, B. C., and R. G. Crane, 2002: Self-organizing maps, Application to synoptic climatology. *Clim. Res.*, **22**, 13–26, doi:10.3354/cr022013.

Hoell, A., C. Funk, J. Zinke, and L. Harrison, 2017a: Modulation of the Southern Africa precipitation response to the El Niño Southern Oscillation by the subtropical Indian Ocean Dipole. *Clim. Dyn.*, **48**, 2529–2540, doi:10.1007/s00382-016-3220-6.

——, M. Hoerling, J. Eischeid, X. W. Quan, and B. Liebmann, 2017b: Reconciling theories for human and natural attribution of recent East Africa drying. *J. Clim.*, **30**, 1939–1957, doi:10.1175/JCLI-D-16-0558.1.

Hope, P. K., W. Drosdowsky, and N. Nicholls, 2006: Shifts in the synoptic systems influencing southwest Western Australia. *Clim. Dyn.*, **26**, 751–764,

doi:10.1007/s00382-006-0115-y.

Houze, R. A., 2012: Orographic effects on precipitating clouds. *Rev. Geophys.*, **50**, 1–47, doi:10.1029/2011RG000365.

Hulme, M., R. Doherty, T. Ngara, M. New, and D. Lister, 2001: African climate change: 1900-2100. *Clim. Res.*, **17**, 145–168, doi:10.3354/cr017145.

IPCC, 2012: *Managing the risks of extreme events and disasters to advance climate change adaptation*. 594 pp.

James, R., and R. Washington, 2013: Changes in African temperature and precipitation associated with degrees of global warming. *Clim. Change*, **117**, 859–872, doi:10.1007/s10584-012-0581-7.

——, ——, and R. Jones, 2015: Process-based assessment of an ensemble of climate projections for West Africa. *J. Geophys. Res.*, **120**, 1–18, doi:10.1002/2014JD022513.

——, and Coauthors, 2018: Evaluating climate models with an African lens. *Bull. Am. Meteorol. Soc.*, **99**, 313–336, doi:10.1175/BAMS-D-16-0090.1.

Jolliffe, I. T., 2002: *Principal Component Analysis*. Springer, 488 pp.

——, and D. B. Stephenson, 2012: *Forecast verification : a practitioner's guide in atmospheric science*. John Wiley & Sons, 304 pp.

Jolliffe, I. T., and J. Cadima, 2016: Principal component analysis: a review and recent developments. *Philos. Trans. R. Soc. A Math. Phys. Eng. Sci.*, **374**, 20150202, doi:10.1098/rsta.2015.0202.

Jury, M. R., and T. Freiman, 2002: The climate of tropical southern Africa during the SAFARI 2000 campaign. *S. Afr. J. Sci.*, **98**, 527–533.

Kendon, E. J., R. A. Stratton, S. Tucker, J. H. Marsham, S. Berthou, D. P. Rowell, and C. A. Senior, 2019: Enhanced future changes in wet and dry extremes over Africa at convection-permitting scale. *Nat. Commun.*, **10**, 1794–1808, doi:10.1038/s41467-019-09776-9.

Kim, H. K., and K. H. Seo, 2016: Cluster analysis of tropical cyclone tracks over the western North Pacific using a self-organizing map. *J. Clim.*, **29**, 3731–3751, doi:10.1175/jcli-d-15-0380.1.

Kim, S. T., and J. Y. Yu, 2012: The two types of ENSO in CMIP5 models. *Geophys. Res. Lett.*, **39**, 1–6, doi:10.1029/2012GL052006.

Klutse, N. A. B., B. J. Abiodun, B. C. Hewitson, W. J. Gutowski, and M. A. Tadross, 2016: Evaluation of two GCMs in simulating rainfall inter-annual variability over

Southern Africa. *Theor. Appl. Climatol.*, **123**, 415–436, doi:10.1007/s00704-014-1356-z.

Knutti, R., 2010: The end of model democracy? *Clim. Change*, **102**, 395–404, doi:10.1007/s10584-010-9800-2.

——, and J. Sedláček, 2013: Robustness and uncertainties in the new CMIP5 climate model projections. *Nat. Clim. Chang.*, **3**, 369–373, doi:10.1038/nclimate1716.

Kohonen, T., 1982: Self-organized formation of topologically correct feature maps. *Biol. Cybern.*, **43**, 59–69, doi:10.1007/BF00337288.

——, 2001: *Self-Organizing Maps*. Springer Berlin Heidelberg, Berlin, Heidelberg,

Lazenby, M. J., M. C. Todd, and Y. Wang, 2016: Climate model simulation of the South Indian Ocean Convergence Zone: Mean state and variability. *Clim. Res.*, **68**, 59–71, doi:10.3354/cr01382.

Lee, C. C., 2017: Reanalysing the impacts of atmospheric teleconnections on cold-season weather using multivariate surface weather types and self-organizing maps. *Int. J. Climatol.*, **3730**, 3714–3730, doi:10.1002/joc.4950.

Lennard, C., and G. C. Hegerl, 2014: Relating changes in synoptic circulation to the surface rainfall response using self-organising maps. *Clim. Dyn.*, **44**, 861–879, doi:10.1007/s00382-014-2169-6.

Lennard, C., L. Coop, D. Morison, and R. Grandin, 2013: *Extreme events: Past and future changes in the attributes of extreme rainfall and the dynamics of their driving processes.* Pretoria, South Africa, Rep. 1960/1/12, 105, 105 pp.

Leppink, J., K. Winston, and P. O'Sullivan, 2016: Statistical significance does not imply a real effect. *Perspect. Med. Educ.*, **5**, 122–124, doi:10.1007/s40037-016-0256-6.

Lever, J., M. Krzywinski, and N. Altman, 2017: Points of Significance: Principal component analysis. *Nat. Methods*, **14**, 641–642, doi:10.1038/nmeth.4346.

Lu, Z., Z. Fu, L. Hua, N. Yuan, and L. Chen, 2018: Evaluation of ENSO simulations in CMIP5 models: A new perspective based on percolation phase transition in complex networks. *Sci. Rep.*, **8**, 1–13, doi:10.1038/s41598-018-33340-y.

Lyon, B., and S. J. Mason, 2007: The 1997-98 Summer Rainfall Season in Southern Africa. Part I: Observations. doi:10.1175/JCLI4225.1.

Mackellar, N., M. Tadross, and B. Hewitson, 2010: Synoptic-based evaluation of climatic response to vegetation change over southern Africa. *Int. J. Climatol. Int. J. Clim.*, **30**, 774–789, doi:10.1002/joc.1925.

Macron, C., B. Pohl, Y. Richard, and M. Bessafi, 2014: How do tropical temperate troughs form and develop over Southern Africa? *J. Clim.*, **27**, 1633–1647, doi:10.1175/JCLI-D-13-00175.1.

Makarau, A., and M. R. Jury, 1997: Seasonal cycle of convective spells over southern Africa during austral summer. *Int. J. Climatol.*, **17**, 1317–1332, doi:10.1002/(SICI)1097-0088(199710)17:12<1317::AID-JOC197<3.0.CO;2-A.

Manatsa, D., T. Mushore, and A. Lenouo, 2017: Improved predictability of droughts over southern Africa using the standardized precipitation evapotranspiration index and ENSO. *Theor. Appl. Climatol.*, **127**, 259–274, doi:10.1007/s00704-015-1632-6.

Maraun, D., and M. Widmann, 2018: *Statistical Downscaling and Bias Correction for Climate Research*. First. Cambridge University Press, Cambridge, 1–341 pp.

Mason, S. J., and M. R. Jury, 1997: Climatic variability and change over southern Africa: a reflection on underlying processes. *Prog. Phys. Geogr.*, **21**, 23–50, doi:10.1177/030913339702100103.

Mastrandrea, M. D., K. J. Mach, G. K. Plattner, O. Edenhofer, T. F. Stocker, C. B. Field, K. L. Ebi, and P. R. Matschoss, 2011: The IPCC AR5 guidance note on consistent treatment of uncertainties: A common approach across the working groups. *Clim. Change*, **108**, 675–691, doi:10.1007/s10584-011-0178-6.

McSweeney, C. F., R. G. Jones, R. W. Lee, and D. P. Rowell, 2015: Selecting CMIP5 GCMs for downscaling over multiple regions. *Clim. Dyn.*, **44**, 3237–3260, doi:10.1007/s00382-014-2418-8.

Meehl, G. A., and C. Tebaldi, 2004: More Intense, More Frequent, and Longer Lasting Heat Waves in the 21st Century. *Science (80).*, **305**, 994–997, doi:10.1126/science.1098704.

Meehl, M., R. Lukas, G. N. Kiladis, K. M. Weickmann, A. J. Matthews, and M. Wheeler, 2001: A conceptual framework for time and space scale interactions in the climate system. *Clim. Dyn.*, **17**, 753–775, doi:10.1007/s003820000143.

Meque, A., and B. J. Abiodun, 2015: Simulating the link between ENSO and summer drought in Southern Africa using regional climate models. *Clim. Dyn.*, **44**, 1881–1900, doi:10.1007/s00382-014-2143-3.

Miao, C., and Coauthors, 2014: Assessment of CMIP5 climate models and projected temperature changes over Northern Eurasia. *Environ. Res. Lett.*, **9**, doi:10.1088/1748-9326/9/5/055007.

Misra, V., 2003: The influence of Pacific SST variability on the precipitation over southern Africa. *J. Clim.*, **16**, 2408–2418, doi:10.1175/2785.1.

Mo, K. C., 2000: Relationships between low-frequency variability in the Southern Hemisphere and sea surface temperature anomalies. *J. Clim.*, **13**, 3599–3610, doi:10.1175/1520-0442(2000)013<3599:RBLFVI>2.0.CO;2.

Moron, V., A. W. Robertson, J.-H. Qian, and M. Ghil, 2015: Weather types across the Maritime Continent: from the diurnal cycle to interannual variations. *Front. Environ. Sci.*, **2**, 65, doi:10.3389/fenvs.2014.00065.

Munday, C., and R. Washington, 2017: Circulation controls on southern African precipitation in coupled models: The role of the Angola Low. *J. Geophys. Res. Atmos.*, 1–17, doi:10.1002/2016JD025736.

Munday, C., and R. Washington, 2018: Systematic climate model rainfall biases over Southern Africa: Links to moisture circulation and topography. *J. Clim.*, **31**, 7533–7548, doi:10.1175/JCLI-D-18-0008.1.

Muñoz, Á. G., X. Yang, G. A. Vecchi, A. W. Robertson, and W. F. Cooke, 2017: A weather-type-based cross-time-scale diagnostic framework for coupled circulation models. *J. Clim.*, **30**, 8951–8972, doi:10.1175/JCLI-D-17-0115.1.

Muñoz, G., L. Goddard, A. W. Robertson, Y. Kushnir, and W. Baethgen, 2015: Cross-time scale interactions and rainfall extreme events in southeastern South America for the austral summer. Part I: Potential predictors. *J. Clim.*, **28**, 7894–7913, doi:10.1175/JCLI-D-14-00693.1.

Niang, I., O. C. Ruppel, M. A. Abdrabo, A. Essel, C. Lennard, J. Padgham, and P. Urquhart, 2014: *Africa. In: Climate Change 2014: Impacts, Adaptation, and Vulnerability. Part B: Regional Aspects. Contribution of Working Group II to the Fifth Assessment Report of the Intergovernmental Panel on Climate Change*. 1199–1265 pp.

Nicholson, S., 2003: Comments on “The South Indian convergence zone and interannual rainfall variability over southern Africa” and the question of ENSO’s influence on southern Africa. *J. Clim.*, **16**, 555–562, doi:10.1175/1520-0442(2003)016<0555:COTSIC>2.0.CO;2.

Nicholson, S. E., 2000: The nature of rainfall variability over Africa on time scales of decades to millenia. *Glob. Planet. Change*, **26**, 137–158, doi:10.1016/S0921-8181(00)00040-0.

Nicholson, S. E., 2011: *Dryland climatology*. 1–516 pp.

Nicholson, S. E., 2018: The ITCZ and the seasonal cycle over equatorial Africa. *Bull. Am. Meteorol. Soc.*, **99**, 337–348, doi:10.1175/BAMS-D-16-0287.1.

Nikulin, G., and B. Hewitson, 2019: A simple set of indices describing the Tropical Rain Belt over central and southern Africa. *Atmos. Sci. Lett.*, **20**, 1–8, doi:10.1002/asl.946.

——, and Coauthors, 2012: Precipitation climatology in an ensemble of CORDEX-Africa regional climate simulations. *J. Clim.*, **25**, 6057–6078, doi:10.1175/JCLI-D-11-00375.1.

O'Gorman, P. A., and M. S. Singh, 2013: Vertical structure of warming consistent with an upward shift in the middle and upper troposphere. *Geophys. Res. Lett.*, **40**, 1838–1842, doi:10.1002/grl.50328.

Pascale, S., B. Pohl, S. B. Kapnick, and H. Zhang, 2019: On the Angola low interannual variability and its role in modulating ENSO effects in southern Africa. *J. Clim.*, **32**, 4783–4803, doi:10.1175/JCLI-D-18-0745.1.

Pathak, R., S. Sahany, S. K. Mishra, and S. K. Dash, 2019: Precipitation Biases in CMIP5 Models over the South Asian Region. *Sci. Rep.*, **9**, 1–13, doi:10.1038/s41598-019-45907-4.

Pedregosa, F., and Coauthors, 2011: Scikit-learn: Machine Learning in Python. *J. Mach. Learn. Res.*, **12**, 2825–2830.

Peres-Neto, P. R., D. A. Jackson, and K. M. Somers, 2005: How many principal components? stopping rules for determining the number of non-trivial axes revisited. *Comput. Stat. Data Anal.*, **49**, 974–997, doi:10.1016/j.csda.2004.06.015.

Pfeifer, S., and Coauthors, 2015: Robustness of ensemble climate projections analyzed with climate signal maps: Seasonal and extreme precipitation for Germany. *Atmosphere (Basel).*, **6**, 677–698, doi:10.22444/IBVS.6227_old.

Philippon, N., M. Rouault, Y. Richard, and A. Favre, 2012: The influence of ENSO on winter rainfall in South Africa. *Int. J. Climatol.*, **32**, 2333–2347, doi:10.1002/joc.3403.

Pinto, I., C. Lennard, M. Tadross, B. Hewitson, A. Dosio, G. Nikulin, H. J. Panitz, and M. E. Shongwe, 2016: Evaluation and projections of extreme precipitation over southern Africa from two CORDEX models. *Clim. Change*, **135**, 655–668, doi:10.1007/s10584-015-1573-1.

——, C. Jack, and B. Hewitson, 2018: Process-based model evaluation and

projections over southern Africa from Coordinated Regional Climate Downscaling Experiment and Coupled Model Intercomparison Project Phase 5 models. *Int. J. Climatol.*, **38**, 4251–4261, doi:10.1002/joc.5666.

Pohl, B., N. Fauchereau, C. J. C. Reason, and M. Rouault, 2010: Relationships between the Antarctic oscillation, the Madden-Julian oscillation, and ENSO, and consequences for rainfall analysis. *J. Clim.*, **23**, 238–254, doi:10.1175/2009JCLI2443.1.

——, B. Dieppois, J. Crétat, D. Lawler, and M. Rouault, 2018: From synoptic to interdecadal variability in southern African rainfall: Toward a unified view across time scales. *J. Clim.*, **31**, 5845–5872, doi:10.1175/JCLI-D-17-0405.1.

Qian, J. H., A. W. Robertson, and V. Moron, 2010: Interactions among ENSO, the Monsoon, and Diurnal Cycle in Rainfall Variability over Java, Indonesia. *J. Atmos. Sci.*, **67**, 3509–3524, doi:10.1175/2010JAS3348.1.

Quagraine, K. A., B. Hewitson, C. Jack, I. Pinto, and C. Lennard, 2019a: A methodological approach to assess the co-behaviour of climate processes over southern Africa. *J. Clim.*, **32**, 2483–2495, doi:10.1175/JCLI-D-18-0689.1.

Quagraine, K. A., B. Hewitson, C. Jack, P. Wolski, I. Pinto, and C. Lennard, 2020: Using Co-Behavior Analysis to Interrogate the Performance of CMIP5 GCMs over Southern Africa. *J. Clim.*, **33**, 2891–2905, doi:10.1175/JCLI-D-19-0472.1.

Raddatz, T. J., and Coauthors, 2007: Will the tropical land biosphere dominate the climate–carbon cycle feedback during the twenty-first century? *Clim. Dyn.*, **29**, 565–574, doi:10.1007/s00382-007-0247-8.

Ramirez-Villegas, J., A. J. Challinor, P. K. Thornton, and A. Jarvis, 2013: Implications of regional improvement in global climate models for agricultural impact research. *Environ. Res. Lett.*, **8**, doi:10.1088/1748-9326/8/2/024018.

Ratna, S. S. B., J. V. Ratnam, S. K. S. Behera, C. J. deW. Rautenbach, T. Ndarana, K. Takahashi, and T. Yamagata, 2014: Performance assessment of three convective parameterization schemes in WRF for downscaling summer rainfall over South Africa. **42**, 2931–2953, doi:10.1007/s00382-013-1918-2.

Reason, C. J. C., 2017: Climate of southern africa. *Oxford Research Encyclopedia, Climate Science*, Oxford University Press, 1–37 https://doi.org/10.1093/acrefore/9780190228620.013.513 .

Reason, C. J. C., and D. Jagadheesha, 2005: A model investigation of recent ENSO impacts over southern Africa. *Meteorol. Atmos. Phys.*, **89**, 181–205,

doi:10.1007/s00703-005-0128-9.

Reason, C. J. C., and M. Rouault, 2005: Links between the Antarctic Oscillation and winter rainfall over western South Africa. *Geophys. Res. Lett.*, **32**, 1–4, doi:10.1029/2005GL022419.

Reason, C. J. C., R. J. Allan, J. A. Lindesay, and T. J. Ansell, 2000: Enso and climatic signals across the Indian Ocean basin in the global context: Part I, Interannual composite patterns. *Int. J. Climatol.*, **20**, 1285–1327, doi:10.1002/1097-0088(200009)20:11<1285::AID-JOC536>3.0.CO;2-R.

Reason, C. J. C., W. Landman, and W. Tennant, 2006: Seasonal to decadal prediction of southern African climate and its links with variability of the Atlantic ocean. *Bull. Am. Meteorol. Soc.*, **87**, 941–955, doi:10.1175/BAMS-87-7-941.

Richardson, A. J., C. Risi En, and F. A. Shillington, 2003: Using self-organizing maps to identify patterns in satellite imagery. *Prog. Oceanogr.*, **59**, 223–239, doi:10.1016/j.pocean.2003.07.006.

Robertson, M. P., N. Caithness, and M. H. Villet, 2001: A PCA-based modelling technique for predicting environmental suitability for organisms from presence records. *Divers*, **7**, 15–27, doi:10.1046/j.1472-4642.2001.00094.x.

Ropelewski, C. F., and M. S. Halpert, 1987: Global and Regional Scale Precipitation Patterns Associated with the El Nino/SOuthern Oscillation. *Mon. Weather Rev.*, **115**, 1606–1626, doi:https://doi.org/10.1175/1520-0493(1987)115<1606:GARSPP>2.0.CO;2.

Rousi, E., C. Anagnostopoulou, K. Tolika, and P. Maheras, 2015: Representing teleconnection patterns over Europe: A comparison of SOM and PCA methods. *Atmos. Res.*, **152**, 123–137, doi:10.1016/j.atmosres.2013.11.010..

Samanta, D., K. B. Karnauskas, and N. F. Goodkin, 2019: Tropical Pacific SST and ITCZ Biases in Climate Models: Double Trouble for Future Rainfall Projections? *Geophys. Res. Lett.*, **46**, 2242–2252, doi:10.1029/2018GL081363.

Sheridan, S., and C. C. Lee, 2012: Synoptic climatology and the analysis of atmospheric teleconnections. *Prog. Phys. Geogr.*, **36**, 548–557, doi:10.1177/0309133312447935.

Shlens, J., 2005: A Tutorial on Principal Component Analysis.

Shulze, R. E., and M. Maharaj, 2007: *Rainfall seasonality. South African Atlas of Climatology and Agrohydrology*. Pretoria, South Africa, Section 6.5 pp.

Stocker, T. F., and Coauthors, 2013: Technical Summary. *Clim. Chang. 2013 Phys.*

Sci. Basis. Contrib. Work. Gr. I to Fifth Assess. Rep. Intergov. Panel Clim. Chang., 33–115, doi:10.1017/ CBO9781107415324.005.

Stopa, Justin, E., and K. F. Cheung, 2014: Periodicity and patterns of ocean wind and wave climate. *J. Geophys. Res. Ocean.*, **119**, 5563–5584, doi:doi:10.1002/2013JC009729.

Su, F., X. Duan, Z. Hao, and L. Cuo, 2013: Evaluation of the Global Climate Models in the CMIP5 over the Tibetan Plateau. *J. Clim.*, **26**, 3187–3208, doi:10.1175/JCLI-D-12-00321.1.

Suzuki, T., 2011: Seasonal variation of the ITCZ and its characteristics over central Africa. *Theor. Appl. Climatol.*, **103**, 39–60, doi:10.1007/s00704-010-0276-9.

Tadross, M., C. Jack, and B. Hewitson, 2005: On RCM-based projections of change in southern African summer climate. *Geophys. Res. Lett.*, **32**, doi:10.1029/2005GL024460.

Taljaard, J. J., 1996: Atmospheric circulation systems, synoptic climatology and weather phenomena of South Africa: Synoptic climatology and weather phenomena of South Africa, rainfall in South Africa. *South African Weather Bur. Tech. Pap.*, **32**, 98.

Tamoffo, A. T., and Coauthors, 2019: Process-oriented assessment of RCA4 regional climate model projections over the Congo Basin under 1.5 ∘ C and 2 ∘ C global warming levels: influence of regional moisture fluxes. *Clim. Dyn.*, **53**, 1911–1935, doi:10.1007/s00382-019-04751-y.

Tang, C., B. Morel, M. Wild, B. Pohl, B. Abiodun, and M. Bessafi, 2019: *Numerical simulation of surface solar radiation over Southern Africa. Part 1: Evaluation of regional and global climate models*. Springer Berlin Heidelberg, 457–477 pp. https://doi.org/10.1007/s00382-019-04817-x.

Taylor, K. E., R. J. Stouffer, and G. A. Meehl, 2012a: An overview of CMIP5 and the experiment design. *Bull. Am. Meteorol. Soc.*, **93**, 485–498, doi:10.1175/BAMS-D-11-00094.1.

Thompson, D. W. J., and J. Wallace, 2000a: Annular modes in the extratropical circulation. Part I: month-to-month variability*. *J. Clim.*, **13**, 1000–1016. https://journals.ametsoc.org/doi/pdf/10.1175/1520-0442%282000%29013%3C1000%3AAMITEC%3E2.0.CO%3B2

Todd, M., and R. Washington, 1999: Circulation anomalies associated with tropical-temperate troughs in southern Africa and the south west Indian Ocean. *Clim.*

Dyn., **15**, 937–951, doi:10.1007/s003820050323.

Trenberth, K. E., 1997: The Definition of El Nino. *Bull. Am. Meteorol. Soc.*, **78**, 2271–2278, doi:https://doi.org/10.1175/1520-0477(1997)078<2771:TDOENO>2.0.CO;2.

——, and D. P. Stepaniak, 2001: LETTERS Indices of El Niñ o Evolution. *J. Clim.*, **14**, 1697–1701, doi:https://doi.org/10.1175/1520-0442(2001)014<1697:LIOENO>2.0.CO;2.

Trujillo, A. P., and H. V. Thurman, 2011: *Essentials of oceanography*. Prentice Hall, 551 pp.

Tyson, P. D., 1986: *Climatic change and variability in Southern Africa*. Oxford University Press, 220 pp.

——, and R. A. Preston-Whyte, 2000: *The weather and climate of southern Africa*. 2nd ed. Oxford University Press, Cape Town ; Oxford, 396 pp.

Tyson, P. D., G. R. J. Cooper, and T. S. McCarthy, 2002: Millennial to multi-decadal variability in the climate of southern Africa. *Int. J. Climatol.*, **22**, 1105–1117, doi:10.1002/joc.787.

Voldoire, A., and Coauthors, 2013: The CNRM-CM5.1 global climate model: Description and basic evaluation. *Clim. Dyn.*, **40**, 2091–2121, doi:10.1007/s00382-011-1259-y.

Washington, R., and M. Todd, 1999: Tropical-temperate links in southern African and Southwest Indian Ocean satellite-derived daily rainfall. *Int. J. Climatol.*, **19**, 1601–1616, doi:10.1002/(SICI)1097-0088(19991130)19:14<1601::AID-JOC407>3.0.CO;2-0.

Watanabe, S., and Coauthors, 2011: MIROC-ESM 2010: Model description and basic results of CMIP5-20c3m experiments. *Geosci. Model Dev.*, **4**, 845–872, doi:10.5194/gmd-4-845-2011.

Weldon, D., and C. J. C. Reason, 2014: Variability of rainfall characteristics over the South Coast region of South Africa. *Theor. Appl. Climatol.*, **115**, 177–185, doi:10.1007/s00704-013-0882-4.

Wilson, L., D. Lettenmaier, and E. Skyllingstad, 1992: A hierarchical stochastic model of large-scale atmospheric circulation patterns and multiple station daily precipitation. *J. Geophys.*, **97**, 2791–2809.

Wolski, P., C. Jack, M. Tadross, L. van Aardenne, and C. Lennard, 2018: Interannual rainfall variability and SOM-based circulation classification. *Clim. Dyn.*, **50**, 479–

492, doi:10.1007/s00382-017-3621-1.

Wolter, K., and M. Timlin, 1993: Monitoring ENSO in COADS with a seasonally adjusted principal component index. *Proc. of the 17th Climate Diagnostics Workshop*.

——, and ——, 1998: Measuring the strength of ENSO events: how does 1997/98 rank? *Weather*,. http://onlinelibrary.wiley.com/doi/10.1002/j.1477-8696.1998.tb06408.x/full

Xu, K.-M., 2006: Using the Bootstrap Method for a Statistical Significance Test of Differences between Summary Histograms. *Mon. Weather Rev.*, **134**, 1442–1453, doi:10.1175/MWR3133.1.

Yang, W., R. Seager, M. A. Cane, and B. Lyon, 2015: The rainfall annual cycle bias over East Africa in CMIP5 coupled climate models. *J. Clim.*, **28**, 9789–9802, doi:10.1175/JCLI-D-15-0323.1.

Yukimoto, S., and Coauthors, 2012: A New Global Climate Model of the Meteorological Research Institute: MRI-CGCM3 ^|^mdash;Model Description and Basic Performance; *J. Meteorol. Soc. Japan*, **90A**, 23–64, doi:10.2151/jmsj.2012-A02.

Zhang, Q., H. Körnich, and K. Holmgren, 2013: How well do reanalyses represent the southern African precipitation? *Clim. Dyn.*, **40**, 951–962, doi:10.1007/s00382-012-1423-z.

Appendix A

Step-wise Methodology Formulation [2]

1. First, a 12-node SOM is produced from standardised 700hPa anomaly fields of circulation pattern.
2. A 3-month frequency of occurrence of each synoptic type is determined where this 3-month frequencies is centered using a 3-month moving average window is used to construct a monthly time series matrix of each synoptic type's frequencies. [3]
3. This matrix of synoptic type frequencies is augmented with additional columns for climate indices for ENSO, AAO and TRBI.
4. PCA is then applied to the matrix; which now consists of synoptic type frequencies and climate indices.
5. The N-rule test is used to retain PCs that are significant at 90% confidence level.
6. A threshold of sufficient response ("strong driver") is set by identifying scores of each of the retained PCs where the scores exceeds plus or minus one standard deviation in the 3-month periods.
7. These responses are then examined by extracting corresponding thresholds from precipitation and temperature anomaly for each of the sub-periods[4] for each of the grid cell using CHIRPS and CRU temperature datasets.
8. Standard errors are determined by means of standard bootstrapping with replacement. Anomalies that exceed 90th percentile of the error estimate are deemed statistically significant.

[2] These methodology steps are repeated for all GCMs used in Chapter 3, where all indices and SOM frequencies are generated for each GCM. However, here the GCMs scores are constrained by the reanalysis as the GCMs are mapped through the reanalysis SOM node space. See Chapter 3 for more details.
[3] The resulting time series is three monthly based, i.e. 1981-JFM, 1981-FMA,…,2013-OND
[4] Refers to the three monthly based time series

Appendix B

Formulations of the Principal Component Analysis

Principal component analysis (PCA) is analysis technique that simplifies the complexity in high-dimensional data while retaining trends and patterns. It does this by transforming the data into fewer dimensions, which act as summaries of features (e.g. Lever et al. 2017).

Here, I provide a general mathematical formulation of the PCA analysis as applied to this study.

Matrix of seasonal frequencies and indices = $\begin{pmatrix} YiCj & \cdots & YiCm \\ \vdots & \ddots & \vdots \\ YnCj & \cdots & YnCm \end{pmatrix}$

Where Yi and Yn is the first and last row, Cj and Cm is the first and last column of the matrix. Here, n is 396 (number of years) and m is 15 (12 SOM nodes + 3 indices).

weights (loadings), $w(k) = (w(i), \dots, w(m))$ where $k = 1, \dots L$

where L is the number of retained PCs (3 in this case)

scores $t(i) = (t1, \dots, tL)(i)$ where $i = 1, \dots, n$

Hence

$t(k,i) = x(i) \,.\, w(k)$ to obtain the scores at position (k,i), the i_{th} row of the variable matrix vectorial is multiplied by the k_{th} column of the loading matrix.

Appendix C

Supplemental Material for Chapter 3

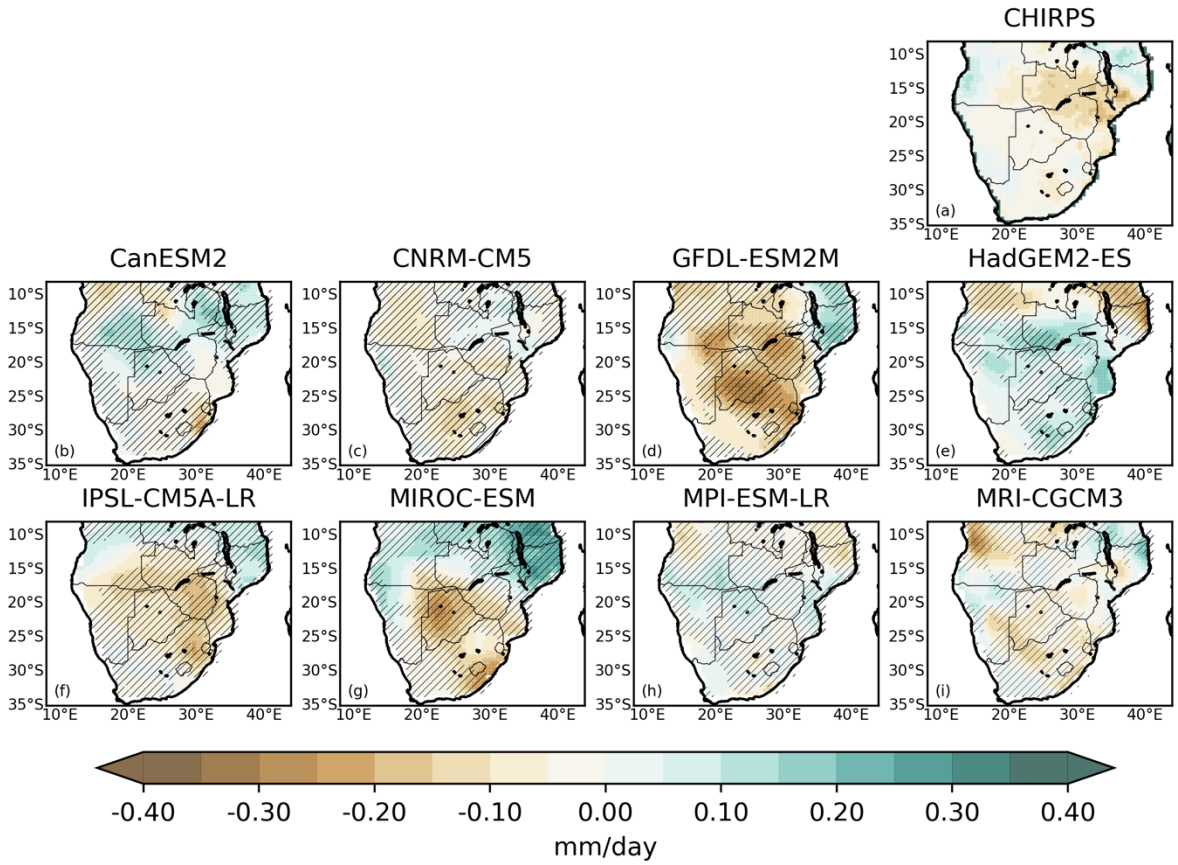

Figure S3.1. Spatial pattern of composite precipitation anomalies for observed (a) and models (b) – (i) for co-behaviour mode two (CM2). Hatching denotes grid cells not statistically significant at 95% level.

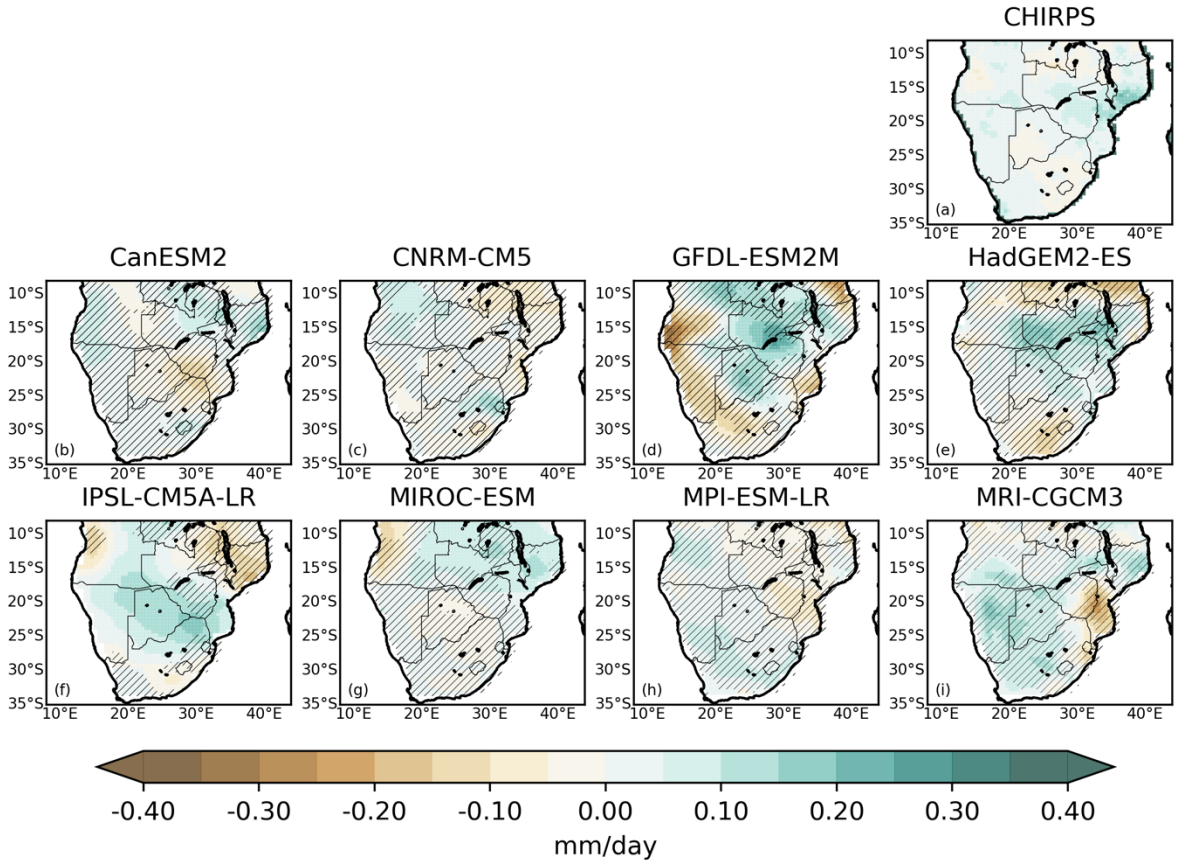

Figure S3.2. Spatial pattern of composite precipitation anomalies for observed (a) and models (b) – (i) for co-behaviour mode three (CM3). Hatching denotes grid cells not statistically significant at 95% level.

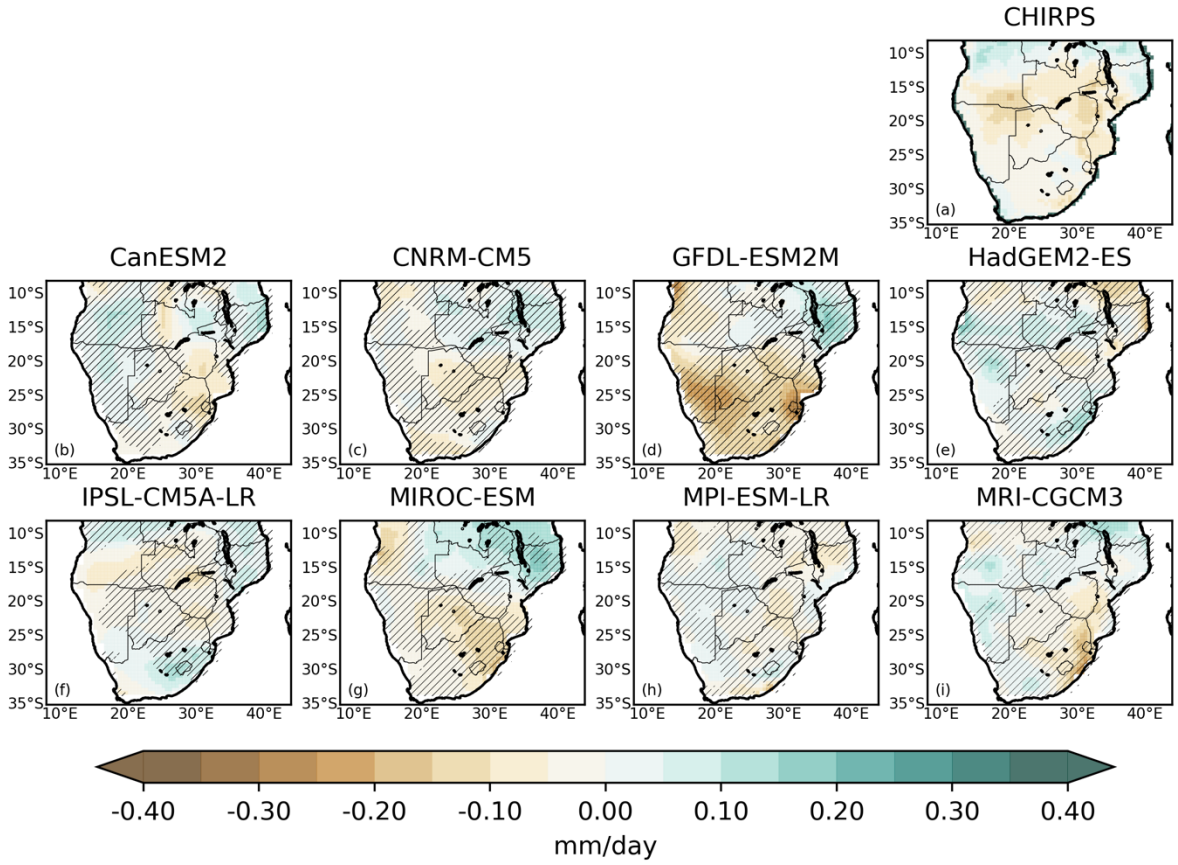

Figure S3 3. Spatial pattern of composite precipitation anomalies for observed (a) and models (b) – (i) for co-behaviour mode five (CM5). Hatching denotes grid cells not statistically significant at 95% level.

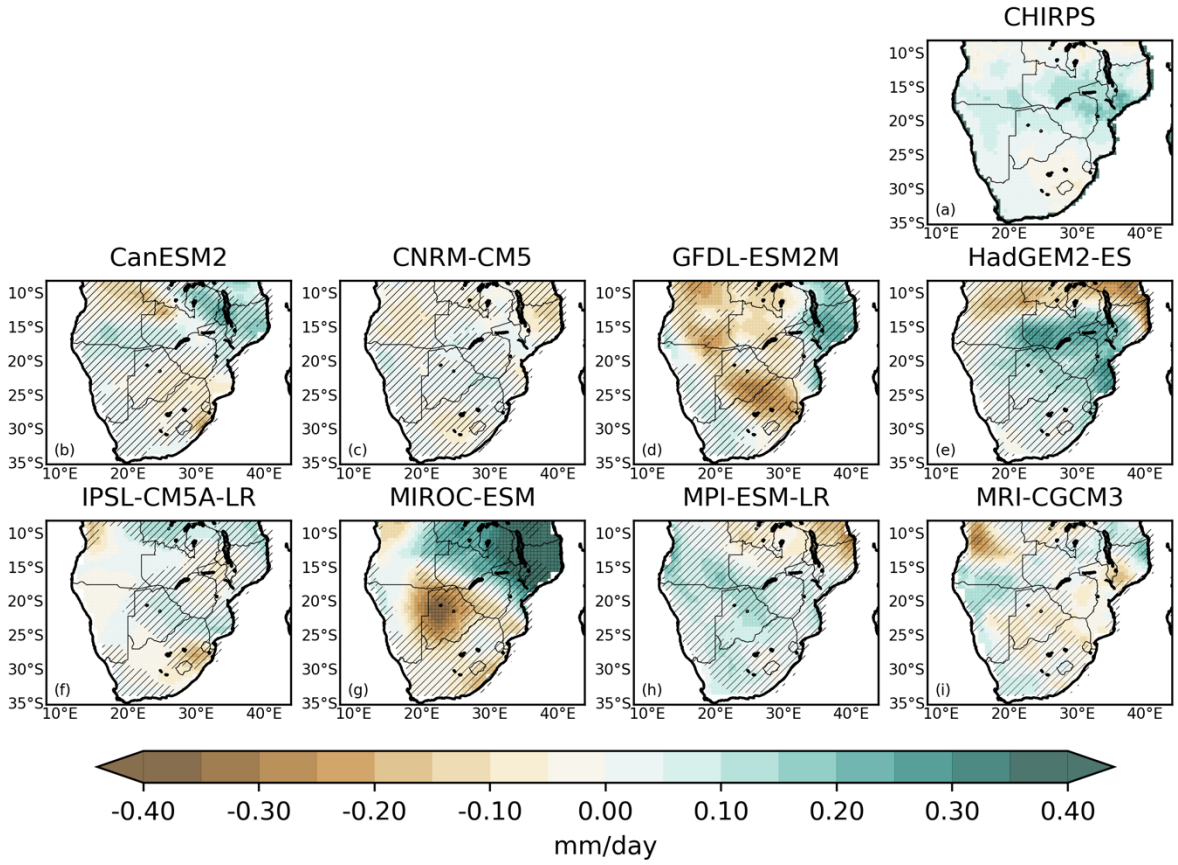

Figure S3.4. Spatial pattern of composite precipitation anomalies for observed (a) and models (b) – (i) for co-behaviour mode six (CM6). Hatching denotes grid cells not statistically significant at 95% level.

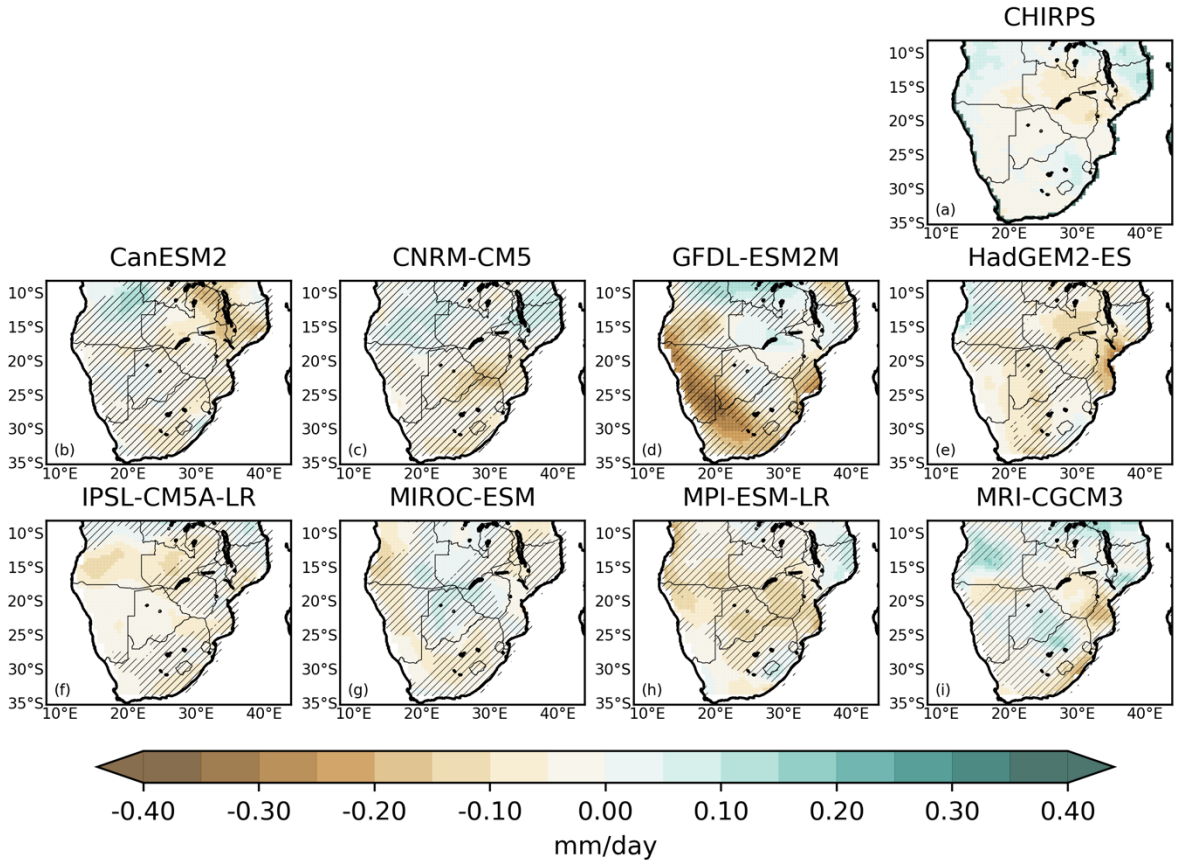

Figure S3 5. Spatial pattern of composite precipitation anomalies for observed (a) and models (b) – (i) for co-behaviour mode seven (CM7). Hatching denotes grid cells not statistically significant at 95% level.

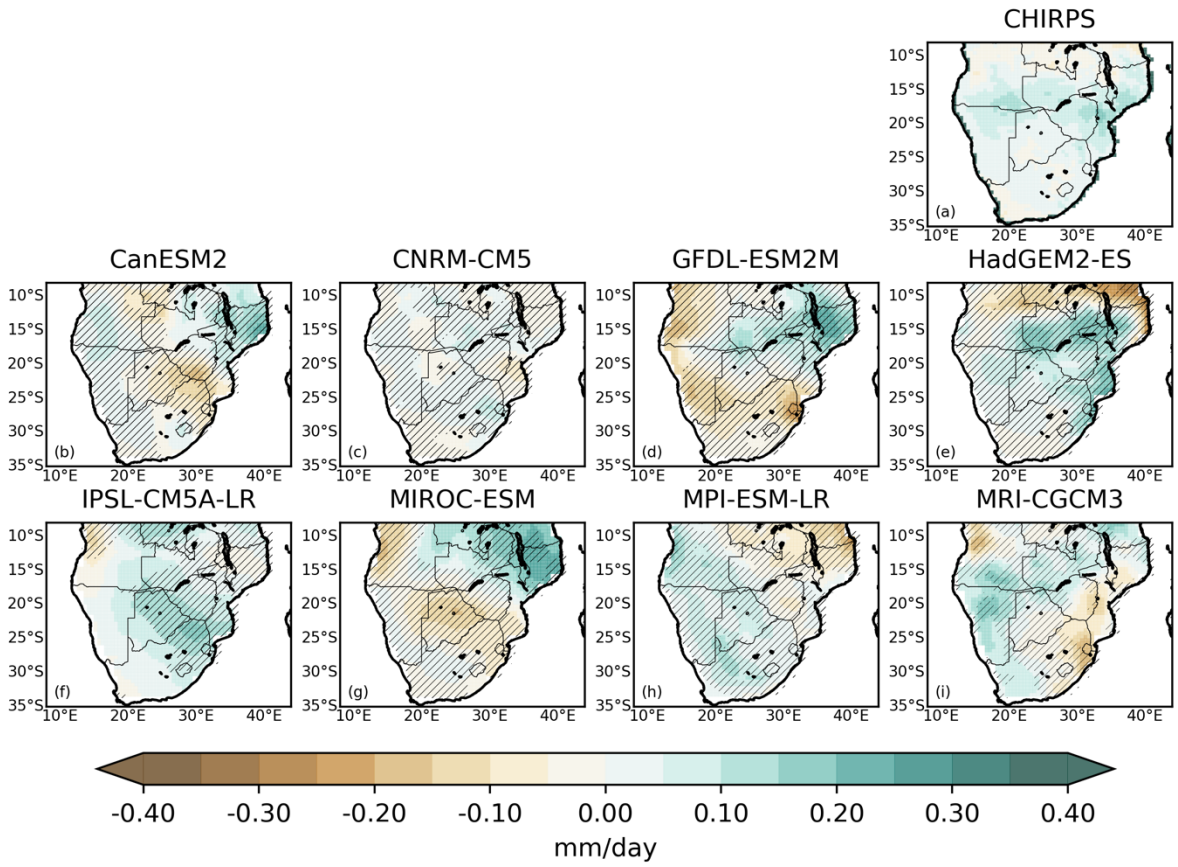

Figure S3.6. Spatial pattern of composite precipitation anomalies for observed (a) and models (b) – (i) for co-behaviour mode eight (CM8). Hatching denotes grid cells not statistically significant at 95% level.

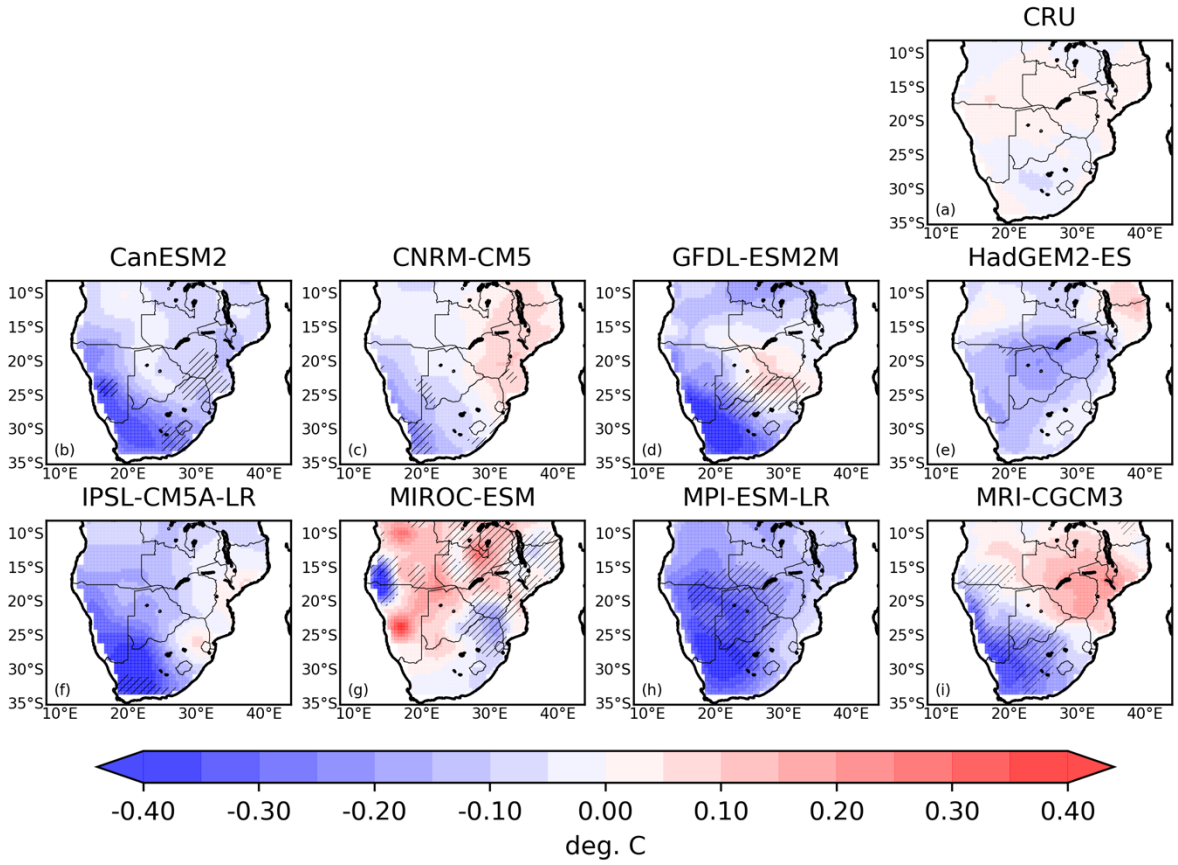

Figure S3.7. Spatial pattern of composite temperature anomalies for observed (a) and models (b) – (i) for co-behaviour mode one (CM1). Hatching denotes grid cells not statistically significant at 95% level.

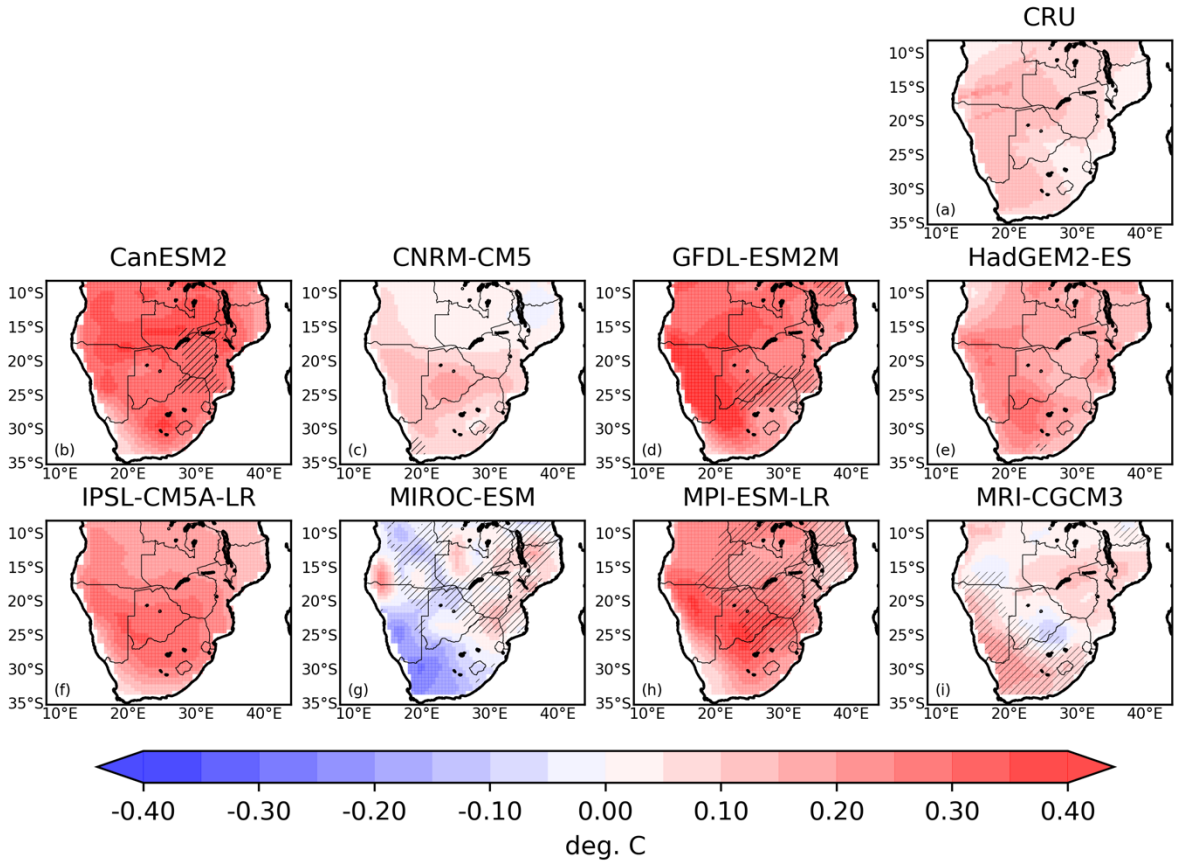

Figure S3.8. Spatial pattern of composite temperature anomalies for observed (a) and models (b) – (i) for co-behaviour mode two (CM2). Hatching denotes grid cells not statistically significant at 95% level.

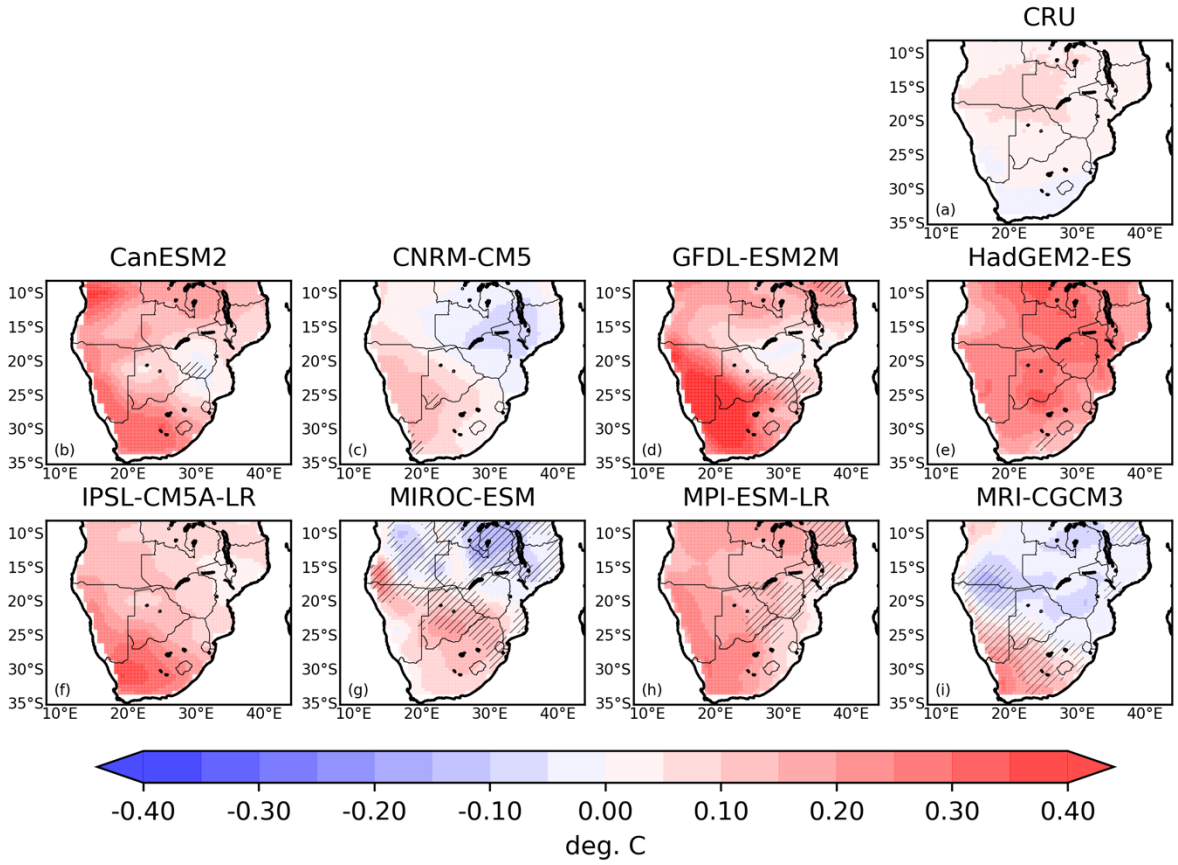

Figure S3.9. Spatial pattern of composite temperature anomalies for observed (a) and models (b) – (i) for co-behaviour mode five (CM5). Hatching denotes grid cells not statistically significant at 95% level.

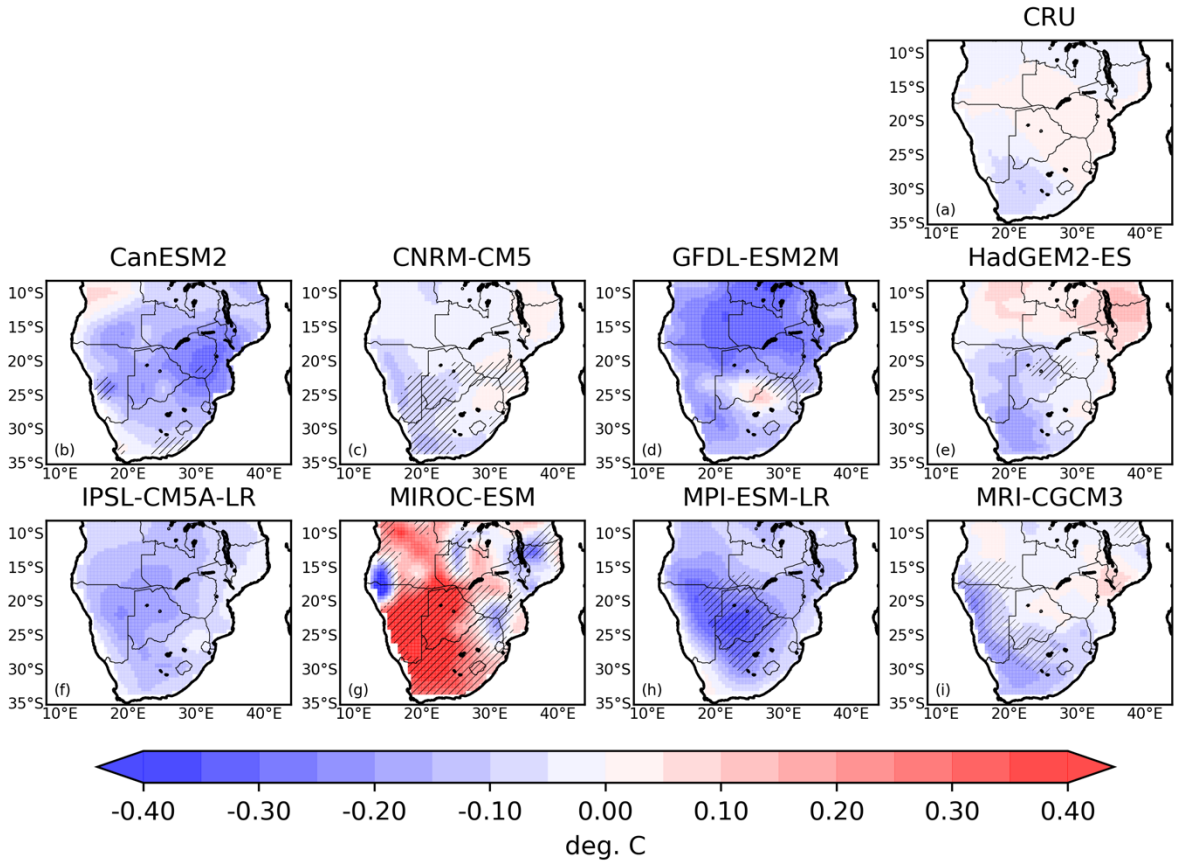

Figure S3.10. Spatial pattern of composite temperature anomalies for observed (a) and models (b) – (i) for co-behaviour mode six (CM6). Hatching denotes grid cells not statistically significant at 95% level.

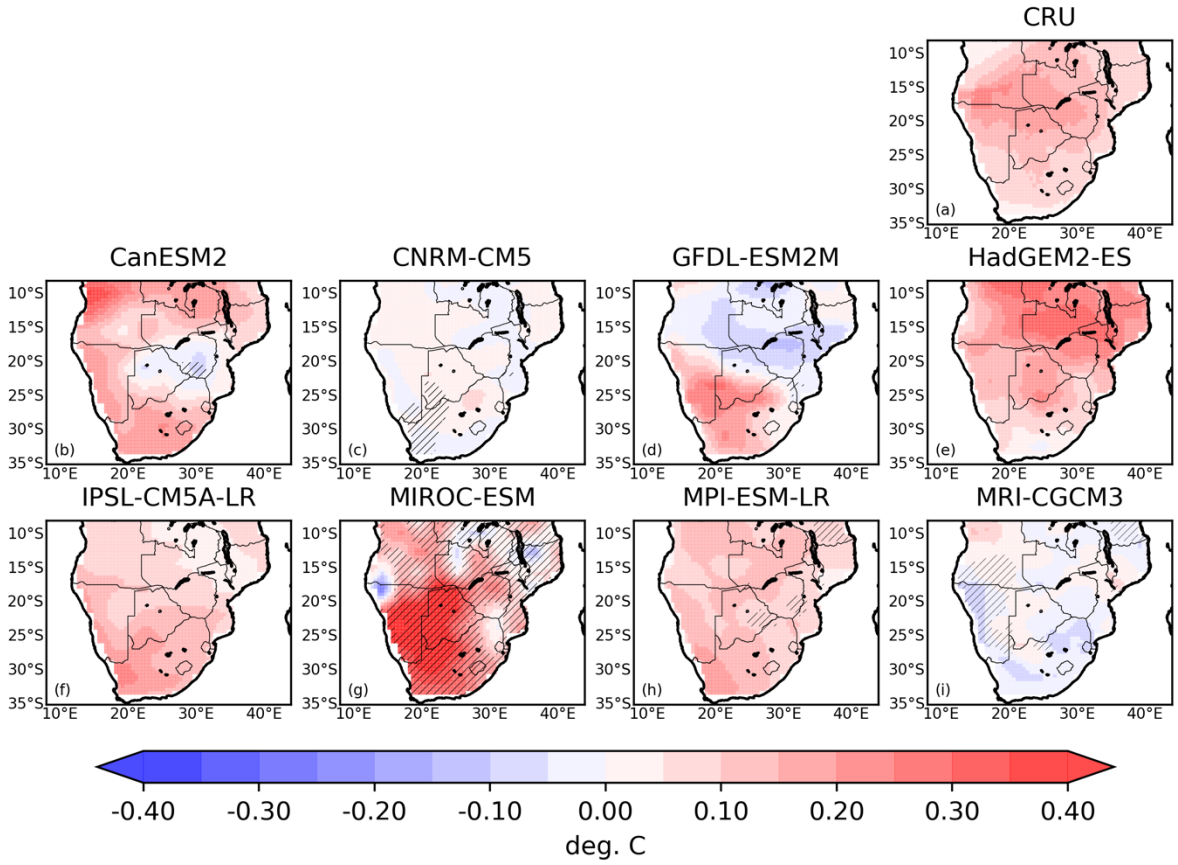

Figure S3.11. Spatial pattern of composite temperature anomalies for observed (a) and models (b) – (i) for co-behaviour mode seven (CM7). Hatching denotes grid cells not statistically significant at 95% level.

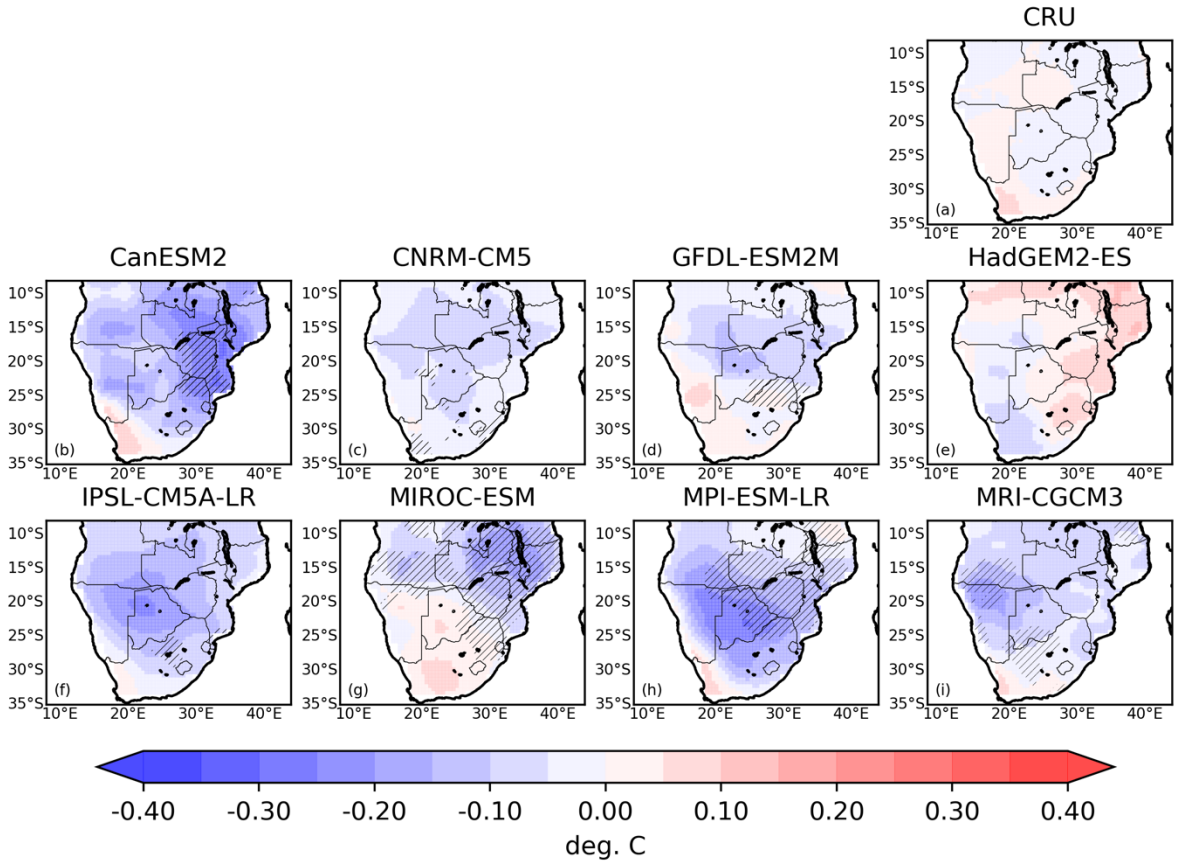

Figure S3 12. Spatial pattern of composite temperature anomalies for observed (a) and models (b) – (i) for co-behaviour mode eight (CM8). Hatches denote grid cells not statistically significant at 95% level.